UNIVERSITÀ DEGLI STUDI DI ROMA
"LA SAPIENZA"

FACOLTÀ DI SCIENZE MATEMATICHE, FISICHE E NATURALI

Characterization of Complex Behaviours in Dynamical Systems: Beyond the Lyapunov Exponents

Dottorato di Ricerca in Fisica
Ph.D. in Physics

XII Ciclo – AA.AA. 1996-1999

Coordinatore: *Prof. Marzio Cassandro*

Supervisor:
Prof. Angelo Vulpiani

Candidate:
Dott. Massimo Cencini

Dedicated to Tito and Giovanni

Almost all I have learnt in these years is mainly due to the continuous and friendly exchange of ideas and discussions I had with the group of people collaborating with Angelo Vulpiani.
I owe them everything.

I'm particularly grateful to Angelo for his friendly way of making research and for stimulating me with questions, ideas and suggestions. I consider myself very lucky for having a master like him.

I'm grateful to Massimo Falcioni (*il saggio*) for his depth in analyzing many issues and his politeness. I would like to thank Luca Biferale, Guido Boffetta and Antonio Celani for the many discussions and the friendly collaborations on turbulence and predictability.
They represent a point of reference not only for my research activity.

I would thank Alessandro Torcini who introduced me to the problem of errors propagation in extended systems, and for his sympathy.

I warmly thank my nice and friendly collaborators Guglielmo Lacorata, Enrico Zambianchi and Patrizia Castiglione, with whom I have learnt many things about "real" problems in geophysics.

I will never forget the nice days spent in working (and fishing) together with my friend Davide Vergni, who encouraged me in many difficult moments and with whom I enjoyed discussing many things.

During the last year I appreciated very much the collaboration of Stefania Espa, Markus Abel, Eckerhard Olbrich and Holger Kantz.

During these three years I received very useful remarks and discussions from K.A. Andersen, F. Bagnoli, R. Baviera, S. Ciliberto, W. Just, R. Livi, A. Mazzino, A. Politi and M. Vergassola.

I would like to acknowledge all the people who, at different levels, contribute to make this experience fruitful and pleasant: F. Ricci-Tersenghi, P. Gori Giorgi, D. Pierotti, A. Perali, L. Benfatto, G. Ruzzi, B. Marani and Lilly.

A special thank to my parents for their patience and support in every moments, and to my brother for his beautiful way to stay close to me and his assistance in coping with my "terrible" English!
Last but not least, I would like to thank Beatrice with whom I have shared beautiful as well as very sad moments.

Piú lontano si va,
meno si sa.

Lao-Tzu

Contents

Introduction

Aside from Poincaré and a few other pioneers, non linear dynamical systems have become subject of intensive research only after the discovery of *deterministic chaos* in a simple system with only three degrees of freedom [1]. The term deterministic chaos was introduced to indicate the irregular behaviors arising in non linear deterministic systems, the main signature of which is the *strong sensitivity to initial conditions*, i.e. the exponential separation of nearby trajectories in phase space.

Nowadays we have a well established dynamical systems theory [2, 3], with a body of concepts and tools (e.g. characteristic Lyapunov exponents, entropies and fractal dimensions of the attractor) for a quantitative characterization of chaos, at least in low dimensional systems. With the characteristic Lyapunov exponents one quantifies the sensitive dependence on initial conditions: two trajectories initially at distance $||\delta \mathbf{x}_0||$ typically separates exponentially in time as

$$||\delta \mathbf{x}(t)|| \simeq ||\delta \mathbf{x}_0|| e^{\lambda t}\,, \tag{0.1}$$

where λ is the maximum Lyapunov exponent: if λ is positive the system is chaotic. Moreover, since the sensitivity on initial conditions can be seen as a source of information [2, 4], one can introduce the Kolmogorov-Sinai entropy [5] which gives the rate of information production induced by the dynamics.

However, this body of knowledge becomes largely unsatisfactory as soon as one considers realistic systems [6]. Indeed, the mathematically well defined basic concepts (e.g. Lyapunov exponents) only refer to asymptotic limits, i.e. infinite time and infinitesimal scales, which are usually unattainable in realistic systems [7, 8, 9, 10]. Moreover, when the spatial aspects are important and the number of degrees of freedom is very high, the dynamical systems concepts and tools developed in the framework of low dimensional systems do not fully characterize the dynamics of these systems, e.g. the Lyapunov exponents only take into account temporal aspects [11, 12].

In this thesis we investigate some aspects of dynamical systems connected with the *predictability problem* which are not taken into account by standard concepts and tools.

The study of predictability, aside from its obvious interest *per se* and for applications (e.g. weather forecasting), can be read, from a conceptual viewpoint, as a way to characterize the *complexity* of dynamical systems. We refer to the concept of complexity as it has been formulated in the context of information theory [13], data compression and algorithmic complexity theory [14]. These approaches are strongly related to the predictability problem [15, 16] because in presence of chaos predictability is limited up to a finite time (related to the first Lyapunov exponent), and, as a consequence, a time sequence obtained from a chaotic system cannot be compressed by an arbitrary factor. Moreover, once analyzed from an algorithmic point of view it results to be *complex* [17]. Without entering into details on this point (see Refs. [16, 18] for a critical and comprehensive discussion on the approaches to complexity) in this thesis we essentially use the term *complex* from a dynamical systems viewpoint as a synonym of *unpredictable*. One relevant advantage of the approach to dynamical systems based on predictability is to enlarge the spectrum of possible "complex" behaviors also to non chaotic systems (i.e. with $\lambda < 0$), where one can observe highly unpredictable behaviors even if the asymptotic dynamics is trivial [3, 19, 20, 21] (see Sect. 2.1).

On the basis of the classical deterministic viewpoint of Laplace [22], it is in principle possible to predict the state of a system, at any time, once the evolution laws and the initial conditions are known. However, initial conditions (and/or evolution equations) are never known with arbitrary precision. Hence, if the system is chaotic, due to the sensitivity to initial conditions (0.1) the prediction of the state of the system is possible only up to a finite time –the *predictability time*–. Indeed, one has to decide a reasonable error tolerance Δ (according to the particular needs) beyond which the state of the system is no more determined with the necessary accuracy. Therefore, if the initial uncertainty is $|\delta \mathbf{x}(0)| = \delta_0$, the typical predictability time is given by

$$T \sim \frac{1}{\lambda} \ln \frac{\Delta}{\delta_0}, \tag{0.2}$$

i.e. the predictability time is essentially given by the inverse of the Lyapunov exponent.

However, the simple relation (0.2) between predictability and maximum Lyapunov exponent fails in generic settings of dynamical systems [6], e.g.: the relation (0.2) is a satisfactory answer to the predictability problem only for δ_0, Δ infinitesimal and for long times. Let us briefly recall some cases in which Eq. (0.2) is unsatisfactory. In *intermittent systems* (even if low dimensional) one has to consider the fluctuations of the predictability time since its typical value (0.2) is not completely relevant [23, 24, 25]. In the context of spatially distributed systems one has to consider not only the way in which an uncertainty grows in time but also the way in which it spreads in space [11, 26] (see Sect. 4.2). In turbulent flows (Sect. 1.2.2 and Sect. 3.2), one has a hierarchy of scales, each of which evolves with its own characteristic time, and the Lyapunov exponents characterize only the smallest fast evolving scales [7, 9, 27]. In addition, in systems displaying an unpredictable character with no positive Lyapunov exponents Eq. (0.2) is completely misleading (see Sect. 2.1).

In the last few years, in order to take into account some of the features which are not described by (0.2) a number of new indicators has been introduced. For instance, the *Comoving Lyapunov exponent* [28], which extends the Lyapunov analysis to a moving frame of reference and turns out to be useful to characterize perturbations which move and amplify (e.g. convective instabilities in open systems such as pipe flows). Other relevant examples are the *spatial* and the *temporal* Lyapunov exponents [12], which give information both on the spatial and temporal evolution of generic perturbations in extended systems (see Sect. 2.2.1). These indicators essentially extend the notion of the Lyapunov exponents in order to give supplementary information on the evolution of perturbation in dynamical systems. However, they are in the framework of linear analysis, i.e. infinitesimal perturbations, so, even if they give supplementary interesting information on the space-time aspects of spatially distributed systems with respect to the usual Lyapunov exponents, they cannot characterize the non linear regime of perturbations growth.

In this thesis we are mainly interested in studying the growth of perturbations which cannot be considered infinitesimal, which are the reasonable ones for the characterization of a realistic predictability problem [8]. To this aim we use the *Finite Size Lyapunov Exponent* (FSLE), recently introduced by Aurell et al. [9, 10] (for a previous attempt to study non infinitesimal perturbations see Ref. [29]). The basic idea of such an analysis is to evaluate the perturbation growth rate at different scales of the perturbation evolution. At very small scales, where the linear analysis applies, the FSLE gives the maximum Lyapunov exponent. At large scales one observes a system dependent behavior, the study of which allows us to characterize the degree of predictability on such scales and, moreover, as we will see, to extract information on the physical processes acting on those scales [10].

For instance, one can characterize systems with many scales and times of motion (e.g. turbulence), indeed at each scale the FSLE identifies the proper characteristic time [9, 10]. It is worth remarking that in such systems the (usual) Lyapunov exponent only refers to the small (fast evolving) scales.

The behavior of the FSLE as a function of the scale also allows us to understand some features of high dimensional systems. For instance: in systems with many interacting microscopic components, the *macroscopic chaos* may appear, i.e. an irregular behavior for some coarse grained variable [30, 31, 32, 33]. Even if we do not know the (hydrodynamical) equations of motion of this coarse grained variables, with the FSLE one can characterize the different dynamical behaviors appearing at different scales. We have also studied a generalization of the FSLE analysis to a moving frame of reference for investigating propagation phenomena in spatially extended systems, for which the linear analysis does not work [34, 35] (Sect. 4.2).

The thesis is organized as follows.

In *Chapter 1* we recall some basic elements of dynamical systems theory and the way in which these results can be extended to high dimensional systems. The issue of the existence of a *thermodynamic limit* for the Lyapunov exponents, i.e. the existence of a Lyapunov density, is also discussed.

In *Chapter 2* we describe the general features of the predictability problem in dynamical systems highlighting the cases in which the standard characterization in terms of Lyapunov exponents fails. We review some recently introduced indicators which take into account both the spatial and the temporal aspects of spatially distributed systems. The last two Sections are devoted to the introduction of the Finite Size Lyapunov Exponents and the related concept of ε-entropy. Moreover, by means of the FSLE we investigate the non linear evolution of perturbations of simple (one-dimensional) maps, showing that the non linear regime may be non trivial also in very low dimensional systems.

In the first part of *Chapter 3* we study systems with many characteristic times with particular attention to the case of turbulence, mainly recalling some known results (see Refs. [7, 9, 10, 36]). The second part is devoted to the study of predictability in systems with uncertainties on the evolution laws, namely we study systems where the small fast evolving scales are unresolved. In such a situation one usually builds a parameterization of such scales in order to take into account their dynamical effects on the resolved degrees of freedom. By means of the FSLE we study the way in which the predictability of the large (resolved) scales is affected by the parameterization of the fast evolving scales.

In the first part of *Chapter 4* we study the collective dynamics of Globally Coupled Maps showing *macroscopic chaos*. By using the FSLE, we are able to characterize these macroscopic behavior: at small values of the perturbation we recover the (microscopic) Lyapunov exponent, while at larger values a sort of macroscopic Lyapunov exponent emerges. In the second part, we discuss the problem of the propagation of an initially localized perturbation in Coupled Map Lattices. This problem is usually characterized in terms of the comoving Lyapunov exponent. However, for some systems this description is not sufficient. We introduce a generalization of the FSLE to a moving frame of reference in terms of which we are able to characterize quantitatively the perturbation propagation.

In *Chapter 5* we discuss an application of the Finite Size Lyapunov Exponent to the study of dispersion properties of passive Lagrangian particles in "non-ideal" flows, in which the asymptotic regime cannot be attained, e.g. in presence of boundaries. We discuss this problem also in the context experimental data.

Chapter 1

Dynamical Systems: an overview

Since the recognition by Lorenz (1963) [1] that even a simple deterministic dynamical system with only three degrees of freedom can generate highly irregular and unpredictable behaviors, many physical and numerical experiments have shown the ubiquity of *deterministic chaos*. In the last few decades, many efforts have been made to develop a satisfactory theory that accounts for such behaviors. Nowadays we have a rather good understanding of low dimensional dynamical systems and a well developed framework of concepts and tools for their characterization. However, as far as high dimensional systems are concerned many questions are still open.

In this Chapter we briefly review the main concepts and tools for the characterization of chaotic behaviors in low dimensional systems and discuss to what extent these concepts apply to high dimensional systems involving time and space, highlighting the many open problems and the few known results.

1.1 Dynamical Systems

Though the evolution of many natural systems is ruled by deterministic laws (i.e. the future state of such systems is completely determined by their present state), often they develop behaviors which can be modeled by stochastic processes, they display *deterministic chaos*. Before discussing how chaos can be characterized, let us start with an abstract definition of what a dynamical system is.

The states of a system are points in an abstract space, the so-called *phase-space*, and the temporal evolution is given by a transformation of the space into on itself. A mathematical model expressing such evolution rule is a *dynamical system* and can be defined as a triple $\{\Omega, \mathbf{S}^t, \mu\}$:

1. Ω is the phase space, usually a compact manifold embedded in space[1] $\Re^n$, where n is an arbitrary dimension.

2. $\mathbf{S}^t$ is the evolution law.

3. μ is the invariant measure under the evolution $\mathbf{S}^t$ (i.e. $\mu(\mathbf{S}^{-t}(E) = \mu(E)$, being E a generic measurable subset of Ω).

Here we only refer to differentiable dynamical systems both in continuous and discrete time t. For the continuous time case, the evolution laws are defined by a set of ordinary differential equations (ODE):

$$\frac{\mathrm{d}\mathbf{x}}{\mathrm{d}t} = \mathbf{F}(\mathbf{x}(t), t)\,, \tag{1.1}$$

or partial differential equations (PDE), if the state variable $\mathbf{v}$ is also a function of spatial coordinates (e.g. the velocity field in a fluid):

$$\partial_t \mathbf{v}(\mathbf{x}, t) = \mathbf{G}[\mathbf{v}(\mathbf{x}, t), t]\,, \tag{1.2}$$

where $\mathbf{G}$ can also include spatial derivatives of the field $\mathbf{v}$. In the discrete time case we have maps:

$$\mathbf{u}(t+1) = \mathbf{F}(\mathbf{u}(t))\,. \tag{1.3}$$

Hereafter we refer essentially to discrete time dynamical systems. The study of maps is indeed not restrictive since maps can be obtained by continuous systems by looking at the intersections of a trajectory with a suitable manifold (the Poincaré section) [2, 37].

A statistical description of the evolution of a dynamical system can be obtained by looking at the properties of the invariant measure μ. More specifically, we make the assumption that for $\mathbf{S}^t$ the *ergodic property* holds [2, 3, 37]. This allows us to replace time averages of an arbitrary observable, ϕ, with averages over the whole phase space weighted according to the invariant measure μ:

$$\lim_{t\to\infty} \frac{1}{T} \int_0^T \phi(\mathbf{S}^t \mathbf{x}_0) dt = \int_\Omega d\mu(\mathbf{x})\phi(\mathbf{x})\,, \tag{1.4}$$

where the equality holds for almost all the initial conditions $\mathbf{x}_0$ with respect to the measure μ. Let us remark that in a generic dynamical system there exist many invariant measures but not all of them are physically relevant [2].

[1] One can also consider other kind of spaces, a dynamical systems can be defined in abstract. However in this thesis we always refer to dynamical systems in $\Re^n$

For instance, a δ-function on an unstable fixed point is invariant under the dynamics but it is not observed. The observed measure is sometimes called the *physical measure* or *natural measure*, i.e. the one selected by the dynamics[2]. Usually one assumes that the physical measure is also *ergodic*, so that (1.4) holds.

A way to describe how the dynamics selects a measure is by introducing the Perron-Frobenius operator [38]. Let us consider a distribution of points in the phase space, e.g. distributed with a non stationary density $\rho(\mathbf{x}, 0)$ at time $t = 0$. The evolution of such a density is given by the Perron-Frobenius operator $\mathcal{L}$, for a map (1.3) one has:

$$\rho(\mathbf{x}, t+1) = \mathcal{L}\,\rho(\mathbf{x}, t) = \int_\Omega \delta^{(d)}(\mathbf{x} - \mathbf{F}(\mathbf{y}))\rho(\mathbf{y}, t) d^d y = \sum_{\{\mathbf{y}_i(\mathbf{x})\}} \frac{\rho(\mathbf{y}_i, t)}{|\nabla \mathbf{F}(\mathbf{y})|}\,, \qquad (1.5)$$

where $\{\mathbf{y}_i(\mathbf{x})\}$ are the pre-images of $\mathbf{x}$. If the system is *mixing*, i.e. the correlation functions (see Sect. 1.1.2) decays exponentially, for almost all the initial distribution one has:

$$\lim_{t\to\infty} \rho(\mathbf{x}, t) = \lim_{t\to\infty} \mathcal{L}^t \rho(\mathbf{x}, 0) = \rho_\mu(\mathbf{x})\,, \qquad (1.6)$$

where $\rho_\mu(\mathbf{x})$ is the invariant density associated to the invariant measure μ (i.e. $\rho_\mu(\mathbf{x}) d\mathbf{x} = d\mu(\mathbf{x})$). The limit is usually (i.e. for "non pathological" systems) attained exponentially fast:

$$||\rho(\mathbf{x}, t) - \rho_\mu(\mathbf{x})|| \sim e^{-|\nu| t}\,, \qquad \text{for} \qquad t \to \infty\,, \qquad (1.7)$$

where ν is the logarithm of the second eigenvalue of the Perron-Frobenius operator. The invariant density $\rho_\mu(\mathbf{x})$ corresponds to the eigenfunction associated with the eigenvalue 1 of $\mathcal{L}$, i.e.

$$\mathcal{L}^t \rho_\mu(\mathbf{x}) = \rho_\mu(\mathbf{x})\,.$$

The traditional distinction among the deterministic dynamical systems is in *conservative* and *dissipative* systems. The first class includes all the systems which preserve the volume in the phase space, among them the most important ones are Hamiltonian systems [37, 39]. In the second class it falls all the systems for which the volume of the phase space shrinks exponentially to zero under the system evolution. After an initial

[2] A possible operative definition of such a measure can be given, following Kolmogorov [2], by adding a small amount of noise, $O(\sigma)$, to evolution laws. In this way there are theorems ensuring the existence of a unique stationary measure μ_σ. Therefore it is rather natural to define the natural measure by taking the limit of zero noise ($\sigma \to 0$), i.e. $\mu = \lim_{\sigma\to 0} \mu_\sigma$. It is worth noting that in numerical computation implicitly one performs this procedure (in this case, the role of noise is played by the round-off errors [27]).

transient (which can be very long) the motion settles onto a zero Lebesgue measure set: the *attractor*[3]. When the motion is regular, the attractors are trivial: the system evolves on fixed points, limit cycles or tori. However, a generic non linear system usually displays chaos and the trajectories evolve in a *strange attractor* which is characterized by peculiar geometric properties. The complex dynamics emerging from this scenario if often named *deterministic chaos*.

One of the most peculiar characteristics of chaos is the *sensitive dependence on initial conditions*, namely initially very close trajectories separate exponentially as time goes on. This phenomenon causes a rapid memory-loss of the initial state, and it is at the origin of the unpredictable character of chaotic dynamics.

1.1.1 Characteristic Lyapunov Exponents

To quantify the sensitive dependence on initial conditions one can introduce a set of numbers which measure the rate of exponential divergence of trajectories along different directions of the phase space. These numbers are called *Characteristic Lyapunov Exponents* (CLEs). Let us start by defining the maximum Lyapunov exponent.

Consider two trajectories: a "reference" one starting at point $\mathbf{x}_0$ and a "perturbed" one starting at $\mathbf{x}_0' = \mathbf{x}_0 + \delta\mathbf{x}_0$, being their distance $d(\mathbf{x}_0, \mathbf{x}_0') = ||\delta\mathbf{x}_0||$ very small (in some norm). During the evolution the distance $d(\mathbf{S}^t\mathbf{x}_0, \mathbf{S}^t\mathbf{x}_0')$ is expected to grow (decrease) exponentially with a typical rate given by:

$$\lambda_{max} = \lim_{t\to\infty} \lim_{d(\mathbf{x}_0,\mathbf{x}_0')\to 0} \frac{1}{t} \ln\left(\frac{d(\mathbf{S}^t\mathbf{x}_0, \mathbf{S}^t\mathbf{x}_0')}{d(\mathbf{x}_0, \mathbf{x}_0')}\right) , \tag{1.8}$$

being λ_{max} the maximum Lyapunov exponent. If $\lambda_{max} < 0$ asymptotically the trajectories reach a fixed point (Fig. 1.1a); if $\lambda_{max} > 0$ one has sensitive dependence on the initial conditions (unpredictability), i.e. chaos (Fig. 1.1c). The case $\lambda_{max} = 0$ corresponds to quasi-periodic motion, e.g. motion on tori or limit cycles (Fig. 1.1b).

A priori the maximum Lyapunov exponent (1.8) may depend on the chosen trajectory and/or on the norm used. For finite dimensional dynamical systems it is possible to demonstrate the equivalence among different norms [40]. However, this problem comes out for infinite dimensional dynamical systems, so, for the moment, we only discuss finite dimensional systems. As far as the (possible) dependence on the trajectory is concerned, we

[3]In conservative systems there are not attractors, the motion take place on the iso-energy surfaces.

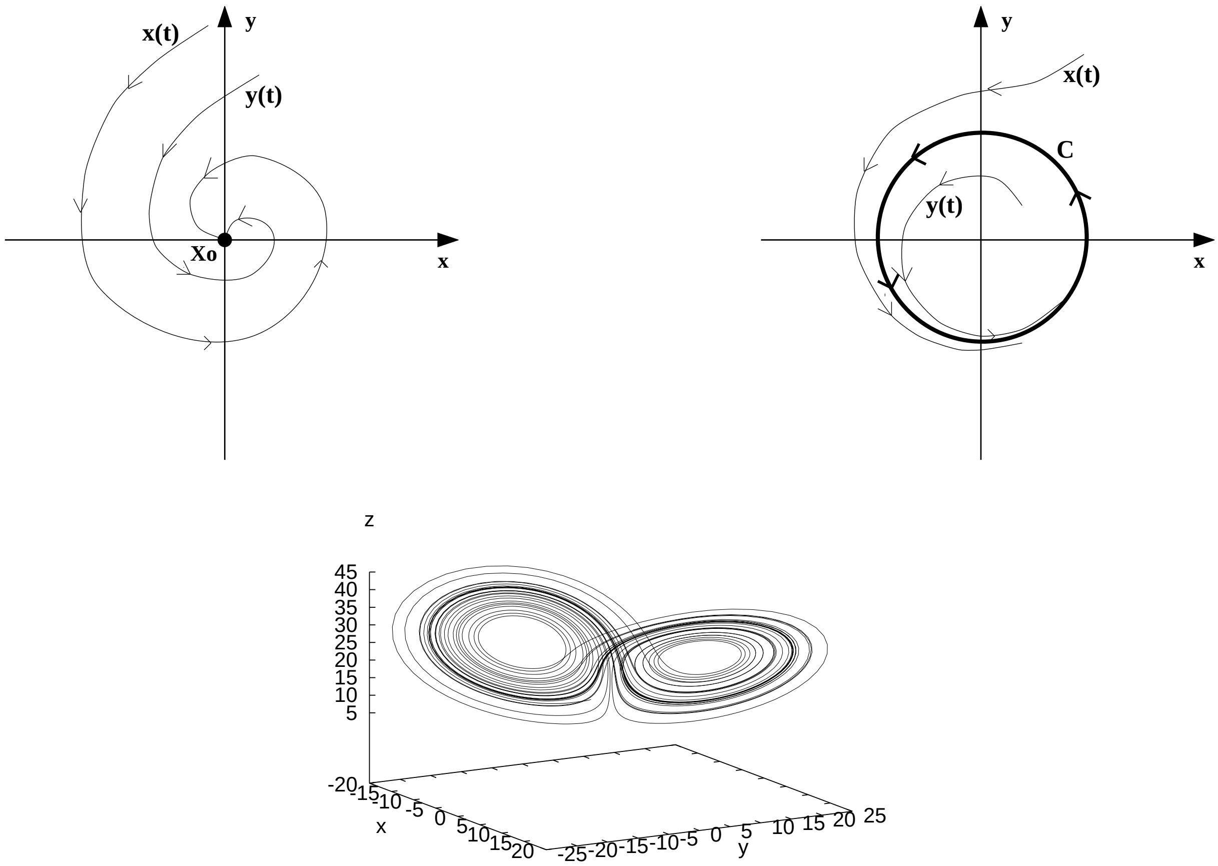

Figure 1.1: The different kinds of attractors are plotted: (a) fixed point, (b) limit cycle, (c) the strange attractor generated by the Lorenz system [1] with the usual choice of the parameters.

can invoke the ergodic theorem (1.4), as a consequence of which the maximum Lyapunov exponent results to be independent on the trajectory for almost all the initial conditions with respect to the natural measure μ. Therefore, for a finite dimensional system the maximum Lyapunov exponent (1.8) is a well defined quantity.

It is worth underlining that the order of the two limits ($t \to \infty$ and $d(\mathbf{x}_0, \mathbf{x}_0') \to 0$) is crucial. The limit $t \to \infty$ is necessary for the ergodic theorem to apply. But, since the motion usually occurs on a bounded attractor (i.e. the distance cannot exceed a certain value), the limit $d(\mathbf{x}_0, \mathbf{x}_0') \to 0$ has to be taken first otherwise the infinite time limit would be trivially zero.

A definition of the Lyapunov exponent, which is more suitable to be implemented on a computer and which allows us to compute all the CLEs spectrum, can be obtained by studying the evolution in *tangent space*[4] [41].

Let us consider a time discrete dynamical system defined by the map:

$$\mathbf{x}(t+1) = \mathbf{F}(\mathbf{x}(t)) \,. \tag{1.9}$$

As far as infinitesimal perturbations are concerned, one can study their motion of by considering the evolution of tangent vectors $\mathbf{z}$, i.e.:

$$\mathbf{z}(t+1) = \hat{D}F[\mathbf{x}(t)]\,\mathbf{z}(t)\,, \tag{1.10}$$

where $\hat{D}F[\mathbf{x}(t)]$ is the Jacobian matrix of the function $\mathbf{F}$

$$\left(\hat{D}F[\mathbf{x}(t)]\right)_{ij} = \left.\frac{\partial F_i(\mathbf{x})}{\partial x_j}\right|_{\mathbf{x}(t)} \tag{1.11}$$

evaluated along the trajectory $\mathbf{x}(t)$. In practice studying the tangent vectors dynamics we take the limit $d(\mathbf{x}_0, \mathbf{x}_0') \to 0$. By iteratively applying (1.10) one has:

$$\mathbf{z}(t) = \hat{D}F[\mathbf{x}(t-1)]\hat{D}F[\mathbf{x}(t-2)]\ldots\hat{D}F[\mathbf{x}_0]\mathbf{z}(0) = \mathcal{A}^t(\mathbf{x}_0)\mathbf{z}(0)\,, \tag{1.12}$$

where $\mathcal{A}^t$ is the evolution operator in tangent space [2]. Finally, by applying the multiplicative ergodic theorem of Oseledec [42], one has that, under general hypothesis, the limiting matrix

$$\hat{\Lambda} = \lim_{t\to\infty}\left[\mathcal{A}^t(\mathbf{x}_0)^\dagger\mathcal{A}^t(\mathbf{x}_0)\right]^{1/2t} \tag{1.13}$$

exists for almost all $\mathbf{x}_0$, where $\dagger$ indicates the adjoint matrix. The matrix $\hat{\Lambda}$ is symmetric and positive definite, with d eigenvalues (α_i, $i = 1\ldots d$) independent on the initial conditions, and by ordering them in a decreasing one has:

$$\lambda_i = \ln \alpha_i\,, \tag{1.14}$$

where λ_i are the Lyapunov exponents (with $\lambda_1 = \lambda_{max}$).

The physical and geometrical interpretation of the first (maximum) Lyapunov exponent is the rate of exponential divergence of two nearby trajectories along the most unstable direction, i.e. in term of the tangent vector one has:

$$\lambda_1 = \lambda_{max} = \lim_{t\to\infty} \ln\frac{||\mathbf{z}(t)||}{||\mathbf{z}(0)||}\,.$$

[4]The linear space spanned by the vectors tangent to the manifold on which the motion takes place.

The meaning of the other Lyapunov exponents can be understood by looking at the evolution of an infinitesimal volume in phase space. In a d-dimensional phase space, we can define a k-dimensional volume, $|Vol_k|$, by means of k independent vectors $(\mathbf{z}_1, \mathbf{z}_2, \ldots, \mathbf{z}_k)$ in tangent space. Due to the dynamics this volume aligns along the most unstable directions and grows exponentially with an average rate given by:

$$\sum_{i=1}^{k} \lambda_i = \lim_{t \to \infty} \frac{1}{t} \ln \frac{|Vol_k(t)|}{|Vol_k(0)|}\,, \tag{1.15}$$

where the sum extends to the first k Lyapunov exponents. It is worth remarking that for a d-dimensional dissipative dynamical systems $\sum_{i=1}^{d} \lambda_i < 0$, indicating that a volume in phase space is contracted. For a conservative dynamical system the sum is zero (the volume is conserved) and, moreover, in symplectic systems [39] the CLE spectrum is symmetric.

Before introducing other quantities, let us underline that the characteristic Lyapunov exponents are global quantities: they define the average rate of expansion. In many situations, e.g., in presence of strong intermittency, one has to take into account not only the average properties but also the fluctuations [23, 24] (see also Sect. 2.1). To properly characterize the fluctuations of the growth rate, one can introduce the *Generalized Lyapunov Exponents*, $L_i(q)$ [24, 43]. Limiting to the maximum one, $L_1(q)$, one has:

$$L_1(q) = \lim_{t \to \infty} \frac{1}{t} \ln \langle R_\tau(t)^q \rangle\,, \tag{1.16}$$

where

$$R_\tau(t) = \frac{|\mathbf{z}(t+\tau)|}{|\mathbf{z}(t)|} \tag{1.17}$$

is the response function defined on a tangent vector. The response function indicates the response of the system after a time interval τ for an unitary perturbation acting at time t. It is possible to show that $L_1(q)$ is a convex function of q and

$$\lambda_1 = \left. \frac{dL(q)}{dq} \right|_{q=0}\,,$$

and, moreover, if there is no intermittency $L_1(q) = \lambda_1 q$ [24, 43]. The generalized Lyapunov exponents are nothing but the moments of the local fluctuations of the rate of expansion along the most unstable direction. For further details see Ref. [24].

1.1.2 Correlation functions, Dimensions and Entropies

Even if the Lyapunov spectrum gives us many information on the degree of *complexity* of a chaotic system, there exists several other indicators highlighting other important features.

I. Correlation functions and power spectrum

Correlation functions are widely used and powerful indicators with applications in many fields. In chaotic systems one usually studies the autocorrelation function of an observable $A(\mathbf{x}(t))$ which depends on the trajectory. Typically one finds the autocorrelation function to be exponentially decreasing in time [2]:

$$C_{AA}(t,t^{'}) = C_{AA}(|t-t^{'}|) = \langle (A(\mathbf{x}(t) - \langle A(\mathbf{x})\rangle)(A(\mathbf{x}(t^{'}) - \langle A(\mathbf{x})\rangle)\rangle \sim e^{-\frac{|t-t^{'}|}{\tau}}, \tag{1.18}$$

where the angular brackets indicate temporal or ensemble average[5]. The exponential decay is another indication of the fast memory-loss induced by the dynamics of such chaotic systems. However, differently from one intuitively expects, the temporal scale τ defined by Eq. (1.18) usually has no relation with the inverse of the first Lyapunov exponent, which is the natural time scale of the memory-loss. Indeed, except pathological systems, one has that $\tau = 1/|\nu|$ where ν (1.7) is the logarithm of the second eigenvalue of the Perron-Frobenius operator (1.5) [38]. Usually, one has that $\tau = 1/|\nu| \geq 1/\lambda_1$. However, there exist systems in which the autocorrelation function decay as a power law (or a stretched exponential, e.g. the Lorenz system [1] at the onset of the strong intermittent regime) even if $\lambda_{max} > 0$.

Through the Wiener-Kinchin theorem [44] which links the Fourier transform of the autocorrelation function with the power spectrum, $S(\omega)$, one has:

$$S(\omega) = \int_{-\infty}^{+\infty} e^{i\omega t} C_{AA}(t) dt.$$

From which it is evident that the power spectrum does not bring any new piece of information with respect to correlation functions. Nevertheless, the power spectrum is usually more suitable to be measured in experimental settings. If one looks at $S(\omega)$, he has that while for regular signals the power spectrum consists of sharp peaks, in chaotic systems it develops a broad continuous component possibly associated with a peaked structure corresponding to some almost periodic recurrences. The continuous band is usually the

[5]Note that in Eq. (1.18) we have implicitly assumed the dynamics to be stationary in time.

signature of chaos [2] (of course, if the there are good reasons to consider the signal produced by a deterministic law).

II. Strange attractor and fractal dimensions

Since the seventies, it was realized the ubiquity of *fractals* in nature [45]. Strange attractors in dissipative chaotic systems are typically fractal objects with self-similar structures [24]. The whole conceptual and technical apparatus developed for the characterization of geometric properties of fractal objects has been successfully applied to chaotic system and it has provided a very powerful tool for a quantitative characterization of the *strangeness* of strange attractors [2, 46].

A first characterization of a fractal object can be obtained by defining the *fractal dimension* (or Hausdorff dimension), D_F, which is a natural extension of the *topological dimension* D (i.e. the minimum dimension of space $\Re^D$ where the object can be embedded, e.g. $D = 1$ for curves, $D = 2$ for surfaces and so on). A geometrical definition of D_F can be given by considering a partition of the space into non-overlapping boxes of size ε, $B_i(\varepsilon)$, and then counting the number of boxes, $N(\varepsilon)$, containing at least one point of the attracting set. The fractal dimension is thus given by:

$$D_F = \lim_{\varepsilon \to 0} \frac{\ln N(\varepsilon)}{\ln(1/\varepsilon)} \,. \tag{1.19}$$

D_F is sometimes referred as the box counting dimension, however in most cases it is equal to Hausdorff dimension [2, 24, 45]. It is worth remarking that $D_F = 1$ for continuous smooth curves, or $D_F = 2$ for surfaces, while $D_F \notin \mathbb{N}$ for fractal objects.

D_F only characterizes the geometrical properties of attractors, i.e. it weights in the same way regions having different visit frequencies. In other words, D_F only characterizes the support of the natural measure. However, in general, the measure is not homogeneous on the attractor, so that only accounting the fractal properties of its support is not satisfactory. If one takes into account the dishomogeneities one speaks of *multifractal objects* and has to introduce other "dimensions" to properly characterize the measure [24, 47, 48]. Among these dimensions the most important one, from the point of view of physicists, is the so-called *information dimension*, D_I, which takes into account the visit frequencies of different portions of the attractor,

A "physical" definition of D_I can be obtained in terms of the scaling behavior of the entropy which measures the amount of information necessary to describe the invariant measure at a resolution ε. As before one introduces a partition of the phase-space in boxes $B_i(\varepsilon)$ and then measures the coarse-grained probability distribution induced by the measure μ:

$$P_i(\varepsilon) = \int_{B_i(\varepsilon)} d\mu(\mathbf{x})\,. \tag{1.20}$$

The entropy associated to this distribution is given by [13, 49]:

$$E(\varepsilon) = -\sum_i P_i(\varepsilon) \ln P_i(\varepsilon)\,, \tag{1.21}$$

and the information dimension is given by

$$D_I = \lim_{\varepsilon \to 0} \frac{\ln E(\varepsilon)}{\ln(1/\varepsilon)}\,. \tag{1.22}$$

In order to fully characterize the measure on the attractor one can introduce the so-called generalized dimensions D_q [18, 24, 38] (D_I is only one of them, probably the most physically relevant), which are very similar to the generalized Lyapunov exponents (1.16). Such generalized dimensions can be defined analogously to Eqs. (1.21-1.22) introducing the quantities (Renyi entropies) [43]

$$Z(\varepsilon, q) = \sum_i P_i(\varepsilon)^q P_i(\varepsilon)\,, \tag{1.23}$$

D_q are defined as

$$D_q = \frac{1}{q-1} \lim_{\varepsilon \to 0} \frac{\ln Z(\varepsilon, q)}{\ln(1/\varepsilon)}\,.$$

Without entering in further details (see Refs. [24, 38] for a detailed discussion), we just mention that by using these quantities it is possible to build a statistical mechanics of chaos [18, 38]. Practically, the most popular way to compute the attractor dimension is in terms of the correlation integral introduced by Grassberger and Procaccia [46], which corresponds to evaluating D_2.

From a dynamical systems point of view, the importance of the fractal dimension relies on the fact that it estimates the number of "effective" degrees of freedom, i.e. the minimal number of variables necessary to describe the motion on the attractor, which are roughly given by $[D_F] + 1$ [2, 3] (being [...] the integer part).

At this point one can wonder if there exist some relation between the Lyapunov exponents and the attractor dimension. In this respect, there is an important conjecture due to Kaplan and York [50] (rigorously proved only in some special cases) which states a relationship between the fractal dimension and the Lyapunov spectrum. Indicating

$N_\lambda(k) = \sum_{i=1,k} \lambda_i$ the sum of the first k Lyapunov exponents (ordered in a decreasing way), one can extend $N_\lambda(k)$ to real numbers by an interpolation between k and $k+1$, i.e. if $k \le x \le k+1$:

$$N_\lambda(x) = N_\lambda(k) + (x-k)\lambda_{k+1}\,. \tag{1.24}$$

Kaplan and York have conjectured that the fractal dimension D_F can be estimated as the value $\tilde{x}$ at which $N_\lambda(x) = 0$, so that:

$$D_F \sim \tilde{x} = k + \frac{\sum_{i=1}^{k} \lambda_i}{|\lambda_{k+1}|}\,. \tag{1.25}$$

Such a conjecture has been numerically verified for many chaotic systems [2].

III. Information and Entropy

In chaotic systems, due to the sensitive dependence on the initial conditions, two trajectories initially different but indistinguishable (within a certain precision) evolve into distinguishable states after a finite time. This process can be seen as a *flow of information* in *bit space* [4], i.e. any uncertainties on the seemingly insignificant digits of the number sequence specifying the initial conditions spreads with time towards the significant ones, *creating* information [2, 5].

After the seminal work of Shannon (1948) [13], it is now well established by *Information Theory* [49] that a quantitative measure of the information contained in a message (in our case in a trajectory) is given by the *entropy* of the message. In dynamical system this concept was introduced by Kolmogorov [5], who originally was searching for an invariant under isomorphisms (smooth change of variables). He discovered such an invariant the *Kolmogorov-Sinai entropy* (KS-entropy), which we are going to define.

We shall limit our discussion to time discrete dynamical systems, the extension to the continuous case is straightforward. We consider a dynamical system defined by the triple $\{\Omega, \mathbf{S}^t, \mu\}$. First of all we have to make a partition of the phase space Ω, or, better, of the support of the ergodic measure μ. For simplicity we can consider a partition in boxes of side ε as done in the previous Section, in such a way that we can put in correspondence any point $\mathbf{x} \in \Omega$ with a symbol (e.g. an integer encoding the box which contains the point), i.e.:

$$\mathbf{x} \to \omega_k \qquad \text{if} \qquad \mathbf{x} \in B_{\omega_k}(\varepsilon)\,. \tag{1.26}$$

By means of such an encoding procedure, a trajectory can be mapped on a sequence of symbols $\{\omega_i\}$:

$$\{\mathbf{x}(0)\,,\ \mathbf{x}(1) = \mathbf{S}^1\mathbf{x}(0)\,,\ \mathbf{x}(2) = \mathbf{S}^2\mathbf{x}(0)\ \ldots\} \rightarrow \{\omega_0\,,\ \omega_1\,,\ \omega_2\ \ldots\}\,. \tag{1.27}$$

In this way a trajectory up to a time N and with a resolution ε turns out to be specified by a sequence of symbols accordingly to the visited boxes. Now we can introduce the joint probability

$$P_\varepsilon(\omega_0,\ldots,\omega_N) = P\left\{\mathbf{x}(0) \in B_{\omega_0}(\varepsilon),\ldots,\mathbf{x}(N) \in B_{\omega_N}(\varepsilon)\right\} \tag{1.28}$$

and we can compute the N-block entropy associated to such probability which is given by:

$$H_N(\varepsilon) = -\sum_{\omega_0,\ldots,\omega_N} P_\varepsilon(\omega_0,\ldots,\omega_N) \ln P_\varepsilon(\omega_0,\ldots,\omega_N)\,. \tag{1.29}$$

From the N-block entropies one can define the entropy rate

$$h_N(\varepsilon) = H_N(\varepsilon) - H_{N-1}(\varepsilon) \qquad (N \geq 0\,,\ H_0 = 0)\,, \tag{1.30}$$

which measures the average information contained in N steps of the sequence. If $h_N(\varepsilon) = 0$ one has the maximum of information, i.e. the next step can be predicted with certitude. On the contrary, when $h_N(\varepsilon)$ attains its maximum (given by the logarithm of the number of symbols, i.e. $\ln N(\varepsilon)$, where $N(\varepsilon)$ indicates the number of cells at resolution ε) no information is available, predicting the future value is a random guess. Since, more of the past is known more it is the amount of information stored, the entropy rate (1.30) cannot decrease when N increases [49]. The Shannon entropy [13]

$$h(\varepsilon) = \lim_{N\to\infty} h_N(\varepsilon) \tag{1.31}$$

measures the amount of information contained the whole past history, moreover if the limit

$$h_{KS} = \lim_{\varepsilon\to 0} h(\varepsilon) \tag{1.32}$$

exists, it defines the Kolmogorov-Sinai entropy (KS-entropy) which measures the mean rate of creation of information induced by the dynamics. The limit $\varepsilon \to 0$ ensures that each sequence corresponds to a single trajectory [2, 3].

A more rigorous definition of the KS-entropy can be obtained by defining a generic partition $\{\mathcal{P}_i\}$ in which the cells are not necessarily equals and then defining a partition dependent entropy $h(\mathcal{P})$ by exactly following steps analogous to ($1.29 \to 1.31$). Finally taking the supremum[6] over all the admissible partitions, one has:

$$h_{KS} = \sup_{\{\mathcal{P}\}} \{h(\mathcal{P})\}\,. \tag{1.33}$$

For a rigorous definition of the KS-entropy see, e.g., Ref. [2]. In practices, the limit $\varepsilon \to 0$ in Eq. (1.32) is performed in order to take automatically the sup.

In terms of information theory the Kolmogorov-Sinai entropy corresponds to the numbers of bits per unit time necessary and sufficient to encode without ambiguity a trajectory during its evolution. Analogously to the characteristic Lyapunov exponents, the KS-entropy vanishes for periodic or quasi-periodic dynamics while it is positive for chaotic systems. Indeed, it is possible to show that the KS-entropy is related to the positive Lyapunov exponents. In fact, the following equality (Pesin equality) [51] is expected to hold:

$$h_{KS} = \sum_{\lambda_i > 0} \lambda_i\,. \tag{1.34}$$

Unfortunately, this equality can be proved only in particular cases. More in general one has the inequality [2]:

$$h_{KS} \le \sum_{\lambda_i > 0} \lambda_i\,.$$

Equation (1.34) tells us a rather intuitive idea: since information creation is induced by sensitivity on initial conditions, the entropy (which measures information) and (positive) Lyapunov exponents (which quantify sensitivity) must be strongly related.

The way we have followed in defining the KS-entropy calls rather naturally for the introduction of the concept of ε-entropy, which is roughly the entropy rate at resolution ε, we shall return on this concept elsewhere (see Sect. 2.4).

1.2 High dimensional dynamical systems

The above introduced quantities are rather satisfactory for characterizing few degrees of freedom dynamical systems. The situation becomes different when one considers high dimensional systems. In such a case one has to deal with a huge number of (interacting)

---

[6] It is worth remarking that there exist partitions, called *generating partitions*, for which the supremum (1.33) is automatically attained, but apart very simple dynamical systems it is an hard task to find them ([2, 3]).

degrees of freedom and, as a consequence, an increasing number of characteristic exponents. Therefore, it is almost impossible to compute all of them, and, sometimes, useless when, e.g., spatial aspects of the system become important (see Chapter 2). Indeed, in such systems, one is faced with a *plethora* of new phenomena which call for new and (often) *ad hoc* characterizations. Among the many new features we just mention that: in presence of different characteristic times in the dynamics the Lyapunov exponents only characterize the small/fast scales developments; in spatially distributed systems many important phenomena are related to transport processes which are not characterized by the above introduced quantities [28]. Moreover, unpredictable (*complex*) behaviors may also arise in absence local instabilities [3, 19, 20, 21]. We shall discuss extensively such issues in the next Chapters.

In the following part of this Chapter, we aim at giving a brief overview of high dimensional dynamical systems, summarizing some well established results and, mainly, highlighting the difficulties and the still open problems. Let us start by introducing a phenomenological and heuristic picture of what a high dimensional system is. First of all we have to specify that some systems, seemingly of very high dimension, may indeed be described in the framework of low-dimensional systems. For instance, the hydrodynamical motion of a fluid, which in principle is infinite dimensional, can be laminar (regular) and, close to the transition to turbulence, chaotic but with a low number of active degrees of freedom, i.e. the attractor of the motion is characterized by a low fractal dimension, D_F. However, there is not an universal and well accepted value of D_F (i.e. of number of degrees of freedom) for distinguishing between low and high dimensional systems.

In order to make such a distinction we follow the approach suggested in Ref. [52], where it is proposed to distinguish the character (low or high dimensional) of a system in terms of three different characteristic lengths. Let us consider a system depending both on space and time. Let us assume that L is the system size (we limit to one spatial dimension, the discussion obviously generalizes to higher dimensions). We can distinguish three characteristic lengths, respectively connected to dissipation[7], excitation and correlation. The *dissipation* length, ℓ_D, is the characteristic length scale at which energy is dissipated. Scales smaller than ℓ_D can be considered as non-active degrees of freedom, at least from a dynamical point of view. The *excitation* length, ℓ_E, represents the scale at which energy is injected into the system. Finally, the *correlation* length, ξ,

[7]Here we are assuming that the system is dissipative

can operationally be defined in terms of a suitable correlation function, e.g. if $\mathbf{u}(\mathbf{x}, t)$ is a space-time dependent vector field:

$$C_{i,j}(\mathbf{x}_1 - \mathbf{x}_2) = \langle (u_i(\mathbf{x}_1, t) - \langle u_i \rangle)(u_j(\mathbf{x}_2, t) - \langle u_j \rangle) \rangle \,, \tag{1.35}$$

where the angular brackets denote a time average or, equivalently, an *ensemble* average. If the large distance behavior is

$$C_{i,j}(\mathbf{r}) \sim \exp\left(-\frac{|\mathbf{r}|}{\xi}\right) \qquad (\mathbf{r} = \mathbf{x}_1 - \mathbf{x}_2) \tag{1.36}$$

then ξ is the correlation length[8].

In terms of these three characteristic lengths one can now introduce the notions of *temporal* and *spatio-temporal* chaos, i.e. *Small* versus *Large* systems [52]. Let us assume that there is a control parameter, R, in the system which can be increased until the dynamics becomes irregular (chaotic), e.g. the Reynolds number in turbulence. We can now distinguish two limiting cases:

- *Small Systems*: $L \sim \ell_D$, if the system size is of the order of the dissipation length we expect also the correlation length to be of the same order. The active degrees of freedom are constrained by the geometry of the problem to a low value, hence the system is expected to be described by a "low" dimensional dynamical system. Since, in such a case, the spatial aspects may be of little relevance one also speaks of *temporal chaos*.

- *Large Systems*: $L \gg \ell_D$. In this case the system involves many degrees of freedom which increase with the system size (i.e. with the ratio L/ℓ_D). Correspondingly the attractor dimension is expected to increase with L. Here the spatial aspects are very important and one usually speaks of *spatio-temporal chaos*. In such a case one also expects $L \gg \xi \gg \ell_D$, so that regions of the system whose distance is greater than ξ are very poorly correlated, so that such systems are also called *extended systems*. With this term one means that the number of (active) degrees of freedom and consequently the number of positive Lyapunov exponents, the Kolmogorov-Sinai entropy and the attractor dimension are extensive quantities, i.e. they increase with the system size, L.

[8]Of course the behavior of $C_{i,j}(\mathbf{r})$ can be considerably more complicated, but let us assume that it is possible to define anyway a correlation length for the system.

Of course, the above simplified picture is not the most general one. Indeed it is very difficult to identify an unifying scenario of transition to high dimensionality. Indeed, the simplest way to reach high dimensionality is that of fixing the control parameter, R, and increasing the system size, $L \to \infty$. Another possibility is to increase R at fixed L. If this is the case, we expect that the number of excited degrees of freedom increases with R. From this point of view the case of turbulence deserves some specifications. In turbulence the control parameter, the Reynolds number, can be expressed as $Re \approx (\ell_E/\ell_D)^{4/3}$ (see Sect. 1.2.2). Since it is more easy to decrease ℓ_D than to increase L (which is typically greater than ℓ_E); we expect this second scenario to hold.

With the hope that now the notion of spatio-temporal chaos is clear[9], we list, without entering in details, some phenomena which are for their intrinsic nature high dimensional, e.g.: *Turbulence* in fluids [6, 53] (see Sect. 1.2.2); *Pattern formation*, i.e. the spontaneous generation of well defined spatial patterns from initially incoherent structures which appear in many fields ranging from optics to chemistry [18, 52, 54]; *Propagation phenomena*, a typical example is the convective instabilities in fluids, i.e. the propagation of unstable regimes throughout a fluid or the chaotic patterns arising in convection or other fluid systems, such as Rayleigh-Bérnard convection or Taylor-Couette flow [55, 56].

It is worth to remark that a common feature of such systems is that they are kept far from equilibrium (e.g. in turbulence one puts continuously energy into the system) by external forcing, so that they have to be inserted in the framework of *out-of-equilibrium statistical mechanics* [57]. However, since there is not yet a general theory of out-of-equilibrium phenomena, most of the approaches to spatio-temporal chaos are essentially based on the extension of concepts and tools developed in the context of low dimensional systems. This explains the introduction of "densities" for quantities such as the Lyapunov exponents, the Kolmogorov-Sinai entropy or the attractor dimensions [58]. This kind of approach is in principle based on the idea that, due to the fast spatio-temporal decorrelation induced by the dynamics (i.e. $\xi \ll L$), one can consider the whole system as composed by many (weakly coupled) low dimensional systems [6, 52]. Even if such conjecture is sometimes justified and has led to many good results, it is often too naive.

From the conceptual viewpoint, one of the most important problems are the existence of a well defined *thermodynamic limit* behavior for very large systems and the under-

[9] In the following we often speak interchangely of spatio-temporal chaos and high dimensional chaos, indeed (as seen) the distinction is largely arbitrary.

standing of relations between the statistical description and the dynamical behavior in phase-space. In any case the existence of the extensivity property for the chaotic indicators (i.e. of a well defined thermodynamic limit) can be consider as the first important step towards a statistical-mechanics description of high dimensional chaos [58, 59]. In the next Section we discuss this issue in a prototypical model for spatio-temporal chaos: the *Coupled Map Lattices* (CML) [60, 61].

1.2.1 Coupled Map Lattices and the Thermodynamic limit in extended systems

Spatio-temporal phenomena usually arise in the context of PDE:

$$\frac{\partial \mathbf{v}}{\partial t} = \mathbf{G}(\mathbf{v}, \nabla \mathbf{v}, \ldots)\,, \tag{1.37}$$

a very popular example is the Navier-Stokes equations [53] which we will examine in the next Section. Another important example is the PDE usually employed in modeling the *reaction-diffusion* mechanisms occurring in some chemical reactions [52, 62]:

$$\frac{\partial \mathbf{C}}{\partial t} = \hat{\mathbf{D}}\nabla^2 \mathbf{C} + \mathbf{F}(\mathbf{C})\,, \tag{1.38}$$

where $\mathbf{C}(\mathbf{x}, t) = \{c_1(\mathbf{x}, t), c_2(\mathbf{x}, t), \ldots\}$ denotes the local concentrations of some reagents, $\hat{\mathbf{D}}$ the diffusion tensor and $\mathbf{F}(\mathbf{C})$ is a non linear function representing the kinetics of the reaction.

However, there exists other classes of systems, possessing the basic phenomenology of spatio-temporal chaos, which are more convenient from a computational point of view such as *Cellular Automata* (CA) [18, 63] and *Coupled Map Lattices* (CML) [60]. Since CA have discrete time, space and phase-space they present some conceptual problems when one wants to study them as models of spatio-temporal chaos[10] so for the moment we only study CMLs.

CMLs are maps defined on the sites of a discrete lattice interacting each other, the most popular and studied example is the diffusively coupled CML, which for a 1-dimensional lattice can be written as [60]:

$$\mathbf{u}_i(t+1) = (1-\epsilon)\mathbf{f}_a[\mathbf{u}_i(t)] + \frac{\epsilon}{2}\left(\mathbf{f}_a[\mathbf{u}_{i+1}(t)] + \mathbf{f}_a[\mathbf{u}_{i-1}(t)]\right)\,, \tag{1.39}$$

[10] Due to the discreteness of the phase-space the number of possible states is finite, as a consequence the motion cannot be considered chaotic in the sense discussed in the previous Sections [6, 18]. Nowadays there is not yet a well accepted definition of chaos in such systems so we do not discuss this problem in details. In Section 4.2.3 we discuss this points comparing CA with a certain class of CML.

where $i = 1, L$, being L the lattice size, $\mathbf{u} \in \Re^n$ is the state variable which depends one the site and time, ϵ measures the strength of the coupling. $\mathbf{f}_a \in \Re^n \to \Re^n$ is a non linear map driving the local dynamics and depending on a control parameter a which quantifies the degree of non linearity. Usually, for one dimensional state variables ($n = 1$), one study coupled logistic maps, $f_a(x) = ax(1-x)$ or tent maps, $f_a(x) = a|1/2 - |x - 1/2||$. In Fig. 1.2 we show the typical space-time behavior of a 1-dimensional CML in the regime of fully developed spatio-temporal chaos. Of course, the extension in more than one-

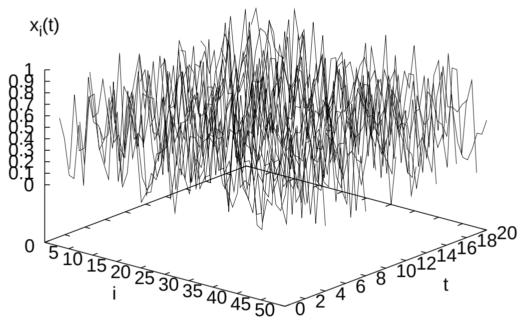

Figure 1.2: The plot shows 20 iterates of 50 couple logistic maps with $a = 4$ and $\epsilon = 1/3$. For this choice of the parameters one observes a well developed spatio-temporal chaotic regime.

dimension is straightforward: one can define a d-dimensional lattice or, for instance, a mean field version of (1.39) (see Sect. 4.1). The coupling in Eq. (1.39) is chosen as the discrete approximation of the Laplacian, however it can be misleading to consider a CML simply as the discrete approximation of PDE. Indeed usually the local map $\mathbf{f}_a$ is chaotic so that chaos in CML is the non trivial result of many interacting chaotic sub-systems. Therefore, the correspondence between the instability mechanisms in the two type of models is usually rather obscure [52].

However, the spatio-temporal phenomenology of CMLs is so wide to be considered a good school to learn much of the spatio-temporal chaotic regime. The hope, often well posed, is to extend the results obtained on such systems to more realistic and difficult systems.

Thermodynamic limit in extended systems

The characteristic Lyapunov exponents (Sect. 1.1.1) as well as fractal dimensions we have defined in the context of low dimensional systems can be defined (and, at least the CLE, computed) also for CMLs. Indeed, if $L < \infty$ the CMLs have finite dimensional phase space and the above quantities are well defined. However, a fundamental question can be raised on the properties of the Lyapunov exponents: the existence of a good thermodynamic limit for the Lyapunov spectrum $\{\lambda_i(L)\}_{i=1,L}$ which obviously depends on the system size L[11]. In other words, one can wonder about the existence of the following limit [58]

$$\lim_{L\to\infty} \lambda\left(\frac{i}{L}\right) = \Lambda(x)\,, \tag{1.40}$$

where x is a continuous index (i.e. $x = i/L$ in the limit $L \to \infty$) and $\Lambda(x)$ is a non increasing function of x with support in $[0, 1]$ (indeed we suppose the Lyapunov exponents to be ordered in a decreasing way). Of course if such limit does not exist the idea to make a statistical mechanics of spatio-temporal chaos would be hopeless: in absence of a good $L \to \infty$ behavior the phenomenology of these systems would depend on L. $\Lambda(x)$ can be viewed as a *Lyapunov exponents density* (see Fig. 1.3). Once proved the existence of a

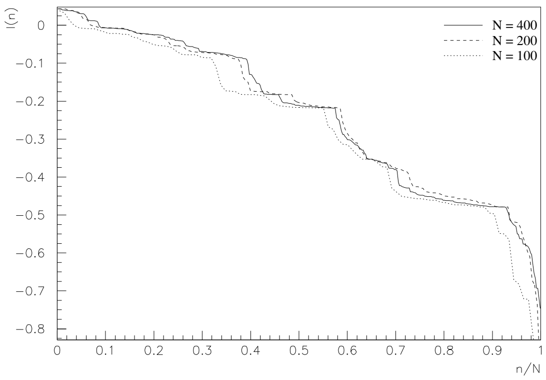

Figure 1.3: $\Lambda(i/N)$ at increasing N for a CML of coupled logistic maps. For large N one can see the development of a well defined Lyapunov density.

Lyapunov density as $L \to \infty$, one can also try to extend some results obtained for low dimensional systems, namely the Kaplan-Yorke conjecture (1.25) and the Pesin equality (1.34), for estimating the KS-entropy and the attractor dimension of such systems, which

[11] here we consider 1-dimensional in space systems but the discussion can be extended to more than one dimension.

are expected to be extensive as well as the Lyapunov exponents [11, 59]. Therefore one can expect the *entropy density* to be given as

$$\mathcal{H}_{KS} = \int_0^1 dx \Lambda(x) \Theta(x) \,, \tag{1.41}$$

being $\Theta(x)$ the step function. Where the entropy density is nothing but

$$\mathcal{H}_{KS} = \lim_{L\to\infty} \frac{h_{KS}}{L} \,,$$

indeed due to extensivity $h_{KS} \propto L$. In the same way one can suppose the existence of a *dimension density* $\mathcal{D}_F$, that is to say a density of active degrees of freedom, i.e.

$$\mathcal{D}_F = \lim_{L\to\infty} \frac{D_F}{L}$$

which by the Kaplan-Yorke [50] (Sect. 1.1.2) conjecture for densities should be given by [11]:

$$\int_0^{\mathcal{D}_F} dx \Lambda(x) = 0 \,. \tag{1.42}$$

These definitions on the density of CLE, entropy and dimension are analogous to the introductions of "intensive" quantities from "extensive" quantities in thermodynamics.

Unfortunately the existence of a good thermodynamic limit has been proved only for very particular CMLs [59], e.g. for diffusively coupled shift maps, $f(x) = \{\beta x \mod 1\}$, $\Lambda(x)$ can be analytically computed

$$\Lambda(x) = \ln\left[\beta\left(1 + \epsilon \cos\left(2\pi x\right)\right)\right] \,.$$

More recently Eckmann and Collet [64] have proved the existence of a density of degrees of freedom in the complex Ginzburg-Landau equation. See also Refs. [11, 59] and references therein for a discussion on such problems.

It is worth noting that the existence of a thermodynamic limit in extended systems poses also many problems when one adopts a time series analysis point of view [11]. In low dimensional systems the embedding theorem [65] ensures that from the analysis of a local observable one can, in principle, reconstruct the phase space and measure the attractor dimension and the Lyapunov exponents. On the other hand in high dimensional systems (where the attractor dimension is really huge) many doubts on the possibility to perform similar analysis may be raised [65, 66]. Without entering into a detailed discussion let us say that when one only looks at a local observable (e.g. the evolution of one site, $x_i(t)$, in a CML) the huge number of unobserved degrees of freedom may play a role very similar to dynamical noise on deterministic equations [11] (see also Ref. [67] and references therein).

As far as space-time continuous systems (where the phase-space is truly infinite dimensional) are concerned, the problem of the Lyapunov exponents is even more difficult than CMLs. In such a case other difficulties (beyond those already cited) arise, indeed in infinite dimensional systems the Lyapunov exponents may depend on the norm which is used [40]. In particular, it could be cases in which also the sign of the Lyapunov exponent may depend on the norm, that is to say that also the definition of chaotic behavior may be unclear [68].

1.2.2 Fully Developed Turbulence

Perhaps the most important example of high dimensional chaotic (both in time and space) system is *three dimensional fully developed turbulence*[12] in fluids. As for the notion of spatio-temporal chaos, there is not an unique well accepted definition of turbulence. So that we avoid to give a definition and go to describe its main features. The equations ruling the evolution of the velocity field in a fluid are the Navier-Stokes equations:

$$\begin{aligned} \partial_t \mathbf{u} + (\mathbf{u}\cdot\nabla)\mathbf{u} &= -\nabla P + \nu\nabla^2\mathbf{u} + \mathbf{F} \\ \nabla\mathbf{u} &= 0 \\ + \,\mathrm{boundary} - \mathrm{conditions} & \end{aligned} \tag{1.43}$$

where $\mathbf{u}$ is the velocity field, P the pressure and ν the kinematic viscosity. F represents an external force which ensures that a stationary state can be attained [6, 53]. The second equation is the incompressibility constraint.

Coming back to the three characteristic lengths defined in Sect. 1.2, in turbulence we have that ℓ_E, i.e. the energy injection scale, is roughly given by the characteristic length scale of the support of the forcing $\mathbf{F}$ (or, more generally, by the geometry imposed by the boundary conditions). Then due to the non linear term in Eq. (1.43), we have a cascade process which transports the energy from ℓ_E through different length scales ($\ell < \ell_E$) down to the dissipative length scale ℓ_D, named the Kolmogorov scale. This is the famous cascade picture *à la* Richardson [53].

[12] Here we present the general features of the problem, we come back to turbulence with further details in Chapter 3.

The control parameter of the process is the Reynolds number:

$$Re = \frac{\ell_E V_E}{\nu}, \tag{1.44}$$

where V_E is the typical velocity at scale ℓ_E. As soon as Re is much greater than a critical value, which depends on the system, one has the so-called fully developed turbulence turbulence (strictly speaking fully developed turbulence corresponds to the limit $Re \to \infty$). For these values of the Reynolds number the velocity field appears very irregular both in its temporal evolution and in its spatial development. In particular, a lot of different scales becomes excited: the *inertial range* ($\ell_D \ll \ell \ll \ell_E$).

Kolmogorov (1941) through dimensional arguments predicted that the energy cascade process leads to a self-similar velocity field (in the limit $Re \to \infty$) the signature of which is the scaling behavior of the moments of the velocity differences [53], i.e.

$$\langle (\mathbf{u}(\mathbf{x} + \ell) - \mathbf{u}(\mathbf{x})^p \rangle \sim \left(\frac{\ell}{\ell_E} \right)^{\zeta_p}, \tag{1.45}$$

where the average is an ensemble average. In particular, Kolmogorov predicted $\zeta_p = p/3$, actually there are small deviation from this value due to *intermittency* [53]. Most of the current studies on turbulence have as final goal the comprehension of intermittency [6, 53]. However for the moment we ignore intermittency corrections.

A consequence of the Kolmogorov theory is that, as Re increases, the dissipative scale decreases as

$$\ell_D \sim \ell_E Re^{-3/4},$$

from this formula we can understand that high dimensional chaos develops in turbulence essentially at fixed L (system size) but at increasing Re. Hence all the behaviors we have described for spatio-temporal chaos as $L \to \infty$ are here expected in the limit of $Re \to \infty$ [52]. In particular, we expect that a Lyapunov exponent density develops in this limit [58]. Seemingly we expect the number of active degrees of freedom to increase with Re, indeed in the framework of Kolmogorov theory one expects that the number of degrees of freedom (ndf) increases as

$$\left(\frac{L}{\ell_D} \right)^3 \propto Re^{9/4}.$$

Indeed the huge ndf is a fundamental limitation in direct numerical simulation of turbulence [24, 69].

Stating the existence of a Lyapunov exponents density is an hard task already in the context of CMLs, but in turbulence it is completely beyond our current possibilities. Indeed, due to the huge number of degrees of freedom and to the non linear terms of the Navier-Stokes equation it is impossible a numerical or analytical verification of such a conjecture. Recently it was introduced a class of very simplified models, the so-called *Shell Models* [6, 70], which share many of the features of turbulence for which there was a numerical evidence that such thermodynamic limit can be attained [70]. The equations defining such model are:

$$\frac{du_n}{dt} = i\left(k_{n+1}u_{n+1}u_{n+2} - \frac{1}{2}k_n u_{n-1}u_{n+1} + \frac{1}{2}k_{n-1}u_{n-2}u_{n-1}\right)^* - \nu k_n^2 u_n + f_n\,, \qquad (1.46)$$

where $k_n = k_0 2^n$ represents a division in octaves of k-space, ν is kinematic viscosity and f_n is a forcing term which is restricted only to the first two shells (in order to mimic large scale energy injection); u_n are complex variables which play the role of velocity differences on scale $1/k_n$.

Without going in detail, we recall that the Shell Model (1.46) displays an energy cascade *à la* Richardson from large scales (small n) to dissipative scales ($n \sim N$) with a statistical stationary energy flux, and it is possible to develop for them a theory very similar to that developed for turbulence. For further details we refer to the recent book [6], where there are discussed the important steps towards the the development of a dynamical systems approach to turbulence obtained by studying such models.

We believe that one of the most relevant properties of turbulence, from a dynamical system point of view, is that it develops spatio-temporal chaos. At variance with other already described behaviors of spatio-temporal chaotic systems, in turbulence we have the peculiar characteristics that many (spatial) scales become active and each scale has its own typical evolution time [7, 9, 71]. Since the fastest evolving scales are associated with the dissipative scales, one intuitively expects that the maximum Lyapunov exponent is associated to these dissipative scales [27], i.e.

$$\lambda_{max} \propto Re^{1/2}$$

(see also Chapter 3). However, despite its theoretical relevance, it is clear that the mere Lyapunov analysis is too poor for a good characterization of turbulence and its complex spatial developments through different scales. We shall come back on this point in the following where we discuss the properties of systems with many characteristic scales of motion.

Chapter 2

Characterization of predictability beyond the Lyapunov Exponent

In the previous Chapter we have seen how and to what extent it is possible to characterize geometric and dynamical properties of low dimensional systems in terms of Lyapunov exponents, fractal dimensions and entropies, and the way in which these quantities generalize to Lyapunov, dimension and entropy densities in high dimensional systems.

Here we address the problem of the dynamics of perturbations in such systems. This problem is obviously connected to the *predictability problem*. Indeed the sensitivity to initial conditions (perturbations) severely limits our ability to make prediction on the evolution of these systems. In particular, we shall see that the usual identification of the *predictability time* (i.e. the maximum time at which one can forecast the state of a system) with the inverse of the Lyapunov exponent is too naive. Indeed the huge phenomenology of spatio-temporal chaotic systems together with the necessity to determine the limits of predictability in realistic systems require more sophisticated indicators than the Lyapunov exponents.

We discuss such questions with a number of examples in which the limits of the standard tools clearly appear. In the last two Sections we introduce some indicators which have been recently developed for characterizing unpredictable behaviors missed by the usual analysis. In particular, we discuss in details the Finite Size Lyapunov Exponent (FSLE), which is a generalization of the usual Lyapunov exponent to finite (non-infinitesimal) perturbations. We also discuss the relations between the FSLE and the ε-entropy.

2.1 Predictability in dynamical systems

From a conceptual point of view, the study of irregular behaviors in deterministic systems has represented an important conceptual step in our way to conceive the idea of "prediction" in natural phenomena. The ability to predict has surely been the single most important qualifier of what constitutes scientific knowledge. Indeed, the famous statement of Laplace (1814) [22] that an *intelligent being* with complete knowledge of the present and the mathematical control of the laws of *Nature* will know the future for all time, assumes that the future is completely predicated by the past, and therefore the perfect prediction would in principle be possible. A mathematical reformulation of this statement is that *Nature* is ultimately described by differential equations, and if one knows them and how to solve them, one knows all there is to know about the world.

However, Laplacian determinism is always conditioned by the fact that in the real world initial conditions (or the finer details of the evolution laws) can never be known with arbitrary accuracy. Now it is well evident that even an infinitesimally small uncertainty in presence of deterministic chaos amplifies exponentially severely limiting our predictability. Moreover, by the recognition of the ubiquity of chaos it is realized that many systems can only be predicted for a finite time, and since prediction of the future state of a system is problem with an obvious practical interest in many fields ranging from astronomy to geophysics arriving to economics, it deserves a detailed discussion.

The simplest approach to the *predictability problem* in deterministic chaotic systems can be described as follows. Due to the sensitive dependence on initial conditions, one has that, typically, an uncertainty on the present state of a system, $\delta\mathbf{x}(0)$, increases as

$$||\delta\mathbf{x}(t)|| \simeq ||\delta\mathbf{x}(0)|| e^{\lambda_{max} t} , \tag{2.1}$$

where λ_{max} is the maximum Lyapunov exponent of the system (see Sect. 1.1.1). As a consequence of (2.1), an observer will consider the system predictable up to the time, T_p, at which the uncertainty reaches a certain (preassigned) tolerance Δ. Therefore if the initial uncertainty is $||\delta\mathbf{x}(0)|| = \delta_0$ the *predictability time* is

$$T_p \sim \frac{1}{\lambda} \ln\left(\frac{\Delta}{\delta_0}\right) . \tag{2.2}$$

Eq. (2.2) tells us that the predictability time is, essentially, given by the inverse of the Lyapunov exponent, since the dependence on the precision of the measure and the tolerance is (only logarithmic) so weak to be neglected, at least in first approximation.

However, the identification of the predictability time simply with the inverse of Lyapunov exponent is too naive. Indeed, Eq. (2.2) only holds for very simple low dimensional systems and, in order to apply the linear analysis (which is necessary to define the CLE spectrum), only for both δ_0 and Δ infinitesimal. As soon as one considers less simple low dimensional systems and, more dramatically, enough high dimensional systems or more realistic uncertainties (which are usually not infinitesimal) the relation (2.2) becomes unsatisfactory and often wrong. In fact, already in the framework of infinitesimal perturbations and low dimensional systems, (2.2) takes into account only the typical behavior and in presence of intermittency (fluctuation of the growth rates) is not sufficient [23]. This inadequacy becomes dramatically evident when the spatial aspects are important as well as the temporal ones, the only considered by the above treatment.

Moreover, when one leaves the realm of infinitesimal perturbations to study the non linear regime of perturbations growth the Lyapunov analysis can lead to apparent paradoxes. Just to give an example, atmosphere is expected to have a very large positive Lyapunov exponents ($O(1\, s^{-1})$), due to the fast evolution of small scale turbulence (always present), but it is of common experience that some atmospheric phenomena are predictable for times ($O(1\, day)$) much longer than the inverse of the Lyapunov exponent. This can be explained, as we will see, only taking into account the large scale-separation existing between the two regimes (see Chapter 3).

In the remaining part of this Section we list some complex (unpredictable) behaviors arising both in low and high dimensional systems which cannot be characterized only in terms of Lyapunov exponents. In the second part of the Chapter, we describe and discuss some recently introduced indicators which have been demonstrated more suitable to understand and characterize some of such complex behaviors. In particular, in Sects. 2.3 and 2.4, we examine the case of non infinitesimal perturbations.

-A- Intermittency and fluctuations of the predictability time

The Lyapunov exponent λ_{max} (1.8) is a global quantity: it measures the average exponential rate of divergence of nearby trajectories. In general there exist finite-time fluctuations of this rate and it is possible to define an "instantaneous" rate, called *effective* Lyapunov exponent, $\gamma_t(\tau)$ as [23, 24, 43]:

$$\gamma_t(\tau) = \frac{1}{\tau} \ln(R_\tau(t)) = \frac{1}{\tau} \ln \left(\frac{||\delta \mathbf{x}(t+\tau)||}{||\delta \mathbf{x}(\tau)||} \right) , \tag{2.3}$$

where $R_\tau(t)$ is the response function (1.17). For finite τ, $\gamma_t(\tau)$ depends on the particular point of the trajectory (it measure the local rate of divergence), and averaging along the trajectory one has $< \gamma_t(\tau) >_t = \lambda_{max}$. At the fluctuations of $\gamma_t(\tau)$ correspond fluctuations of the predictability time, T.

If intermittency is weak the probability distribution function of $\gamma_t(\tau)$ is peaked around λ_{max} and the average predictability time (2.2) is meaningful. Otherwise, one has to consider the PDF of the predictability time. To quantify the degree of intermittency one can introduce the following parameter [24]:

$$\mu = \lim_{t\to\infty} \frac{1}{t} \left(\left\langle \ln^2(R_\tau(t)) \right\rangle - \langle \ln(R_\tau(t)) \rangle^2 \right) . \tag{2.4}$$

When $\mu/\lambda \gg 1$ one has strong intermittency and the PDF of the predictability time has long exponential tails, while for $\mu/\lambda \leq 1$ it is peaked around (2.2) [23, 25, 43].

It is possible to understand such features by using a very simple stochastic model[1]. As a first (rough) approximation one can mimic the perturbation evolution as [23]:

$$\ln \left(\frac{||\delta \mathbf{x}(t)||}{||\delta \mathbf{x}(0)||} \right) = \lambda t + \sqrt{\mu} w(t) , \tag{2.5}$$

where $w(t)$ is a zero mean Wiener process [44] with $w(0) = 0$ and $\langle w(t)w(t')\rangle = \min(t, t')$. Within this approximation the evaluation of the predictability time is reduced to a first exit time problem [44], i.e. T is the largest time such that: $\sqrt{\mu}w(t) \leq \ln(\Delta/\delta_0) - \lambda t$. The solution of this problem [72] gives the following PDF for T:

$$P(T) = \frac{\ln(\Delta/\delta_0)}{\sqrt{2\pi\mu T^3}} \exp \left[-\frac{(\lambda T - \ln(\Delta/\delta_0))^2}{2\mu T} \right] . \tag{2.6}$$

By studying the above relation one has: for weak intermittency ($\mu/\lambda \leq 1$), $P(T)$ is almost Gaussian and the average value is close to the most probable value $T_p \approx 1/\lambda \ln(\Delta/\delta_0)$ which is (2.2); for strong intermittency ($\mu/\lambda \gg 1$) the PDF develops long exponential tails. So that the *effective* predictability time is longer than (2.2) due to the effects of the "laminar" periods which characterize the dynamics of intermittent systems [24, 25].

-B- Unpredictability without chaos

Usually unpredictability in deterministic systems is identified with the presence of at least one positive Lyapunov exponent, from which (2.2). However, there exist systems exhibiting unpredictable behaviors without chaos (i.e. with $\lambda_{max} < 0$). Remaining in

[1]For an exhaustive review on the treatment of intermittency in chaotic systems and turbulence see Ref. [24] where the characterization in terms of Generalized Lyapunov exponents (1.16) is presented and connections with the multifractal properties of chaotic attractors are highlighted.

the framework of low dimension systems, one can have: systems with *fractal basins of attraction* [3], *transient chaotic* systems [73, 74] and systems with *strange non chaotic attractors* [75].

In the first class it falls systems with trivial attractors (fixed points) but with complex basin of attraction, i.e.: the set of points that asymptotically reach a given fixed point is fractal, as a consequence very close trajectories may attain different asymptotic states, leading to unpredictability. In such systems unpredictability has its source in the geometrical complexity instead of in the dynamical instabilities (information on the future evolution is stored in the complexity of the geometry of the basins of attraction).

As far as transient chaotic regimes are concerned, one has that there exist systems with regular asymptotic behavior but with very long disordered (chaotic) transient dynamics, so long that the only observable regime is often the transient one[2]. Among the many chaotic transient phenomena we cite the *chaotic scattering* phenomenon [74].

-C- Localized chaos in spatially extended systems

As soon as one considers spatially distributed systems, the spatial developments of the dynamics compels us to take into account other phenomena. Among these an important example is the emergence of *localized chaos* (frozen random patterns, see Fig. 2.1) [61]. Indeed in space-time systems, one can have strongly localized regions of chaotic character (sometimes, slowly moving in space [61]) embedded in an almost quiescent space. An extreme limit of such behavior is *spatio-temporal intermittency*[3] where one can have both laminar and turbulent burst in space-time [61, 76] (see Fig. 2.1).

As far as localized chaos is concerned, one has, e.g. in CMLs of logistic maps [61], that the Lyapunov spectrum is characterized by a small number of positive Lyapunov exponents, proportional to the number of chaotic regions. However, the Lyapunov spectrum does not give any information about the spatial distribution of such regions (see Fig. 2.1). This information can be obtained by looking at the dynamics of the Lyapunov vectors (which identify the directions associated to the Lyapunov exponents). The Lyapunov vectors are defined as the eigen-vector for the long times product of the Jacobian matrix (see Sect. 1.1.1). In most cases one has that the Lyapunov vectors associated to positive

[2]In the following we give an example of such systems in the context of high dimensional systems where transient times may grow with the systems size, so that in the thermodynamic limit are the only observable regimes [19, 20]

[3]However, such last regime is at the transition between fully developed spatio-temporal chaos and ordered or almost ordered patterns. Often it is studied in the context of percolation phenomena [76]. But we do not want to enter into details.

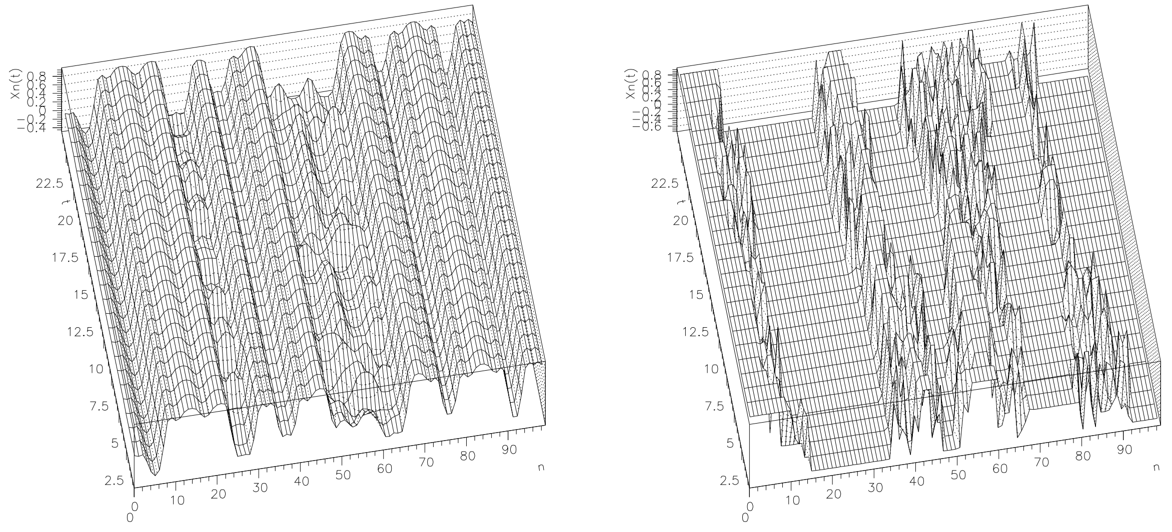

Figure 2.1: (a)Space time plot of a CML 1.39 of logistic map with $a = 1.5$ and $\epsilon = 0.4$, in such a case one has strongly localized chaotic regions. (b) the same of Fig. (a) but for $a = 1.752$ and $\epsilon = 0.001$ where one observes spatio-temporal intermittency.

Lyapunov exponents are localized in space [61]. As we shall see this problem is connected to Anderson localization of wave-functions in disordered materials [77, 78] and it has lead to the introduction of the "spatial" Lyapunov exponent [12] (see also Sect. 2.2).

-D- Unpredictability of the attractor

Another important example of unpredictability which cannot be characterized in terms of the Lyapunov exponents is the difficulty to predict, in systems which many possible (strange) attractors, on which attractor the motion settles asymptotically. This problem is indeed very difficult to address: in high dimensional systems usually there exists a huge number of possible attractors [18, 61], and there is not any systematic way (apart from very particular systems) to understand (and control) on which of them the motion asymptotically takes place. This problem is really very poorly understood in spite of is importance: the understanding of *climate change* is indeed connected with this problem.

-E- Information propagation in distributed systems

As in low dimensional systems an uncertainty on the insignificant digits (specifying the initial conditions of two nearby trajectories) flows in *bit space* reaching the significant ones [4]. The same phenomenon appears in spatially distributed systems. In the latter, however, one has also a flow of information in *real space* due to spatial coupling [11]. This features can be understood, e.g., looking at the evolution of localized perturbations in CMLs [11, 34] (see Sect. 4.2). The temporal growth of localized perturbations is accounted by the Lyapunov exponents but their spreading in space needs for other indicators to be characterized, e.g. one can introduce the velocity of errors spreading [11, 34]. In order to account such problem in the following we introduce the Comoving Lyapunov Exponents, and, in Sect. 4.2, we show how also this last indicator must be generalized in some cases [34, 79].

-F- Convective chaos versus Absolute chaos in open flows

In many situations, such as pipe flows, there is a privileged direction: the mean flow. In order to study such systems (*flow systems*), it was introduced other classes of CMLs, one possibility is the one-way coupling CMLs [80, 61, 21]:

$$x_i(t+1) = (1-\epsilon) f_a(x_i(t)) + \epsilon f_a(x_{i-1}(t)) \,, \tag{2.7}$$

where the boundary conditions can be chosen in different ways (e.g. periodic or open). Of course there exist also PDE describing such systems, a relevant example is the time dependent Complex Ginzburg-Landau equation [28], also ODE have been used to study such systems [81].

In such systems a number of new phenomena appear. Let us mention that beyond the phenomenology of spatio-temporal systems from ordered motion up to fully developed spatio-temporal chaos, one can also have regular temporal evolution but chaos in space (*spatial chaos*) or *convective* chaos opposite to *absolute* chaos. The spatial chaos is a novel discovery of such systems [61], it is obvious that the usual CLE are inadequate in such a case. A more detailed discussion is needed for the problem of *convective* and *absolute* chaos [21, 61].

One usually speaks about absolute chaos when an initially spatially localized perturbation grows at the same place where it was imposed. The perturbation spreads only due to diffusion. By convective chaos [61, 80] one designs the case in which a perturbation, initially spatially localized, starts to move along the flow growing in sites different from that where it is seeded (see Fig. 2.2). During its motion the perturbation may leave the system (free boundary condition) so that after a certain period of time the system becomes regular (i.e. $\lambda < 0$), however such time is usually proportional to the system size: it is a sort of long chaotic transient. It is well evident that such systems cannot be fully characterized by their Lyapunov spectrum.

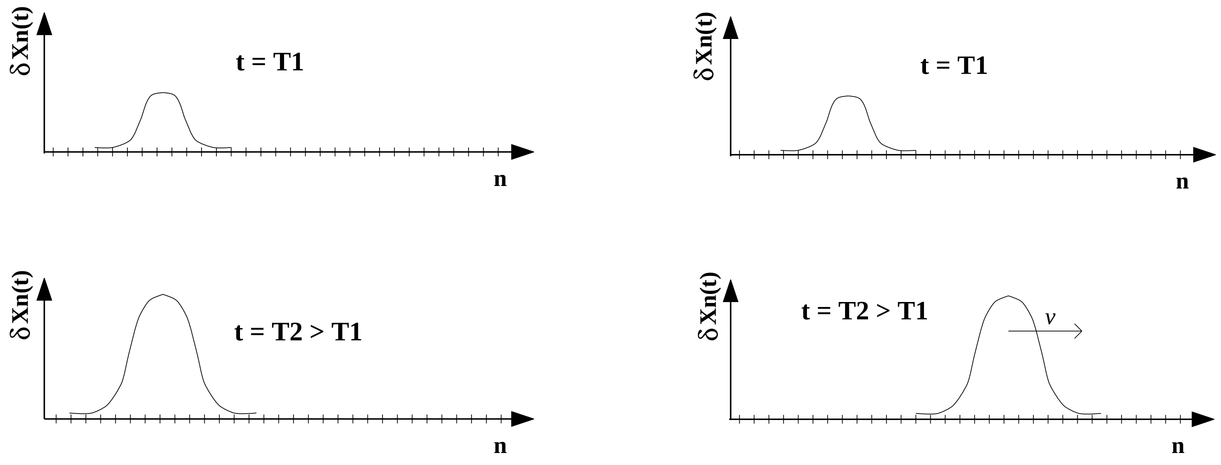

Figure 2.2: This plot show the main differences between absolute chaos (on the left) and convective chaos (on the right). A perturbation localized in space at time $T1$ grows in time ($T2$) in the same place where it is seeded in the case of absolute chaos and speads due to the coupling with neighbor sites. In the convective case the perturbation grows on sites different from where it is initialized.

In addition, in open flows one can also have another kind of sensitivity: if one forces at each time step the system (say) on the first site from which the perturbation starts to move and grow at increasing the distance from the boundary, there could be a *sensitivity to the boundary conditions* [21, 82].

-G- "Chaos" in stable coupled map lattices

In 1988 Crutchfield and Kaneko [19] found that CMLs of stable maps (i.e. with $\lambda_{max} < 0$) may give rise to an unpredictable dynamics on times which grows exponentially with the system size [20] even if asymptotically the motion settles onto a regular attractor. In addition, in such CML, even the maximum Lyapunov exponent computed during the disordered transient has found to be negative [20]. Such phenomenon raised an interesting conceptual question signified by the title of the work of Crutchfield and Kaneko [19]: "Are attractors relevant to Turbulence?". That is to say that, due to the fact that in the thermodynamic limit such systems leads to a disordered (unpredictable) asymptotic motion, the statistical hypothesis underlining the strange attractor explanation of fluid turbulence [83], and other systems, can be unnecessary.

Apart from this interesting new point of view on deterministic irregular phenomena, for us the interesting point is that many behaviors displayed by such systems cannot be caught by simply studying their Lyapunov spectrum. We shall discuss this point in the context of the study of the non linear regime of these maps (see Sect. 2.2.2).

-H- Large scale predictability in systems with many different scales

In nature many interesting problems are connected with turbulence, e.g.: turbulence is always present in atmosphere where we live. As seen in Sect. 1.2.2 one relevant property of turbulence is the presence of many characteristic length scales and times [7, 71]. In such situations it is very important to consider non infinitesimal perturbations (δ), or non infinitesimal tolerance (Δ), so that our ability to predict the future, quantified by the predictability time, is determined by the detailed non linear mechanisms of transfer of errors through the different scales present in the system. It is evident that in this case the linear analysis is useless: the predictability time may have no relation with λ_{max} [7, 36, 84].

In order to address such problems we discuss in the following the use of the Finite Size Lyapunov exponent which extends the usual Lyapunov analysis to the non linear regime of perturbations evolution [9, 10].

In certain systems the presence of many (spatial and temporal) scales is intrinsically contained in the evolution laws (e.g. turbulence). However, there exist also cases in which it is dynamically generated [32, 33]. In Sect. 4.1, we examine the motion of a *macroscopic* variable in a Globally Coupled Maps system, defined by:

$$x_n(t+1) = (1-\epsilon) f_a(x_n(t)) + \frac{\epsilon}{N} \sum_{i=1}^{N} f_a(x_i(t)) \,. \tag{2.8}$$

For any finite N the motion of the center of mass, $m(t) = 1/N \sum x_i(t)$, may be chaotic but with a typical time longer than the evolution time of the *microscopic* components, which is roughly given by the inverse of the Lyapunov exponent of (2.8). Therefore, if one is interested in characterizing the *macroscopic* motion he has to go beyond the Lyapunov analysis (see Sect. 4.1).

-I- Dispersion properties in fluids due to chaotic advection

An interesting field for the application of dynamical systems theory is the advection of particles in a fluid flow through the phenomenon of *Chaotic Advection* [85, 86, 87]. In this field one has to distinguish two situation: the velocity field is chaotic (advection in presence of Eulerian chaos), or the velocity field is periodic (regular) [6]. Intuitively one expects that the behavior of passive tracers reflects that one of the velocity field. Actually, the situation is more complex: one can have chaotic Lagrangian motion in absence of Eulerian chaos or, sometimes, (even if less frequently) the opposite situation [87].

However, such a problem is interesting also for other reasons. In particular, with the CLE one can understand that for infinitesimal perturbations (here perturbations are simple two or more nearby tracers) the growth is exponential. But, usually, one is interested in characterizing the dispersion properties, which are related to the case in which there if a finite separation between particles. In such a regime the standard analysis is to examine the relative (two particles) or absolute (one particles) dispersion properties in terms of diffusion coefficients. However, also such analysis is often unsatisfactory [88, 89]. From a dynamical systems point of view, the dispersion properties are related to the non linear regime of perturbations evolution. In Chapter 5 we will see the way one can study such a problem by means of the Finite Size Lyapunov Exponent [88], in particular, we also discuss its computation in experimental data analysis [90].

2.2 Lyapunov exponents for "generalized" perturbations in extended systems

In extended systems the spatial dependence of the state variable requires to consider not only the instability causing the divergence of nearby trajectories but also propagation phenomena [28] and spatial inhomogeneities [12, 52, 82]. The complete characterization of generic perturbations requires the evaluation of both its *temporal* and *spatial* growth rates as a complementary measure of its instability properties [12, 21]. In recent years there were developed various tools for achieving this scope. Among the many we cite the introduction of the *local* Lyapunov exponent [82], the *comoving* Lyapunov exponent [28], the *spatial* and *temporal* Lyapunov exponents [12, 78, 91]. All these indicators account for the instability properties of generic (space-time) perturbations. However not all of them are independent [12] as we shall show in the following. In the next Sections we mainly discuss the comoving Lyapunov exponent and the *spatial* and *temporal* Lyapunov exponents. For sake of completeness we cite the review article of Kaneko [61] in which other possible indicators are discussed and the paper of Pikovsky [82] where the *local* Lyapunov exponent is introduced and its relation with other indicators is discussed.

Let us start now with the notion of *spatial* and *temporal* Lyapunov exponents, we mainly follow Ref. [12].

2.2.1 "Spatial" and "temporal" Lyapunov exponents

Let us consider a generic CML, e.g.:

$$x_i(t+1) = f_a\left((1-\epsilon)x_i(t) + \frac{\epsilon}{2}(x_{i-1}(t) + x_{i+1}(t))\right) \tag{2.9}$$

with t, i being respectively space and time indices, $i = 1, L$ where L is the lattice size and ϵ measures the coupling strength[4]. When one wants to describe the evolution of a perturbation involving both space and time (i.e. the most generic perturbation), one has to consider both the temporal and the spatial growth rates. The former coincides with the evaluation of the standard CLE, even if more general perturbations (e.g. exponentially shaped in space) can be considered [34, 91]. The latter is particularly useful for highlighting localization properties of Lyapunov vectors and it has lead to the introduction of the *spatial* Lyapunov exponent.

A generalized version of the CLE spectrum can be obtained assuming perturbation with a given spatial shape. In Ref. [91] it was considered an exponentially shaped profile, i.e. $\delta x_i(t) = \Phi_i(t)e^{\eta i}$, which has lead to the introduction of the so called *temporal* (or *specific*) Lyapunov exponents (note that $\eta = 0$ corresponds to the usual CLE). The evolution in tangent space of $\Phi_i(t)$ is given by

$$\Phi_i(t) = m_i(t)\left[\frac{\epsilon}{2}e^{-\eta}\Phi_{i-1}(t) + (1-\epsilon)\Phi_i(t) + \frac{\epsilon}{2}e^{\eta}\Phi_{i+1}(t)\right], \tag{2.10}$$

where $m_i(t) = f'[(1-\epsilon)x_i(n) + \epsilon/2(x_{i-1}(t) + x_{i+1}(t))]$ is the local multiplier and periodic boundary conditions are assumed. Then by using standard algorithm [41] one can compute the complete Lyapunov spectrum $\lambda_i(\eta)$ with $i = 1, L$ for each η, these are the *temporal* or *specific* Lyapunov exponents. It is also shown that in the thermodynamic limit a density of such exponents exists [12], i.e.

$$\Lambda(\eta, n_\lambda) = \lambda_j(\eta) \qquad n_\lambda = \frac{j}{L}. \tag{2.11}$$

The use of such exponents will clearly appear when we study the problem of the propagation of localized perturbations (see Sect. 4.2).

In the same spirit, in order to investigate the properties of the (temporal) Lyapunov vectors it was introduced the *spatial* Lyapunov exponents [78]. One assumes a temporal

[4] Let us note that Eq. (2.9) is slightly different from Eq. (1.39), however with a simple change of variables ($y_i(t) = f_a(x_i(t))$ one show that the two model are equivalent.

exponential profile for the perturbation, i.e. $\delta x_i(t) = e^{\lambda t}\Psi_i(t)$, and studies its evolution in tangent space, i.e.

$$\Psi_i(t+1) = e^{-\lambda} m_i(t) \left[\frac{\epsilon}{2}\Psi_{i-1}(t) + (1-\epsilon)\Psi_i(t) + \frac{\epsilon}{2}\Psi_{i+1}(t) \right] , \tag{2.12}$$

which can also be written as a spatial recursive equation:

$$\begin{aligned} \Theta_{i+1}(t) &= \Psi_i(t) \\ \Psi_{i+1}(t) &= -2\frac{(1-\epsilon)}{\epsilon}\Psi_i(t) + \frac{2e^{\lambda}}{\epsilon m_i(t)}\Psi_{i+1}(t) - \Theta_i(t) \end{aligned} \tag{2.13}$$

with $\Theta_i(T+1) = \Theta_i(1)$ and $\Psi_i(T+1) = \Psi_i(1)$. Eq. (2.13) can then been solved by a transfer matrix approach by introducing the vector $\mathbf{V}_i = (\Theta_i(1), \ldots, \Theta_i(T); \Psi_i(1), \ldots, \Psi_i(T))$ and the evolution matrix:

$$\hat{S}_i = \begin{pmatrix} \mathbf{0} & \mathbf{I} \\ -\mathbf{I} & \mathbf{A_i} \end{pmatrix} , \tag{2.14}$$

where $\mathbf{I}$ and $\mathbf{0}$ are the $(T \times T)$ identity and null matrices, and $\mathbf{A_i}$ is a bidiagonal matrix with $(\mathbf{A_i})_{n,n} = -2(1-\epsilon)/\epsilon$ and $(\mathbf{A_i})_{n,n+1} = 2e^{\lambda}/(\epsilon m_i(n))$. Note that the dynamics produced by the matrix product is conservative (i.e. $det(\hat{S}_i) = 1$). Numerical computation requires an *a priori* knowledge of the local multipliers, which depends on the trajectory[5]. As usual one assumes that boundary conditions are not important in the limit $T \to \infty$ and that initial conditions chosen according to the *natural measure* are equivalent. By following the usual procedure for the computation of Lyapunov exponents of random matrices [77] one obtain $2T$ Lyapunov exponents η_i (because of the conservative dynamics and the fact that the matrices (2.14) are symplectic [77] one has that $\eta_j = -\eta_{T+1-j}$, however, this is true only for diffusive coupled maps). In complete analogy with $\lambda_i(\eta)$ for $T \to \infty$ one has a *spatial* Lyapunov exponent density [12, 78]:

$$\eta(\lambda, n_\eta) = \eta_j(\lambda) \qquad n_\eta = \frac{j - 1/2}{T} - 1 , \tag{2.15}$$

where $n_\eta \in [-1, 1]$ and $(j - 1/2)/T - 1$ is to fix the center of symmetry on $n_\eta = 0$ independently of T.

In analogy with disordered systems [77] it is possible to show that $\eta(\lambda, 0)$ can be interpreted as the inverse of the localization length, ℓ_{loc}, of the Lyapunov vector associated to λ, provided that λ belongs to the CLE. This analogy can be understood considering

[5] Actually the direct numerical computation of the spatial Lyapunov exponent suffers of some problems so that one has to resort to some precautions [12].

the problem of Anderson localization in the discrete version of the 2D (infinite strip) Schrödinger equation [77] in the tight-binding approximation (note that here the disorder play the same role of the fluctuations of the local multipliers) [78, 12]:

$$\psi_{n,m+1} + \psi_{n,m-1} + \psi_{n-1,m} + \psi_{n+1,m} = (E - V_{n,m})\psi_{n,m} , \tag{2.16}$$

where $n = 1, 2\ldots$ and $m = 1, \ldots, D$, $\psi_{m,n}$ and $V_{m,n}$ are respectively the wave function and a random potential on the site (n, m) with $\psi_{n;D+1} = \psi_{n,1}$ The theoretical analysis of this model predicts the existence of exponentially localized wave function for arbitrary small disorder, in the same way one as localization of Lyapunov vectors in CMLs.

It is worth noting that the analogy between Lyapunov vectors localization and wave functions localization in disordered systems fails when $\eta(\lambda, 0) = 0$. Nevertheless, in such a case there was found that the behavior of $\eta(\lambda, n_\lambda)$ for n_λ close to 0 can give some insight on possible others phenomena, e.g., stretched exponential localization [12]. In addition, also a power law localization may appear [92]. Such a power law behavior has been connected with *roughening* phenomena in statistical mechanics. Indeed, it is possible to show [92] that the dynamics of $h_i(t) = \ln(\delta x_i(t))$ can be mapped in a discrete version of the Kardar-Parisi-Zhang equation [93] for the scalar field $h(x, t)$, where the role of noise is replaced by the fluctuating local multipliers[6].

The analogies here discussed between spatio-temporal chaotic dynamics and other phenomena such as Anderson localization and roughening processes demonstrate that we need an unifying approach to relate the dynamical description with the statistical mechanics representation of extended chaotic systems.

To conclude this Section we cite that in Ref. [12] that the exploration of the (η, Λ)-plane (i.e. the complementary analysis of both these Lyapunov indicators) has been proposed as a comprehensive description of phenomena occurring in the context of one dimensional (in space) systems.

2.2.2 The Comoving Lyapunov Exponent

In spatially distributed dynamical systems *propagation phenomena* are very important [11]. An important piece of information about such properties is contained in the (space-time) *correlation functions*. Indeed, if the state of the system is described in terms of a

[6]However such an approach is rather delicate when the multipliers change of signs [12, 92].

d-dimensional vector field $\mathbf{u}(\mathbf{x},t) = \{u_1(\mathbf{x},t), u_2(\mathbf{x},t), \ldots, u_d(\mathbf{x},t)\}$ one can introduce the (space-time) correlation tensor as:

$$C_{i,j}(\mathbf{x},\mathbf{x}';t,t') = \langle u_i(\mathbf{x},t)u_j(\mathbf{x}',t')\rangle - \langle u_i(\mathbf{x},t)\rangle\langle u_j(\mathbf{x}',t')\rangle\,, \tag{2.17}$$

where $i,j = 1,\ldots,d$ and $\langle[\ldots]\rangle$ indicates an *ensemble* average. If the system is statistically stationary and invariant under translation one has $C_{i,j}(\mathbf{x},\mathbf{x}';t,t') = C_{i,j}(\mathbf{x}-\mathbf{x}';|t-t'|)$. Studying the shape of the correlation function, if the dynamics yields to propagation phenomena one can obtain information about the propagation velocity by looking at the peaks of $C_{i,j}$. Indeed, one expects a peak for $||\mathbf{x}-\mathbf{x}'|| \approx v|t-t'|$, being v the propagation velocity.

However, the correlation tensor (2.17) is usually hard to compute in experimental setting and in numerical computation is very (CPU) time consuming. In order to give a good characterization of propagation in space-time systems and to characterize phenomena such as *convective chaos*, in recent years it was introduced the idea of a velocity dependent Lyapunov exponent [28]. In a nutshell the basic idea is to compute the Lyapunov exponent in a frame of reference comoving with respect to the systems: the *comoving* Lyapunov Exponent (comoving-LE) [28].

Let us start with a simple example related to CMLs (extension to the continuous time and space are straightforward[7]. Let us consider two identical CML and suppose to initialize a (localized) perturbation on W sites of a lattice:

$$\delta x_i(0) \neq 0 \qquad \text{only for} \qquad i \in [-W/2, W/2]$$

without loss of generality we have considered a perturbation centered on the center of the lattice.

If we are interested in following the perturbation and its growth, we can define a norm which measures the amplitude of a localized perturbation on W sites, after t steps in a frame of reference comoving (with the perturbation) with velocity v, as:

$$\Delta(W;t,v) = \sqrt{\sum_{j=vt-W/2}^{vt+W/2} \delta x_j(t)^2}\,. \tag{2.18}$$

Of course, one can also work in tangent space, i.e. $\delta\mathbf{x}(t) \to \mathbf{z}(t)$, being $\mathbf{z}$ the tangent vector.

[7]Indeed Kaneko and Deissler introduced the comoving-LE for the complex Landau-Ginzburg equation [28]

One can expect that for times enough long (2.18) grows exponentially, i.e.

$$\Delta(W;t,v) \approx \Delta(W;0,v)e^{\lambda(v,W)t}\,. \tag{2.19}$$

Therefore, we can define the (maximum) comoving Lyapunov exponent as:

$$\lambda(v) = \lim_{t\to\infty} \lim_{\Delta(W;0,v)\to 0} \frac{1}{t}\ln\left(\frac{\Delta(W;t,v)}{\Delta(W;0,v)}\right)\,, \tag{2.20}$$

if this limit exists and it is independent on W (for W large enough). The rationale for the order of the two limit in (2.20) should be clear from the discussion of Sect. 1.1.1.

Working in tangent space and defining the comoving Jacobian matrix:

$$\left(\hat{J}_t(v,\mathbf{x}(t))\right)_{i,j} = \frac{\partial x_{i+[v(t+1)]}(t+1)}{\partial x_{j+[vt]}(t)}\,, \tag{2.21}$$

where $[\ldots]$ indicate the integer part, one can built the same theory described in Sect. 1.1.1 and then to invoke the Oseledec theorem [42]. However, since we are interested only in computing the maximum comoving Lyapunov exponent we limit our discussion to the definition given above (2.20). Indeed, the meaning of the whole comoving spectrum is still questionable.

Coming back to Eq. (2.20), it is important to say that the limit $t \to \infty$ implies the infinite size limit (i.e. $L \to \infty$), so that numerical computations of $\lambda(v)$ have to be performed with care. Let us note that $\lambda(v)$ is connected with the *temporal* (*specific*) Lyapunov exponents (2.11). Indeed, Eq. (2.19) can be rewritten as [12, 91]

$$\delta x_i(t) = \delta x_0(0)\exp(\lambda(v = i/t)\,t)\,, \tag{2.22}$$

from which one has a perturbation having a locally exponential profile given by $\eta = d\lambda(v)/dv$ in the point $i = vt$. From Sect. 2.2.1 we know that such a profile evolves as:

$$x_{vt}(t) \sim \exp\{\lambda(\eta)t + \eta v t\}\,. \tag{2.23}$$

From the last two equations one finally has:

$$\lambda(v) = \lambda(\eta) + \eta\frac{d\lambda(\eta)}{d\eta}\,, \tag{2.24}$$

which can be interpreted as a Legendre transform from $(\lambda(v), v)$ to $(\lambda(\eta), \eta)$ [91]. By inverting the transformation one also obtains that $v = d\lambda(\eta)/\eta$ (see also Sect. 4.2).

The comoving Lyapunov exponent, $\lambda(v)$, is a measure of the rate of amplification for perturbations which move with a velocity v. In closed systems with symmetric coupling

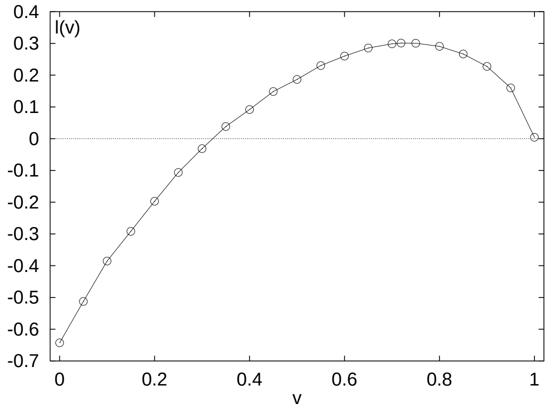

Figure 2.3: $\lambda(v)$ versus v computed for the system (2.7) for the logistic map with $a = 3.85$ and $\epsilon = 0.7$. As it is possible to see even if the Lyapunov exponent is negative ($\lambda = \lambda(v=0) < 0$) there is a range of velocities for which the comoving Lyapunov exponent is positive.

$\lambda(v) = \lambda(-v)$ and $\lambda(v=0) = \lambda_{max}$, in Sect. 4.2 we shall see that the velocity for which $\lambda(v) = 0$ corresponds to the propagation velocity of an initially localized perturbation.

In the problem of characterizing *convective* and *absolute* chaos in flow system, the comoving Lyapunov exponent has revealed to be the natural indicator. If $\lambda(v=0) > 0$ the system is absolutely unstable: the perturbation grows on site (Fig. 2.2). If $\lambda(v=0) < 0$ the flow is absolutely stable, but if it exists a velocity value v^* for which $\lambda(v^*) > 0$ (Fig. 2.3) we have convective chaos: the perturbation initially localized moves with a velocity v^* and grows with a rate $\lambda(v^*)$ (see Fig. 2.2). Let us underline that the behavior described in Figure 2.2 can appear on in systems with a mean flow[8].

In Ref. [21] it was proposed to characterize by means of the comoving Lyapunov exponents also the *sensitivity to boundary conditions* in flow systems. Indeed one can consider the uncertainty $\delta x_n(t)$, on the determination of the variable at the site n, as given by the superposition of the evolved $\delta x_0(t-\tau)$ with $\tau = n/v$:

$$\delta x_n(t) \sim \int \delta x_0(t-\tau) e^{\lambda(v)\tau} dv = \epsilon \int e^{[\lambda(v)/v]n} dv \,. \tag{2.25}$$

Since one is interested in the asymptotic spatial behavior, i.e.:

$$\lambda_S = \lim_{n\to\infty} \frac{1}{n} \left\langle \ln \frac{|\delta x_n|}{|\delta x_0|} \right\rangle , \tag{2.26}$$

[8]In such a case one can doubt about the utility of $\lambda(v)$ by saying that the perturbation leaves the the system in a finite time. However, usually such systems are externally forced so that there is a continuous input of perturbations.

where the quantity λ_S can be considered a sort of spatial-complexity-index, see Ref. [21]. In the limit of large n and neglecting the intermittency, one can use a saddle point estimate of Eq. (2.25), i.e.:

$$\lambda_S = \max_v \left\{ \frac{\lambda(v)}{v} \right\} . \tag{2.27}$$

Actually, taking into account intermittency one has $\lambda_S \geq \max\{\lambda(v)/v\}$. In Ref. [21] it was shown that this puts a relation between the convective instability of a system and its sensitivity to the boundary conditions.

2.3 Growth of non infinitesimal perturbations

In complex dynamical systems, such as spatially distributed systems, one needs to take into account different kinds of perturbations and, as a consequence, to enlarge the set of indicators. This has lead to the *spatial* and *temporal* Lyapunov exponent, *comoving* Lyapunov exponents. As a matter of fact the above mentioned indicators are defined for infinitesimal perturbations, i.e. they remain in the philosophy of the linear analysis.

However, as seen in Sect. 2.1, there exist many interesting problems which cannot be addressed in the framework of linear analysis, among which we just mention: the characterization of systems with many characteristic temporal and spatial scales [7, 10, 36], and the "chaotic-like" behaviors appearing in certain stable CMLs [19, 20].

In the following we discuss in detail an approach introduce by Aurell et al [9, 10] in the context of predictability in turbulence. This approach is based on the *Finite Size Lyapunov Exponents*, i.e. on the idea of generalizing the Lyapunov analysis to finite (non infinitesimal) perturbations (see Ref. [29] where the idea of studying perturbation of finite perturbations is proposed in terms of higher order Lyapunov exponents).

2.3.1 The Finite Size Lyapunov Exponent

The natural starting point to approach non infinitesimal uncertainties is in terms of the predictability time. In Sect. 2.1 we have defined the predictability time for a perturbation of size δ and tolerance Δ in terms of the inverse of the Lyapunov exponent (2.2). One can relax the requirement that δ and Δ are infinitesimal and thus define the predictability time, $T(\delta, \Delta)$, for a perturbation δ with an error tolerance Δ, where now (δ, Δ) may be non infinitesimal. Typically, such a time will fluctuate, so that the natural definition for the Finite Size Lyapunov Exponent (FSLE) is a "suitable" average of some function of this time, i.e. by inverting (2.2) one has [9, 10]

$$\lambda(\delta,\Delta)=\left\langle \frac{1}{T(\delta,\Delta)}\right\rangle \ln\left(\frac{\Delta}{\delta}\right), \tag{2.28}$$

where $\langle[\ldots]\rangle$ is an average along the trajectory (in the following we shall specify the way in which this average has to be intended). In principle, at variance with the maximum Lyapunov exponent $\lambda(\delta,\Delta)$ may depend both on δ and Δ. However, if Δ is not much larger than δ one can expect only a dependence on δ. Moreover,when δ,Δ are both infinitesimal, this definition gives the maximum Lyapunov exponent (i.e. is also independent of δ). In the following we describe in detail the procedure for the computation of the FSLE.

Let us suppose to integrate the equations of motion of a certain system on a computer. After a long integration time in order to reach a statistically stationary state, we introduce a very small perturbation, i.e. we consider the "reference" trajectory $\mathbf{x}(0)$, which is supposed to be on the attractor, and generate a "perturbed" trajectory $\mathbf{x}'(0)=\mathbf{x}(0)+\delta\mathbf{x}(0)$. We have to take care that such a perturbation is initially very small $\delta(0)=||\delta\mathbf{x}(0)||=\delta_{min}\ll 1$ (measured in some norm). After one defines a set of thresholds δ_n: a natural choice is $\delta_n=\delta_0 r^n$ with $1\gg\delta_0\gg\delta_{min}$ and $n=1,\ldots,N$ with $\delta_N<\langle||\mathbf{x}-\mathbf{y}||\rangle_\mu$ for $\mathbf{x},\mathbf{y}$ generic points on the attractor. This last condition ensures that one studies only perturbations with a size below the average size of the attractor, on which all the perturbations will saturate. Note that r should be >1 but not very large in order to avoid interferences of different length scales. Typically, one chooses $r=2$ (or $r=\sqrt{2}$), however any value in, e.g., $[1,2]$ is good. Then one integrate the two trajectories until $\delta(t)=\delta_0$, this integration ensures that the trajectories are on the attractor and it selects the most unstable direction[9]. After one measures the time, $\tau_i(\delta_0,r)$, the perturbation needs to grow from δ_0 up to δ_1. Then the "perturbed" trajectory is rescaled to distance δ_0 from the "reference" one and one measures the time $\tau_2(\delta_0,r)$ to reach δ_1. If $r=2$ we can call them "doubling" times, i.e. the times the perturbation takes to double its amplitude. One has to repeat this procedure a large number of times, $\mathcal{N}$, (number of doubling time experiments) for each δ_n[10]. See Fig. 2.4 for a sketch of the method.

At the end we have a set doubling times, $\{\tau_i(\delta_n,r)\}_{i=1,\mathcal{N};n=1,N}$, for each perturbation size δ_n and, we can define the average of an arbitrary observable, A, on the set of doubling

[9]Actually it selects also a particular measure see Appendix A for a detailed discussion on this point.
[10]For instance one can iterate simultaneously N copies of the system each of which is take at a distance δ_n from the reference one.

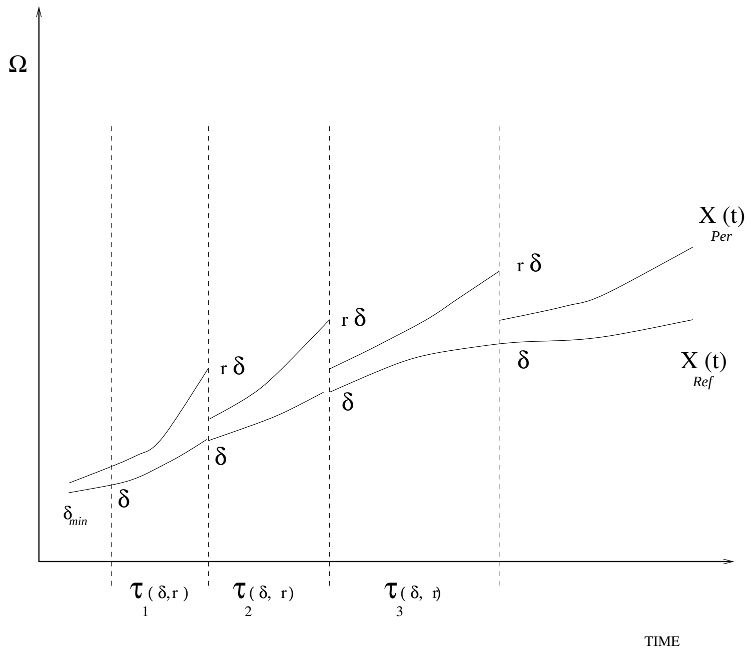

Figure 2.4: A sketch of the FSLE algorithm: one makes a perturbation δ_{min} and after the chosen scale δ is reached, he starts to measure the doubling times $\tau_1(\delta, r)$. One has to repeat this procedure for each chosen δ.

time measurements as:

$$\langle A \rangle_e = \frac{1}{\mathcal{N}} \sum_i^{\mathcal{N}} A_i \,. \tag{2.29}$$

Let us stress that the average $\langle [\ldots] \rangle_e$ is not the same as taking a time-average, since different error doubling experiments may take different times[11]. The usual time average $\langle [\ldots] \rangle_T$ can be linked to the average on the doubling time experiments (2.29) by the following relation [10]

$$\langle A(t) \rangle_T = \frac{1}{T} \int_0^T A(t) dt = \frac{\sum_{i=1}^{\mathcal{N}} A(\tau_i) \tau_i}{\sum_{i=1}^{\mathcal{N}} \tau_i} = \frac{\langle A\tau \rangle_e}{\langle \tau \rangle_e} \,, \tag{2.30}$$

where $T = \sum_i \tau_i$, here we have dropped the dependence of the doubling times on δ and r. Coming back to Eq. (2.28) we have:

$$\lambda(\delta_n) = \left\langle \frac{1}{\tau(\delta_n, r)} \right\rangle_T \ln r = \frac{1}{\langle \tau(\delta_n, r) \rangle_e} \ln r \,, \tag{2.31}$$

which defines the Finite Size Lyapunov Exponent [9, 10]. Let us note that the dependence on r is not very important if r is not very large. In fact, performing numerical computations with $r \in]1, 2]$ we have not found any important dependency on r (see Fig. 2.5).

[11] *Viz.* Eq. (2.29) is a time average only if the doubling time are equals, i.e. $\tau_i(\delta_n, r) = \tau_j(\delta_n, r)$ for each i, j.

The above described method assumes that the distance between two states is continuous in time. This is not true for maps (or experimental data, which are usually sampled at fixed times), so that the method has to be slightly modified. In the time discrete case $\tau(\delta_n, r)$ is the minimum time such that the distance between the two trajectories (initially of size δ_n) becomes larger or equal to δ_{n+1} (i.e. $\tau(\delta_n, r) = \max_\tau\{\delta(\tau) \geq \delta_{n+1}\}$). At difference with the continuous case now $||\delta\mathbf{x}(\tau(\delta_n, r))||$ is a fluctuating quantity so that Eq. (2.31) must be replaced with:

$$\lambda(\delta_n) = \frac{1}{\langle \tau(\delta_n, r) \rangle_e} \left\langle \ln \left(\frac{||\delta\mathbf{x}(\tau(\delta_n, r))||}{\delta_n} \right) \right\rangle_e . \tag{2.32}$$

In Fig. 2.5 we show $\lambda(\delta)$ versus δ for both a continuous time system (the Lorenz system [1]) and a time discrete one (the logistic map $f(x) = ax(1-x)$ for $a = 4$) for three different choices of $r \in]1, 2]$. As it is possible to see $\lambda(\delta)$ practically does not depend on r . At $\delta \ll 1$, when the perturbation can be considered infinitesimal one has $\lambda(\delta) = \lambda_{max}$, while at larger δ one can see a decreasing of the growth rate, essentially, due to the trajectories folding (the attractor is a bounded set)[12].

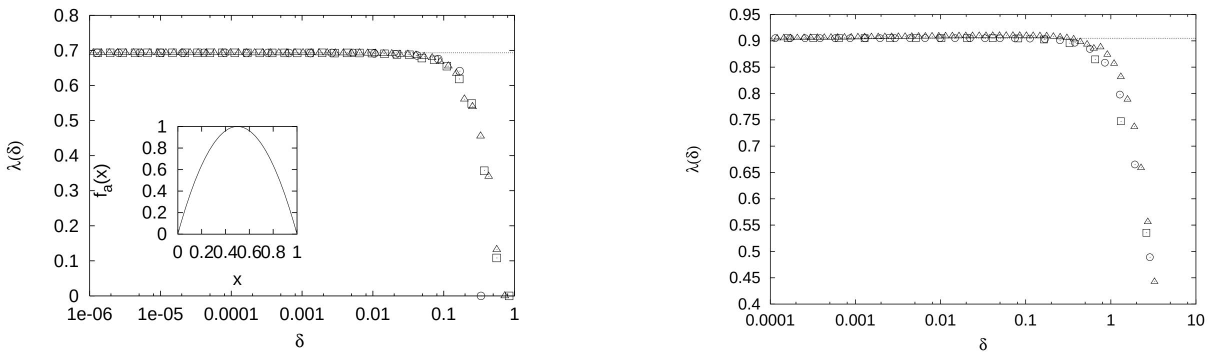

Figure 2.5: $\lambda(\delta)$ versus δ: (a) for the Lorenz [1] model with the usual choice for the parameters for $r = 1.3$ ($\triangle$), $r = 1.6$ ($\bigcirc$) and $r = 2$ ($\square$) (b) for the logistic map (shown in the inset) for $r = 1.2$ ($\triangle$), $r = 1.5$ ($\bigcirc$) and $r = 2$ ($\square$). The straight lines corresponds to λ_{max}.

At difference with λ_{max}, $\lambda(\delta)$ may also depend on the norm one chooses. This fact, apparently not very positive, is however physically very reasonable: when one looks at the non linear regime, for instance, for the predictability problem the answer may depends on the observable one chooses. A similar problem appears in infinite dimensional system

[12] However, in the next Section we shall see that there exist systems displaying a different behavior.

where the norms are not equivalent [40]. Also in such a case one has to choose a norm according to a physical idea [95].

A further aspect of the above defined Finite Size Lyapunov Exponent is that it answer to a physically very reasonable criteria. In many dynamical systems, the physical mechanism driving perturbation dynamics is typically related to some dynamical properties of the system at length scales of the order of the perturbation size (e.g. a typical example is turbulence). Therefore, the idea to fix the scale and to look at the times is more natural than to fix a certain time delay, t_d, and to look at the growth rate on such t_d [10, 88]. The above described method to compute the FSLE can be slightly modified in order to

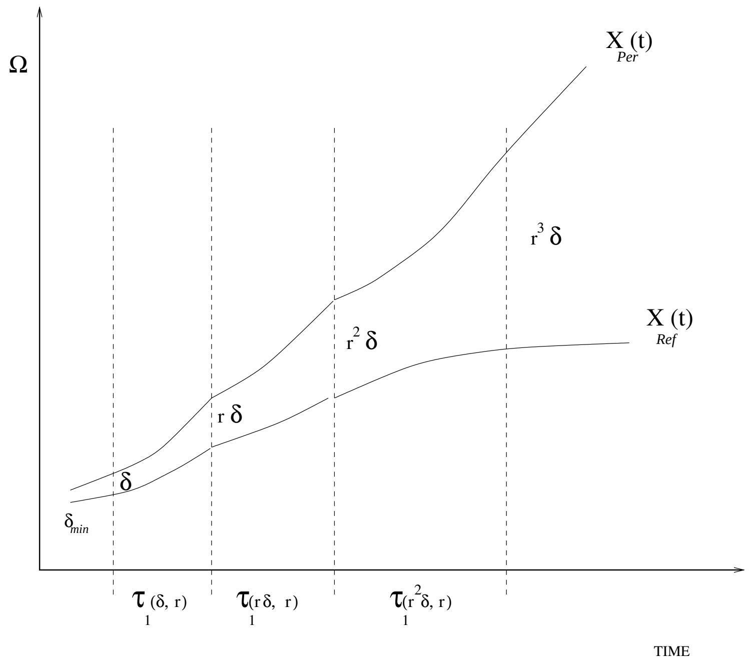

Figure 2.6: A sketch of the second algorithm, one measures with only two trajectories (the reference and the perturbed) all doubling times $\tau(\delta_n, r)$ at different amplitudes δ_n of the perturbation. When the last chosen threshold is reached, the perturbed trajectory is rescaled to δ_{min}.

be computationally more efficient. Instead of measuring the time $\tau_i(\delta_n, r)$ to go from δ_n to δ_{n+1} and then rescaling the "perturbed" trajectory to δ_n, one can follow the whole perturbation growth from δ_0 up to the maximum attainable scale δ_N and then measure the times to from one threshold to the other during the evolution. After the last scale δ_N is reached the perturbed trajectory is rescaled to δ_{min} and one reiterates the procedure (see Fig. 2.6). $\lambda(\delta)$ is then evaluated according to Eqs. (2.31) or (2.32).

These two described methods give the same results in the limit of very small perturbations but may give slightly different values of $\lambda(\delta)$ at large δ, indeed numerically we verified that such differences are not dramatic (see Fig. 2.7). In any case in most of this thesis we shall use the second described method which is particularly suitable for many degrees of freedom dynamical systems such as the ones here studied.

It is worth to note that the first method may give rise to some problems [10]. Indeed, in its definition we have implicitly assumed that the statistically stationary state of the system is homogeneous with respect to perturbations of finite size. But, one may plausibly argue that the structure of the attractor in phase space on which the motion takes place may be fractal, and not equally dense at all distances from a given point. So that the first proposed procedure would not necessarily exactly sample the motion on the attractor. Of course, this problem disappears at very small δ, where the dynamics is practically on the tangent space. The second method proposed does not suffer of this problem since the trajectories live on the attractor during their whole evolution[13].

One can also think to remove the threshold condition used for defining the doubling times $\tau(\delta_n, r)$ and simply compute the average error growth rate after a given time interval Δt, e.g. at every time step. In other words, at every Δt of the integration, the perturbed trajectory $\mathbf{x}'(t)$ can be rescaled to the original distance δ, keeping the direction $\mathbf{x}'(t)-\mathbf{x}(t)$ constant. However, in order to have a sensible result Δt should not be too large in order to avoid interferences of different scales.

Within this scheme the FSLE is given by

$$\lambda(\delta) = \frac{1}{\Delta t} \left\langle \ln \left(\frac{||\delta \mathbf{x}(t+\Delta t)||}{||\delta \mathbf{x}(t)||} \right) \right\rangle_T . \tag{2.33}$$

This algorithm moreover can be generalized to the computation of the sub-leading FSLEs by the standard ortho-normalization procedure on k trajectories[14] [41].

We conclude this Section by showing in Fig. 2.7 the FSLE for the same systems as in Fig. 2.5 computed according to the three different methods. As it is possible to see there are not dramatic differences between the three different methods: the problem of

[13]Indeed, for this second method one can wonder that the formula (2.31) may not lead to the usual Lyapunov exponent for small perturbations, since the pieces of trajectories referring to the same δ_n are not consecutive in time, however in Appendix A we shall show that this problem may be overcome. Moreover, numerically we always find a good estimate of the maximum Lyapunov exponent also with this method.

[14]However we have again the problem of the implicitly assumed homogeneity of the attractor, and also a problem of isotropy when we re-orthogonalized the perturbations. We just note that this last could be a more serious problem. In the following we shall limit to the first (maximum) FSLE.

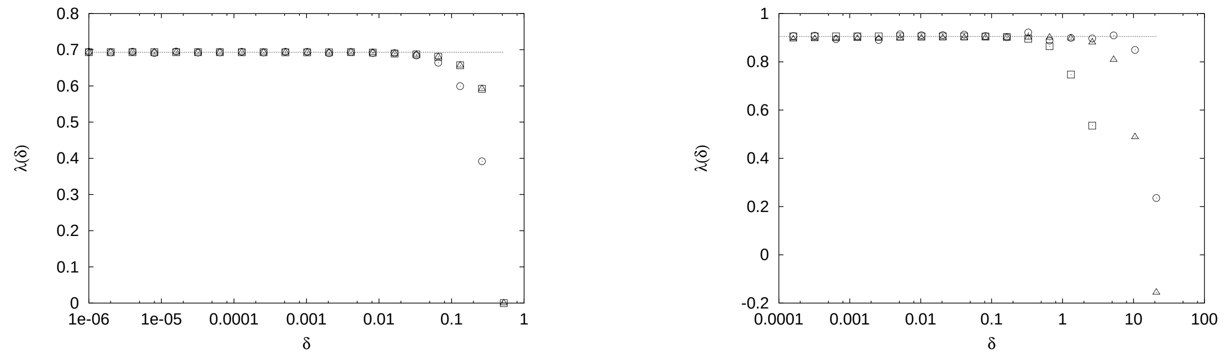

Figure 2.7: $\lambda(\delta)$ versus δ for the same systems as Fig. 2.5 computed with the three different algorithms: ($\square$) the first, ($\bigcirc$) the second and ($\triangle$) the third.

the homogeneity of the attractor may cause slight differences visible at large δ. In the following we shall adopt essentially the second method which is the more efficient from a computational point of view and does not suffer of the problem of the homogeneity of the attractor. It is worth underlining that defining the FSLE in terms of the doubling time one cannot measure negative Lyapunov exponents: time by definition is a positive quantity. However, this is not very important in the systems we shall study.

In the next Section we shall show that enlarging our observations to non infinitesimal perturbations, there appear interesting behaviors even in very simple dynamical systems.

2.3.2 "Non-Linear Chaos" in simple systems

The above described non linear analysis is typically very difficult so that in most of interesting cases one can only perform numerical computation of $\lambda(\delta)$. In the following we study two very simple maps of the unit interval for which the computation can be performed analytically [34]. These examples, even if extremely simple, highlight that in the non linear regime one can have very peculiar situations.

Let us start with the tent map

$$f(x) = \begin{cases} 2x & x \in [0, 1/2[\\ -2x + 2 & x \in [1/2, 1] \, . \end{cases} \tag{2.34}$$

This map is indeed very simple: the invariant density is uniform in the unit interval (i.e. $\rho_\mu(x) = 1$), and, moreover, the map is piecewise linear: the absolute value of the slope does not fluctuate. For this map the maximum Lyapunov exponent is easily computable as follows

$$\lambda_{max} = \lim_{\delta\to 0} \left\langle \ln \left| \frac{f(x+\delta/2) - f(x-\delta/2)}{\delta} \right| \right\rangle_\mu = \int_0^1 dx \rho_\mu(x) \ln |f'(x)| = \ln 2 \,. \tag{2.35}$$

It is then natural to relax the request $\delta \to 0$ and compute the FSLE as:

$$\lambda(\delta) = \left\langle \ln \left| \frac{f(x+\delta/2) - f(x-\delta/2)}{\delta} \right| \right\rangle_\mu = \langle I(x,\delta) \rangle_\mu \,, \tag{2.36}$$

of course by Eq. (2.35), in the limit $\delta \to 0$ one has $\langle I(x,\delta)\rangle_\mu = \lambda_{max} = \ln 2$. It is easy to see that (for $\delta < 1/2$) $I(x,\delta)$ is given by:

$$I(x,\delta) = \begin{cases} \ln 2 & x \in [0, 1/2 - \delta/2[\ ]1/2+\delta/2, 1] \\ \ln \dfrac{|2(2x-1)|}{\delta} & \text{otherwise}\,. \end{cases} \tag{2.37}$$

By computing the average (2.36), for $\delta < 1/2$, one has

$$\lambda(\delta) = \ln 2 - \delta \,, \tag{2.38}$$

which is in very good agreement with the numerically computed[15] $\lambda(\delta)$ (see Fig. 2.8). In this case going from infinitesimal to finite uncertainties the stability properties of the map are enhanced, i.e. the value of Lyapunov exponent (2.35) is decreased (2.38).

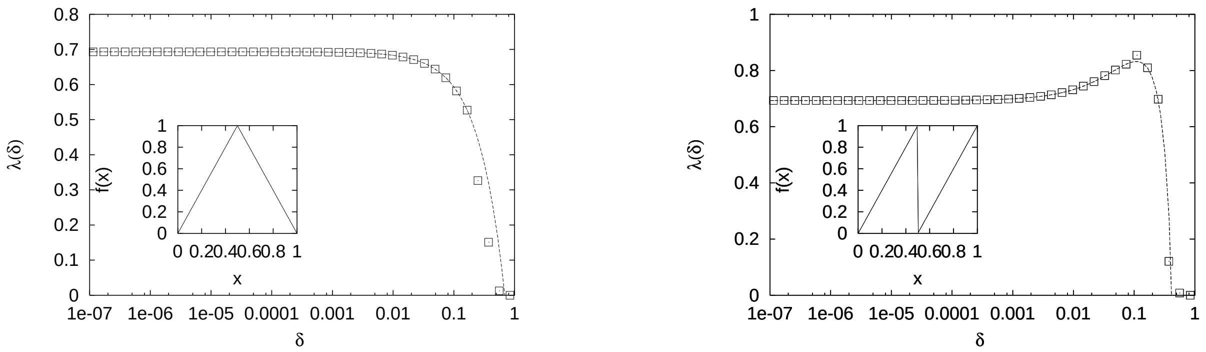

Figure 2.8: $\lambda(\delta)$ versus δ for the tent map (left) and the shift map with $\beta = 2$ (right). The continuous lines are the analytically computed FSLE. The two maps are displayed in the insets.

However, although the growth rate of divergence on the infinitesimal scales is given by the Lyapunov exponent, there exist systems for which, at difference with (2.38), the

[15] No matter of the used algorithm.

finite size corrections due to the higher order terms leads to an enhancement of rate of separation at large scales [34]. Such a kind of behavior may have dramatic consequences in marginally stable systems ($\lambda_{max} = 0$) and even in stable systems.

An example of such a behavior is given by the shift map:

$$f(x) = \beta x \qquad \mathrm{mod}\ 1\,, \tag{2.39}$$

which has $\lambda_{max} = \ln\beta$. By using the same procedure as before, for δ not too large one has:

$$I(x,\delta) = \begin{cases} \ln\left[\dfrac{(1-\beta\delta)}{\delta}\right] & x \in [1/\beta - \delta/2, 1/\beta + \delta/2] \\ \ln\beta & \text{otherwise}\,. \end{cases} \tag{2.40}$$

Since, for $\beta = 2$, the invariant density is uniform in the unit interval, the average of $I(x,\delta)$ gives

$$\lambda(\delta) = (1-\delta)\ln 2 + \delta \ln\left(\frac{1-2\delta}{\delta}\right)\,. \tag{2.41}$$

In Fig. 2.8 we show the analytic FSLE compared with the numerically evaluated $\lambda(\delta)$.

In the shift map one has the seemingly anomalous situation for which:

$$\lambda(\delta) > \lambda(\delta \to 0) = \lambda_{max} \qquad \text{for } \delta > 0\,. \tag{2.42}$$

Such a behavior can obviously lead to peculiar phenomena when, e.g., one considers CMLs using as local map the shift map (see Sect. 4.2)

As above mentioned one expects that the possibility to have positive higher order corrections leading to (2.42), may be more dramatic in marginally stable. For example, if one compute $\lambda(\delta)$ for the circle map, $f(x) = \alpha + x \mod 1$ (λ_{max}=0), one obtains

$$\lambda(\delta)=\delta\ln[(1-\delta)\delta]\,, \tag{2.43}$$

which is positive for $0 < \delta < 1/2$. Therefore at small but finite perturbations one has a positive growth rate in spite of the (marginal) stability against infinitesimal perturbations. As a consequence of (2.43), if the system is subject to the action of a small amount of dynamical noise, also infinitesimally small perturbations may be driven into the non linear (unstable) regime. Of course, the role of noise can be played by coupling with other maps, so that for a CML of circle maps one may have behavior resembling (for some aspects) that of a chaotic system (see Sect. 4.2).

As a final example, we consider a more complex systems such as the CMLs introduced in Refs. [19, 20] and briefly discussed in Sect. 2.1. These CMLs present unusually long disordered transients, increasing exponentially with the system size L. Moreover, the maximal Lyapunov exponent (computed on the transient) is negative [20]. The equations which define such a system are the usual CML equation (1.39) (or equivalently (2.9)). The local dynamics can be given by different kinds of (stable) maps, e.g. we have considered the following one [20]:

$$f(x) = \begin{cases} bx & 0 < x < 1/b \\ a + c(x - 1/b) & 1/b \leq x < 1\,. \end{cases} \tag{2.44}$$

For $a = 0.07\,,\ b = 2.7\,,\ c = 0.887$ the un-coupled map possesses a stable period-3 orbit, which is also the most probable asymptotic solution of the coupled system for $\epsilon = 1/3$. Due to the strong contraction region $(1/b \leq x < 1)$ the Lyapunov exponent is negative also in the disordered transient. In Fig. 2.9 we show the numerically computed $\lambda(\delta)$. We

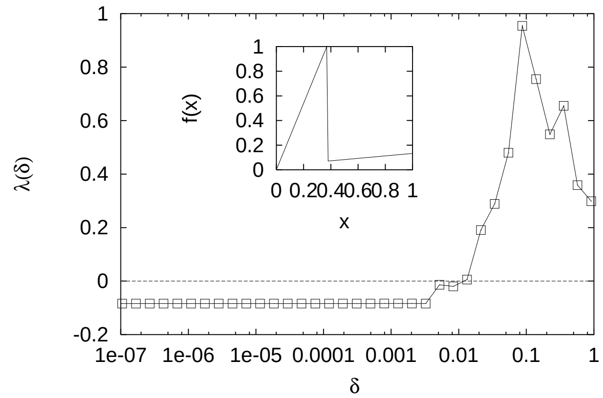

Figure 2.9: $\lambda(\delta)$ versus δ for the map (2.44) (shown in the inset) with $\epsilon = 1/3$ and $L = 35$, the other parameters are described in the text. The straight line corresponds to the maximum Lyapunov exponent of the system, here *negative*.

have used the third proposed algorithm (Eq. 2.33) in order to measure the contractions for small δ. At small scales ($\delta \leq .01$) we found a negative Lyapunov exponent, while for $\delta > 0.01$ one has $\lambda(\delta) > 0$. One can then conjecture that the instabilities which produce the observed spatio-temporal disordered transient may be related to the sensitivity to finite perturbations, which act at each time step on every map due to the coupling with neigh-bourn sites. A similar analysis was performed by Kantz and Letz [96], who have defined a quantity similar to the FSLE adopting a time series analysis point of view.

The common characteristic of these (strongly non linear) maps is that the derivative $f'(x)$ exhibits a δ-singularity. However, as shown in Refs. [35] it is necessary to have an enough narrow peak. For instance, one can define a map such as

$$f(x) = \begin{cases} \beta x & 0 \leq x < 1/\beta \\ -\alpha(x - 1/\beta) + 1 & 1/\beta \leq x < 1/\beta + 1/\alpha \\ \beta(x - 1/\alpha) - 1 & 1/\beta + 1/\alpha \leq x < 1\,, \end{cases} \tag{2.45}$$

for which one can vary with continuity the bandwidth and the height of the peak. Indeed by numerically computing the FSLE [79] (not shown), at varying the parameters, one observes both a tent-like or a shift-like behavior.

2.4 ε-entropy and Finite Size Lyapunov Exponent: towards a scale dependent description of complex behaviors

The Kolmogorov-Sinai entropy, h_{KS}, gives an estimate of the number of bits per unit time which is necessary and sufficient to record without ambiguity a trajectory of a chaotic system [2] (see Sect.1.1.2). In the same philosophy of the FSLE, relaxing the strict requirement of reproducing a trajectory with arbitrary accuracy, one can ask for reproducing the trajectory only within a given tolerance ε. The number of bits per unit time we need for such a purpose is measured by the so-called ε-entropy [97, 17]. Such a quantity was originally introduced by Shannon [98] who calls it "source entropy with respect to a fidelity criterion", and by Kolmogorov [97] who found analytic formulas for Gaussian stationary processes. Recently Gaspard a Wang [17] made use of this concept to characterize a large variety of processes.

The natural starting point to introduce such a quantity is by making a partition of the phase space in cells of diameter ε (see Sect. 1.1.2). Then by following the steps described in Sect. 1.1.2 to compute the KS-entropy, one evaluates the joint probabilities (1.28) and the block entropies $H_N(\varepsilon)$ (1.29). The ε-entropy is nothing but

$$h(\varepsilon) = \lim_{N\to\infty} H_N(\varepsilon) - H_{N-1}(\varepsilon)\,, \tag{2.46}$$

i.e. Eq. (1.31). Actually, the above definition may depend on the partition (for finite ε). To make $h(\varepsilon)$ partition-independent one can define a generic partition of the phase space $\{\mathcal{P}_i\}$ and evaluates the Shannon entropy on this partition: $h(\mathcal{P})$. The ε-entropy is thus defined as the infimum over all partitions for which the diameter of each cell is less than ε [17]:

$$h(\varepsilon) = \inf_{\mathcal{P}:\mathrm{diam}(\mathcal{P}_i)\leq\varepsilon} h(\mathcal{P})\,. \tag{2.47}$$

In numerical evaluation of $h(\varepsilon)$ one usually follows the procedure introduced by Grassberger and Procaccia [46] or by Cohen and Procaccia [99]. It is worth to underline that as the FSLE also the ε-entropy depends on the used norm (with Shannon "by the fidelity criterion adopted"). For $\varepsilon \to 0$ one recovers the Kolmogorov-Sinai entropy (1.32), which is independent on the definition of the diameter.

For time continuous dynamical systems, since the computation of the entropy has to be performed by discretizing not only the phase space but also the time (e.g. introducing an observational time step τ), one has to introduce the concept of (ε, τ)-entropy [17], i.e. the value of the entropy depends also on the sampling time τ, the ε-entropy corresponds to the limit $\tau \to 0$. This problem is absent for time discrete processes. Therefore, in the following we limit the discussion to these last.

It is easy to realize that in systems with only one positive Lyapunov exponent the ε-entropy and the FSLE should give the same information[16] and in the limit $\varepsilon \to 0$ they coincide. For systems with more than one positive Lyapunov exponent the ε-entropy measures the rate of information production on all the direction of the phase space at the scale ε. Intuitively, one can conjecture the existence of the analogous of the Pesin equality (1.34) for finite scales, i.e. assuming to be able to compute the whole spectrum of finite size Lyapunov exponents $\lambda_i(\delta)$ one expects:

$$h(\varepsilon) = \sum_{\lambda_i(\varepsilon)>0} \lambda_i(\varepsilon)\,. \tag{2.48}$$

Unfortunately, as seen in Sect. 2.3.1, it is still not clear how to define (and compute) in a reliable way the non leading Lyapunov exponents, therefore, Eq. (2.48) is, for the moment, an interesting open problem.

However, the ε-entropy does not say all one wants to know about predictability and moreover the computation of $h(\varepsilon)$ is not very easy even in low dimensional systems [65]. Furthermore in high dimensional systems, where one expects extensivity for the entropy $h(\varepsilon)$ is practically uncomputable [11]. In this respect the finite size Lyapunov exponent has the advantage to be easy to compute, indeed its computation is not more expensive of the computation of the Lyapunov exponent.

[16] Actually in some cases this is not true. For instance, for the systems studied in Sect. 2.3.2 where $\lambda(\delta) > \lambda(0)$ one expects that $h(\varepsilon)$ is different from $\lambda(\delta)$. Indeed, by definition $h(\varepsilon) < h(\varepsilon')$ for $\varepsilon > \varepsilon'$.

2.4.1 Stochastic versus deterministic behaviors

In stochastic systems, at variance with chaotic dynamical systems, in the limit $\varepsilon \to 0$ one has $h(\varepsilon) \to \infty$ ($\lambda(\varepsilon) \to \infty$)[17]. Nevertheless, for any finite ε the ε-entropy and the FSLE are finite quantities and their scaling behavior[18] as a function of ε allows us for a characterization of the stochastic process. Indeed, as discussed by Gaspard and Wang [17] one can classify the processes according to the scaling behavior of $h(\varepsilon)$ as a function of ε (see Table 2.1). Without entering into the details of the computation [10], for the

Process	$h(\varepsilon)$
regular	0
chaos	$0 < h_{KS} < \infty$
Brownian Motion	$(1/\varepsilon)^2$
Fractional Brownian	$(1/\varepsilon)^{1/h}$
Time discrete, continuous states	$d\ln(1/\varepsilon)$

Table 2.1: This table summarizes the behaviors of the ε-entropy for some stochastic processes. For more details about the processes and the $h(\varepsilon)$ behaviors we refer to Ref. [17].

FSLE one has similar behaviors. Of course the pre-factor of the scaling behaviors may be different and, for chaotic systems, one recovers only the maximum positive Lyapunov exponent and not the KS-entropy.

In this thesis we are mainly concerned with deterministic dynamical systems. However, often deterministic chaotic systems may generate, on large scales, behaviors which fall into one of the classes above mentioned. As interesting examples we mention the *Chaotic advection* [85, 86, 87] (Chapter 5) for which on large scales one has a diffusive (Brownian motion) behavior induced by chaos, or fully developed turbulence (see Sect. 1.2.2) where the large scales (i.e. in the inertial range) properties can be fairly mimicked by a multi-affine stochastic process (typical of certain random processes) even if the dynamics is deterministic. Therefore, for a comprehensive characterization of chaotic dynamical systems the knowledge of the behavior of $h(\varepsilon)$ and $\lambda(\delta)$ for stochastic processes is indeed very interesting.

[17] In this Section we shall use equivalently δ and ε.

[18] It is worth noting that in the computation of the ε-entropy there often involved many technical problems which may resolve in the practical impossibility to observe such scaling behaviors. Some of these problems have been recently handled by introducing a new method (based on exit times) for computing the ε-entropy. See Ref. [100] for a detailed description

An interesting case in which such an aspect emerges is a dynamical system with an external source of randomness, i.e. the system is driven by dynamical noise. For instance let us consider the following noisy map[19]:

$$x(t+1) = F(x(t)) + \sigma\eta(t)\,, \tag{2.49}$$

where $\eta(t)$ is a random process and σ measures its strength. Let us consider the case in which $\langle\eta(t)\rangle = 0$ and $\langle\eta(t)\eta(t')\rangle = \delta_{t,t'}$, and the map $F(x)$ is originally chaotic with a Lyapunov exponent λ. If $\sigma \neq 0$, a simple computation [10] shows that if $|\delta x(0)| \gg \sigma$ the noise term is negligible, and $\lambda(|\delta x(0)|) \approx \lambda$. On the contrary, if $|\delta x(0)| \ll \sigma$, one has $\delta x(t) \approx \sigma\delta\eta(t-1)$. Thus in one iteration of the map the distance between the two trajectories grows $O(\sigma)$. In such a case by applying the FSLE (2.32) it is easy to recognize that$\lambda(|\delta x(0)|) \sim \ln(\sigma/|\delta x(0)|)$. A computation of the ε-entropy gives exactly the same behavior for $h(\varepsilon)$ as a function of ε [10, 17].

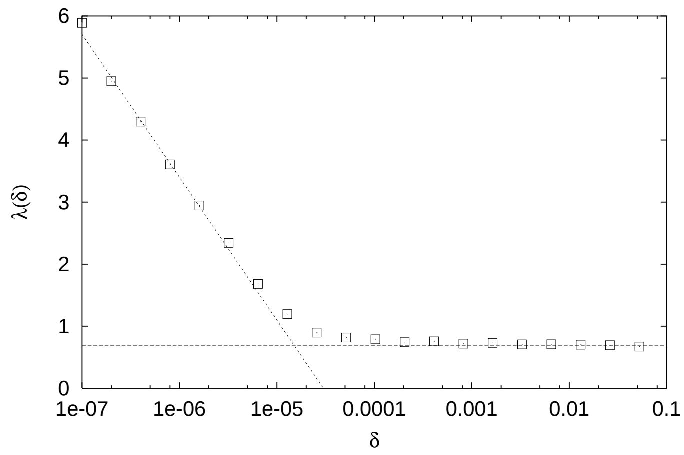

Figure 2.10: FSLE computed for the logistic map (with $a = 4$) plus noise as Eq. (2.49) with $\sigma \approx 10^{-4}$. The lines indicate the behavior (2.50).

Therefore, in dynamical systems with noise of strength σ, one has (see Fig. 2.10):

$$\lambda(\delta) = \begin{cases} \ln\left(\dfrac{\sigma}{\delta}\right) & \delta \ll \sigma \\ \lambda & \delta \gg \sigma \end{cases} \tag{2.50}$$

[19] Actually, the characterization of such a kind of systems is in general highly not trivial, and can be done following two different procedure which give different results. Indeed one can consider the noise as constituting the evolution rule, so that if one computes the Lyapunov exponent he study the evolution of two trajectories with the same realization of the random sequence. Differently one can consider different realization of noise. For a detailed discussion of such systems see Refs. [101].

the same holds for the ε-entropy.

Let us conclude this Section with a brief discussion on the problem of the distinction between deterministic and stochastic systems from a time series analysis perspective. As seen before, the analysis of the dependency of the ε-entropy (or the FSLE) on the scale of observation may help us in identifying the character of a system. Therefore, by evaluating such quantities from a time series one the try to answer the question: Is the process which generates the signal stochastic or deterministic?

Actually, in order to give a definite answer to this question one has to study the behavior of such quantities in the limit $\varepsilon \to 0$, i.e.: if in this limit $h(\varepsilon)$ reaches a finite limiting value the system is deterministic and chaotic; if in this limit $h(\varepsilon) \to \infty$ the system is stochastic. However, since in experimental data one can make measure only up to a finite resolution and cannot analyze infinite sequences[20] one cannot definitively answer to such a question.

Apart from philosophical considerations, one has to resort to a pragmatic definition of the nature of the system. Usually, if for ε enough small one observes $h(\varepsilon) \approx const$, he call such a constant the KS-entropy and the system is considered to be deterministic and chaotic. However, to be honest, one cannot exclude possible randomness of the system which could appear below the resolution with which the signal can be observed.

In our opinion the unique honest point of view to be adopted is the following: one can look at the scale dependency of $h(\varepsilon)$ and $\lambda(\delta)$, and can introduce the notion of "scale dependent character of the system". Let us clarify this point with a simple example.

Let us consider the map:

$$x(t+1) = x(t) + K \sin(2\pi x(t)) + \sigma\eta(t)\,, \tag{2.51}$$

if $\sigma = 0$ this map is chaotic and, moreover, for large x values generate a Brownian motion-like behavior [17], i.e. $\langle|\delta x(t)|^2\rangle \sim t$. If $\sigma \neq 0$, one has the same behavior as before and, in addition, on scales $|\delta x| \ll \sigma$ one observes the behavior (2.50) (see Fig. 2.11).

Let us now assume that we do not know the equations of motion, we only look at a time series generated by Eq. (2.51). If we study the $\lambda(\delta)$ or $h(\varepsilon)$ on such time series, if it is enough long we should observe exactly the behavior of Fig. 2.10.

Since in general we might not be able to reach resolution $\varepsilon \ll \sigma$, in principle we cannot discern the "true" nature of the systems. However, we can use the following pragmatic

[20] We recall that the entropy and the Lyapunov exponent are defined for $t \to \infty$.

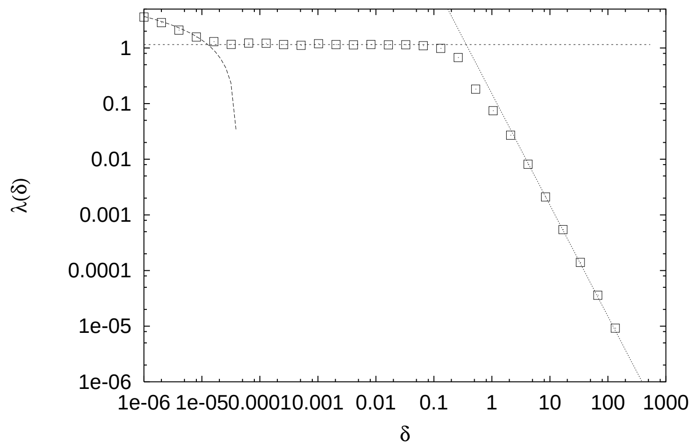

Figure 2.11: $\lambda(\delta)$ versus δ for the map (2.51), with $K = 0.8$ and $\sigma \approx 10^{-4}$. The behaviors (2.50) and the diffusive regime $\lambda(\delta) \approx 1/\delta^2$ are also shown.

classification [102]: since for $\delta \in [\delta_1, \delta_2]$ $\lambda(\delta) = const$ we consider the system having a chaotic character, but *on that scales*. In the same way since for $\delta > \delta_2$ $\lambda(\delta) \approx \delta^{-2}$ we call the system stochastic on such scales (with Brownian motion like behavior). Of course if we can have access to $\delta < \sigma = \delta_1$ we consider the system stochastic on these scales. This pragmatic approach to the distinction between the possible characters of the system avoids for misinterpretations and questionable conclusions which may sometimes appear in data analysis [21].

[21] This approach has been developed in collaboration with the time series analysis group of Dresden. For further details and a critical discussion on the possible difficulties and wrong interpretation which may arise in the context of the distinction between noise and chaos we refer to the current literature see Ref. [65] and references therein.

Chapter 3

Predictability in systems with many scales of motion

In real world one is often faced with the problem of predicting the future evolution of a certain system. This issue is particularly important, for example, in weather forecast where a tempestive prediction of some atmospheric phenomenon (e.g. storms) can be of fundamental importance for many human activities.

In predicting the evolution of systems such as the atmosphere, we are severely limited by the fact that we do not know with arbitrary accuracy both the evolution equations and the initial conditions of the system. Moreover, since these systems are usually chaotic, an infinitesimal uncertainty will amplify exponentially inhibiting our possibility of forecasting even if we had have perfect knowledge of the evolution laws. An relevant property of such systems is that many scales both in their temporal evolution and in their spatial development are involved. This aspect of the problem is particularly important once one wants to determine the limits of our ability to make prediction. In fact, despite the recognition that the evolution of atmospheric fields is chaotic, if one limits himself in searching what features can be predicted for a relatively long time he can hope to obtain partial but very important answers to the predictability problem. To exemplify this aspect, let us mention the fact that despite how the wind blows on the corner of the street is in practice unpredictable from one moment to the next, weather forecast is possible, typically, for about one week on temperate latitudes.

Specifically, in systems with many scales of motion one can hope to make some prediction on the large scales (the slower ones) or on quantities averaged on a certain time window. In this Chapter we shall address the problem of determining a quantitative indication of the amount of predictability on the large scales features of systems with several scales of motion. In particular, we discuss a simplified model characterized by two scales of motion and the predictability problem in turbulence where a hierarchy of scales exist. In the second part of the Chapter we focus on the problem of predicting the large scale features by using truncated models, which mimic the partial knowledge of the equation of motions of a certain systems.

The point of view adopted here is, in some sense, the quantitative counterpart of the "constructive" approach to the predictability problem discussed by Monin in his book [84]: [...] *Determination of the limits of predictability per se is not a constructive task (and should be an end in itself). A constructive solution of the predictability problem for extended periods must be the determination of the characteristics of the meteorological fields that are predictable for these periods.* [...].

3.1 Predictability in presence of different characteristic times

Using ideas and techniques of dynamical systems theory, there have been many progresses in understanding the growth of an uncertainty during the time evolution of a certain system. In particular, as far as infinitesimal uncertainties (δ_0) are concerned, if our purpose is to forecast the system within a tolerance Δ, the future state of the system can be predicted only up to the *predictability time* given by Eq. (2.2), which we repeat here:

$$T_p \sim \frac{1}{\lambda_{max}} \ln\left(\frac{\Delta}{\delta_0}\right) . \tag{3.1}$$

where both $\delta(0)$ and Δ are infinitesimal. Equation (3.1) gives only a first rough answer to the problem (see the discussion of Chapter 2).

In fact, already within the framework of infinitesimal perturbations there are important modifications to (3.1) [23, 25, 82] in presence of intermittency (see Sect. 2.1). Moreover, in systems with many characteristic times, e.g. 3D fully developed turbulence where a hierarchy of different space-time scales do exist, or when the threshold Δ (or the initial error δ_0) is not small, the predictability time T_p is determined by the details of the nonlinear mechanism responsible for the growth of the error through the many degrees of freedom present in the systems [7, 26, 84, 103]. In particular, T_p may have no relation with the maximum Lyapunov exponent which only rules the evolution of infinitesimal errors [9, 10].

If one try to apply blindly Eq. (3.1) to address the predictability problem one is faced with the paradox that, although the Lyapunov exponent, let us say, for the atmosphere (as a whole) is presumably rather large (essentially, due to the small scale turbulence), the large scale behaviors can be forecasted with a good accuracy for several days [84]. To overcome this apparent paradox one has to consider differently the predictability problem. The words predictability and prediction are indeed rather vague by themselves: *one has to specify for predictability of what feature against what perturbation and, in particular, against a perturbation of what size* [10, 36]. In complex and spatially extended systems one typically speaks about large-scale features and small-scale features. The predictability time of the small-scale features against a small-scale perturbation is typically shorter than that of large-scale features against a large-scale perturbation (in Sect. 2.3.2 we have seen possible exception to this behavior). This difference stems from the fact that the smallest scales are usually driven by the smallest characteristic time and spatial scales. However, the errors associated with these scales saturate very quickly and only play a marginal role any more in the error growth [7, 8, 9, 10]. Therefore, the amplification of uncertainties on the large scales evolves with the typical times (much longer) of the largest, energy containing scales [7, 71].

To be more quantitative one can use the Finite Size Lyapunov exponent (Sect. 2.3). Indeed, by spanning on different sizes of the error one is able to quantify the rates of perturbation growth at different scales. In this way one can introduce an average predictability time from an initial error δ to a given tolerance Δ, which now are no longer constrained to be infinitesimal, as [36]:

$$T_p = \int_{\delta}^{\Delta} \frac{\mathrm{d}\log \delta'}{\lambda(\delta')} \tag{3.2}$$

which reduces to (3.1) when $\lambda(\delta) = \lambda$. In generic systems one expects $\lambda(\delta)$ to be a decreasing function of δ as a consequence Eq. (3.2) gives a longer predictability time than Eq. (3.1). We stress that it exists exceptions to such a behavior (Sect. 2.3.2).

In the next Section, we study a simplified model possessing two characteristic scales.

3.1.1 Large scales predictability in a simple two-scale model

The model here considered was introduced by Lorenz [8] as a simplified model for the atmosphere dynamics which includes explicitly both large scales (synoptic scales, slow component) and small scales (convective scales, fast component). We will see that the effect of the small, fast evolving, scales becomes irrelevant for the predictability of large scale motion as soon as one considers large errors [8, 36].

The model consists of a set of large scale, slow evolving, variables x_k (representing the synoptic scales) and small scale, fast evolving, variables $y_{j,k}$ (representing the convective scales). The equation of motion are

$$\begin{aligned} \frac{dx_k}{dt} &= -x_{k-1}\left(x_{k-2}-x_{k+1}\right)-\nu x_k+F-\textstyle\sum_{j=1}^{J} y_{j,k} \\ \frac{dy_{j,k}}{dt} &= -cby_{j+1,k}\left(y_{j+2,k}-y_{j-1,k}\right)-c\nu y_{j,k}+x_k\,, \end{aligned} \tag{3.3}$$

where $k=1,...,K$ and $j=1,...,J$. As in [8] we assume periodic boundary conditions on k ($x_{K+k}=x_k$, $y_{j,K+k}=y_{j,k}$) while for j we impose $y_{J+j,k}=y_{j,k+1}$. The variables x_k represent some large scale atmospheric quantities in K sectors extending on a latitude circle, while the $y_{j,k}$ represent quantities on smaller scales in $J\cdot K$ sectors. The parameter c is the ratio between fast and slow characteristic times and b measures the relative amplitude.

Let us note that (3.3) has the same qualitative structure of a finite mode truncation of Navier-Stokes equation [36], with quadratic inertial terms and viscous dissipation. The coupling (with unit strength) is chosen in order to have the "energy"

$$E=\frac{1}{2}\left(\sum_{k=1}^{K} x_k^2+\sum_{k=1}^{K}\sum_{j=1}^{J} y_{j,k}^2\right) \tag{3.4}$$

conserved in the in-viscid, un-forced limit. The forcing term drives only the large scales and we will consider $F=10$ which is enough for developing chaos [8].

In order to understand the way in which an uncertainty grows we have performed the following numerical experiment with parameters as in [8]: $K=36$, $J=10$, $c=b=10$ implying that the typical y variable is 10 times faster and smaller than the x variable. One can define three different norms: the global Euclidean norm on both the slow and fast variables (energy norm), i.e.

$$\delta_t(t)=\sqrt{\sum_{k=1}^{K}\delta x_k^2+\sum_{k=1}^{K}\sum_{j=1}^{J}\delta y_{j,k}^2}\,, \tag{3.5}$$

a partial norm which take into account only the slow variables:

$$\delta_s(t)=\sqrt{\sum_{k=1}^{K}\delta x_k^2}\,, \tag{3.6}$$

and an analogous norm for the fast ones:

$$\delta_f(t) = \sqrt{\sum_{k=1}^{K} \sum_{j=1}^{J} \delta y_{j,k}^2} \,. \tag{3.7}$$

Then we have initialized two copies of the systems (3.3) putting a small perturbation in

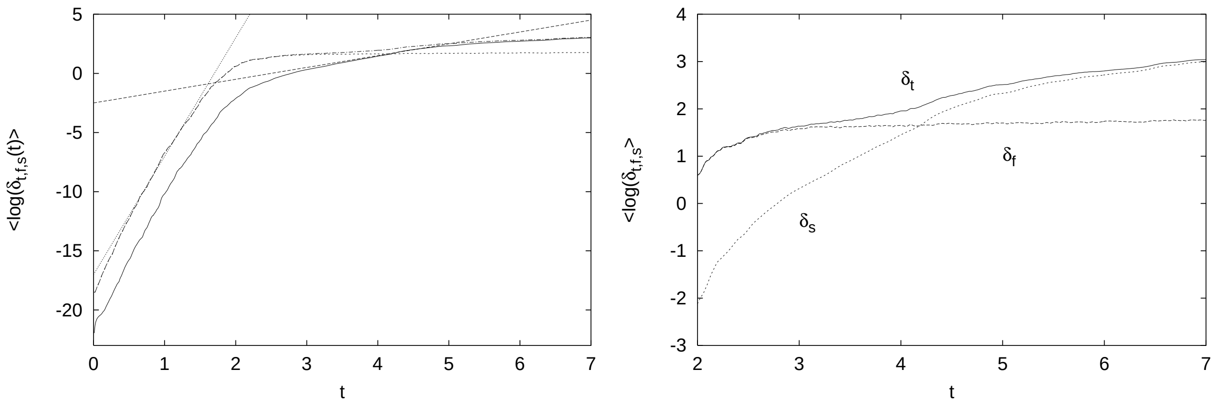

Figure 3.1: $\langle \log(\delta(t)) \rangle$ versus time for the system (3.3) with parameters and initial uncertainty as explained in the text. The three different norms $\delta_{t,s,f}$ are shown. The straight lines show the two exponential regimes as explained in the text. On the right it is shown an enlargement of the region near the saturation in order to better see the behavior of $\langle \log(\delta_t(t)) \rangle$

one of them, specifically the perturbation is taken as a random displacement on the slow and fast variable in such a way that $\delta_s = 10^{-12}$ and $\delta_f = 10^{-8}$. This difference mimics the fact that for the slow variables (the largest) one can typically be more accurate in preparing the initial conditions [36].

In Fig. 3.1 we show $\langle \log(\delta_{t,s,f}(t)) \rangle$ versus time. The following scenario comes out:

- at small times (small scales) the error growth is dominated by the fastest evolving variables. So that the initial average growth rate is given by the maximum Lyapunov exponent $\lambda_{max} \approx 10$, which characterize all the above defined norms.

- After the fastest (smallest) scales saturate to their typical r.m.s. value ($\langle y^2 \rangle^{1/2} \simeq 0.25$), the slow ones (as it is possible to see looking at $\delta_s(t)$) start to grow with the typical rate of the slow variables up to their saturation. Note that the growth is approximately exponential (the rate of which defines a sort of slow variables Lyapunov exponent).

If one looks at the total Euclidean norm (δ_t) he can immediately recognize the two above described behaviors (see the enlargement of the interesting region in Fig. 3.1).

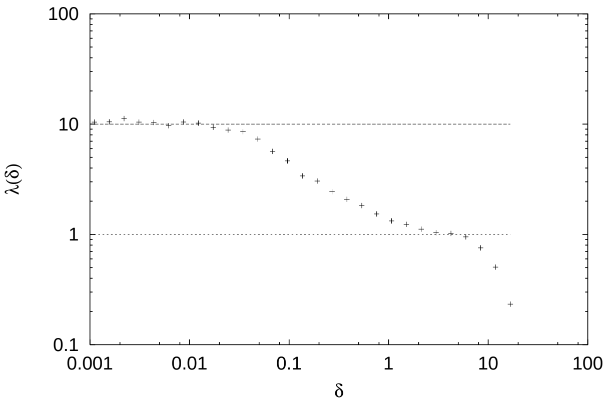

Figure 3.2: $\lambda(\delta)$ versus δ for the same parameters as Fig. 3.1. We take $\delta_{min} = 10^{-8}$ $\delta_0 = 10^{-3}$, $r = \sqrt{2}$ and we average over 1000 doubling experiments. The two lines indicate the Lyapunov exponent of the systems $\lambda_{max} \simeq 10$ and the "slow" variables Lyapunov exponent, the second small plateau at large scales.

We have then performed the computation of the FSLE for the system (3.3), the result is displayed in Fig. 3.2 (where we have used the norm on the slow components). For very small errors we observe the saturation of $\lambda(\delta)$ to the leading Lyapunov exponent of the system λ_{max}. For errors larger than the r.m.s. value of the fast variables we observe a slowing down of $\lambda(\delta)$ towards a second plateau at $\lambda_{slow} \simeq 1$, roughly corresponding to the inverse characteristic time of large scales [36].

Comparing Fig. 3.1 with Fig. 3.2 we can see that the information obtained with the two methods is very similar. Nevertheless by the FSLE one can identify in a better way the dynamical properties associated to different scales. Moreover, in the crossover regions (i.e. near the two saturation) the FSLE, by fixing the scales, prevents us from averaging growth rates which pertain to different physical regimes. Let us briefly clarify this point. Due to fluctuations (intermittency) of the instantaneous growth rate one can reach the saturation level of the fast scales with different times, so that averaging at fixed time delay causes to mix two different dynamical regimes: the fast variable dominated with the slow variable dominated [88]. This point will become much clear in Chapter 5 where we discuss the use of the FSLE in quantifying the dispersion process. Finally, in Figure 3.3 we plot the predictability time (3.2) for fixed initial error $\delta = 10^{-3}$ and different thresholds. We observe an enhancement of the predictability time for large tolerance Δ

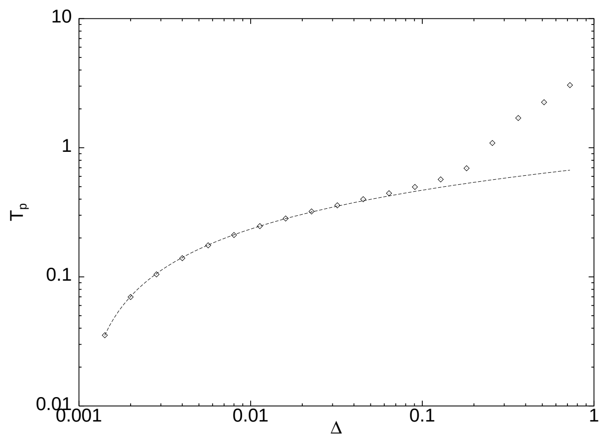

Figure 3.3: Predictability time $T_p(\delta, \Delta)$ obtained by Eq. (3.2) by using $\delta = 10^{-3}$ and varying Δ [36]

with respect to the Lyapunov exponent estimation. For large initial errors (as it is usually the case in numerical weather forecasting) the predictability time is thus independent of the Lyapunov exponent.

3.2 Predictability in Turbulence

The paradigmatic and, for many aspects, most important example of systems with many characteristic time and spatial scales is 3-D fully developed turbulence [7]. In the following we briefly review the theory of predictability for turbulent flows, mainly following the classical approach proposed by Lorenz so far [7], see also Refs. [103, 71]. We also discuss the approach proposed by Aurell et al. [9, 10], who introduced the FSLE to study this problem.

In three dimensional fully developed turbulence (see Sect. 1.2.2), the inverse of the maximum Lyapunov exponent is roughly proportional to the smallest characteristic time of the system, the turn-over time τ_D of eddies of the size of the Kolmogorov length ℓ_D. The argument, due to Ruelle [27], is the following. The Kolmogorov theory (1941) predicts that the longitudinal velocity difference at distance $\ell = |\mathbf{l}|$, in the inertial range ($\ell_D \ll \ell \ll \ell_E$) scales as

$$v(\ell) \equiv |\mathbf{v}(\mathbf{x}+\mathbf{l}) - \mathbf{v}(\mathbf{x})| \sim V_E \left(\frac{\ell}{\ell_E}\right)^h , \tag{3.8}$$

where $h = 1/3$ (see also Sect. 1.2.2). Ignoring intermittency, the Kolmogorov scale ℓ_D can be defined balancing inertial and dissipative terms, i.e. $\nu \sim \ell_D\, v(\ell_D)$, thus from (3.8) one has

$$\eta \sim \ell_E \, Re^{-3/4} \, . \tag{3.9}$$

The corresponding eddy turn-over time, τ_D is

$$\tau_D = \tau(\ell_D) \sim \frac{\ell_D}{v(\ell_D)} \sim T_E \left(\frac{\ell_D}{\ell_E}\right)^{2/3} , \tag{3.10}$$

where $T_E = \ell_E/V_E$ can be thought as the life time of the large scale disturbances.

From these dimensional relations one can estimate the maximum Lyapunov exponent as [27]

$$\lambda_{max} \sim \frac{1}{\tau(\ell_D)} \sim \frac{1}{T_E} \, Re^{1/2} \, . \tag{3.11}$$

As a consequence of Eq. (3.11) one has that the higher is the Reynolds number the shorter is the predictability time, which is identified by the inverse of the Lyapunov exponent. However, this is true only for infinitesimal perturbations and, also in this case, taking into account the intermittency one expects that the presence of laminar periods changes the chaotic features of the fluid flow (Sect. 2.1). The intermittency can be described by introducing a spectrum of singularities h of the velocity differences [6, 47, 48], i.e. assuming a local scaling invariance so that in any point $\mathbf{x}$ of the fluid $v(\ell) \sim \ell^{h(\mathbf{x})}$. In the framework of the multifractal approach, one thus finds [25]

$$\lambda \sim \frac{1}{T_E} \, Re^{\alpha} \, , \qquad \text{with } \alpha = \max_h \left[\frac{D(h) - 2 - h}{1 + h} \right] , \tag{3.12}$$

where $D(h)$ is the fractal dimension of the set of fluid points characterized by a given singularity h. The value of α depends on $D(h)$. By using a $D(h)$ obtained by fitting the exponents ζ_q (1.45) of the velocity structure functions, one finds $\alpha = 0.459...$, slightly smaller than the Ruelle prediction $\alpha = 0.5$ [27]. In any case to characterize predictability on large scales one has to resort to a different approach.

From a different point of view, without considering infinitesimal disturbances, Lorenz [7], see also Ref. [71], proposed the following phenomenological approach to the predictability problem in turbulence. Let us translate the problem in k-space. Consider wave-numbers around k corresponding typical spatial scale $\ell \sim k^{-1}$. The time $\tau(k)$ which needs a perturbation at wavenumber $2k$ to induce a complete uncertainty on the velocity field on the wave number k can be assumed to be proportional to the eddy turn-over time at scale ℓ, i.e., from (3.8):

$$\tau(\ell) \sim \frac{\ell}{v(\ell)} \sim T_E \left(\frac{\ell}{\ell_E}\right)^{2/3} . \tag{3.13}$$

Therefore, a disturbance on the smallest scales, $O(v(\ell_D))$, propagates through an *inverse cascade* from the Kolmogorov scale $\eta \sim k_D^{-1}$ up to the scale of the energy input $\ell_E \sim k_0^{-1}$. The predictability time, T_p, on the large scales is then given by the sum [103]:

$$T_p = \sum_{n=0}^{N} \tau(2^n \ell_E) \,, \tag{3.14}$$

where $N = \log_2(k_D/k_0) \sim \log Re$, we have divided the k space in octaves for simplicity. The leading term of the geometric series (3.14) is given for $n = N$, hence T_p is practically independent of Reynolds number:

$$T_p \sim T_E \sim \ell_E / V_E \,. \tag{3.15}$$

A direct consequence of the Lorenz picture of an inverse cascade of a perturbation is that one can also estimate the growth of a perturbation at intermediate times. After a time t, a perturbation, initially localized on the Kolmogorov length scale, is expected to affect eddies of size ℓ_t such that $\tau(\ell_t) \sim t$. So that by inverting Eq. (3.13) one has

$$\ell_t \sim \ell_E \left(\frac{t}{T_E}\right)^{3/2} \,. \tag{3.16}$$

Then, the amplitude of the difference $\delta\mathbf{v}(t)$ between two velocity fields at time t can be estimated as the typical velocity difference at scale ℓ_t, and thus, from (3.8) and (3.16) it follows [103]

$$|\delta\mathbf{v}(t)| \sim v(\ell_t) \sim V_E \sqrt{t/T_E} \,. \tag{3.17}$$

Hence, perturbations grow as square root of time. It is worth to remark that such perturbations are no longer infinitesimal so that the inverse cascade picture is not in contradiction with the exponential amplification of errors on initial conditions that is always present in chaotic systems.

There are two main predictions of the Lorenz approach: predictability time on large scale independent of Reynolds number and growth of perturbations as a power of time instead of an exponential for scales inside the inertial range. In particular, inverting equation (3.17) and indicating with δ the velocity difference $\delta = |\delta v(t)|$, one has that the predictability time with respect to a perturbation of size δ is given by

$$\tau(\delta) \sim \frac{\ell_E}{V_E} \left(\frac{\delta}{V_E}\right) \tag{3.18}$$

and, therefore, from a computation of the FSLE for a turbulent flows one expects that for enough large perturbations [9]

$$\lambda(\delta) \sim \frac{1}{\tau(\delta)} \sim \delta^{-2} . \tag{3.19}$$

We conclude this Section by noting that this power law is not affected by intermittency correction [9], and that intermittency only play a role in the crossover region between the exponential regime $\lambda(\delta) = \lambda \sim Re^{\alpha}$ and the δ^{-2} regime. See Ref. [9, 10] for further details.

3.3 Predictability of large scales motion in truncated models

In the prediction of the evolution of a system, e.g. the atmosphere, one is severely limited by the fact that we do not know with arbitrary accuracy the initial conditions of the system, which are usually determined only with a finite resolution (i.e. by a finite number of observations) [84].

However, in real systems one must also cope with the lack of knowledge of the evolution equations, and even with perfect knowledge of the evolution laws one is often limited by the finite computational resources. For instance in systems described by PDE, once one wants to make numerical computations he has to make unavoidable approximations such as finite difference approximations and, in order to reduce the number of degrees of freedom, to neglect some components in the equations of motion (typically the fast ones). In this part of the Chapter we address the predictability problem in such a situation. In particular, we have in mind the cases in which one wants to forecast the large scale features of some phenomena by using an imperfect model in which one neglects the small and fast evolving components.

To make more precise our discussion let us start by considering a system described by a differential equation:

$$\frac{d}{dt}\mathbf{x}(t) = \mathbf{f}(\mathbf{x}, t) , \quad \mathbf{x}, \mathbf{f} \in \mathcal{R}^n . \tag{3.20}$$

As a matter of fact we do not know exactly the equations, and we have to devise a model which is different from the "true" dynamics

$$\frac{d}{dt}\mathbf{x}(t) = \mathbf{f}_{\sigma}(\mathbf{x}, t) \quad \text{where} \quad \mathbf{f}_{\sigma}(\mathbf{x}, t) = \mathbf{f}(\mathbf{x}, t) + \sigma\delta\mathbf{f}(\mathbf{x}, t) . \tag{3.21}$$

where σ measures the deviation from the true equations. Therefore, it is natural to wonder about the relation between the true evolution (*reference* or *true* trajectory $\mathbf{x}_T(t)$) given by (3.20) and that one effectively computed (*perturbed* or *model* trajectory $\mathbf{x}_M(t)$) given by (3.21). This problem is referred to as *predictability of the second kind*, in contrast with the case in which one has uncertainties on the initial conditions which is referred as *predictability of the first kind*.

Let us make some general remarks. At the foundation of the second kind predictability problem there is the issue of *structural stability* [37, 2]: since the evolution laws are known only with finite precision it is highly desirable that at least certain properties are not too sensitive on the details of the equations of motion. For example, in a system with a strange attractor, small generic changes in the evolution laws should not change drastically the dynamics (see Ref. [104] for a simple example with non generic perturbation).

In dynamical systems theory, the problems of first and second kind predictability are essentially understood in the limit of infinitesimal perturbations. Indeed, in chaotic systems the effects of a small generic uncertainty on the evolution laws are similar to those due to the finite precision on the initial condition [105]. The model trajectory, $\mathbf{x}_M(t)$, generated by perturbed dynamics (3.21) diverges exponentially from the reference trajectory, $\mathbf{x}_T(t)$, produced by Eq. (3.20) with a mean rate roughly given by the Lyapunov exponent of the original system. The statistical properties (e.g. correlation functions) are not strongly modified[1].

However, as discussed in the first part of the Chapter, as far as finite perturbations are concerned, the leading Lyapunov exponent is not any longer important for the predictability issue and a more suitable characterization can be achieved in terms of the Finite Size Lyapunov Exponent.

Also in the case of second kind predictability one has to deal with errors which are far from being infinitesimal. Indeed, in real systems the size of an uncertainty on the evolution equations is determinable only *a posteriori*, on the basis of the ability of the model equations to reproduce some of the features of the phenomenon. Typical examples are systems described by PDE where in numerical computation one is usually forced to cut some degrees of freedom off (i.e. the small scales components).

In the following we analyze the effects of limited resolution on the predictability of the

[1] This last fact has been frequently related to the *shadowing lemma* [3, 37]: almost all trajectories of the true system can be approximated by a trajectory of the perturbed system starting from a slightly different initial condition. However, the shadowing lemma can be proven only in special cases [37, 105] and therefore it cannot be straightforwardly invoked to explain the statistical *reproducibility* in a generic case.

large scale features. This raises two problems: in first place one has to deal with perturbations of the evolution equations which, in general, cannot be considered small; second, the parameterization of the unresolved modes. The finite size Lyapunov exponent fits very well the first point, being able to characterize and quantify the effects of uncertainty on the evolution laws at different scales. As regards the second point, one can define the optimal parameterization as that one for which the predictability on the large scales is not worse than the *intrinsic predictability* of the system (i.e. due to uncertainties on the initial conditions) [106]. We shall show that with some phenomenological parameterizations one can recover on large scales the intrinsic predictability of the system. This is highly not obvious in systems with some *feedback* from the large scales toward the small ones.

3.3.1 Effects of small uncertainties and structural stability

In the *second kind predictability problem*, we can distinguish three general cases depending on the original dynamics. In particular, equation (3.20) may display:

(i) trivial attractors: asymptotically stable fixed points or attracting periodic orbits;

(ii) marginally stable fixed points or periodic/quasi-periodic orbits as in integrable Hamiltonian systems;

(iii) chaotic behavior.

In case (i) small changes in the equations of motion do not modify the qualitative features of the dynamics. Case (ii) is not generic and the outcome strongly depends on the specific perturbation $\delta\mathbf{f}$, i.e. it is not structurally stable. In the chaotic case (iii) one expects that the perturbed dynamics is still chaotic. Here we will consider only the case (iii).

Let us also mention that in numerical computations of evolution equations (e.g. differential equations) there are two unavoidable sources of errors: the finite precision representation of the numbers, which causes the computer phase space to be necessarily discrete, and the round-off errors, which introduces a sort of noise. Because of the discrete nature of the phase space of the system studied on computer, orbits numerically computed have to be periodic. Nevertheless the period is usually very large, apart for very low computer precision [105]. We do not consider here this source of difficulties. The round-off produces on Eq. (3.20) a perturbation which can be written as $\delta\mathbf{f}(\mathbf{x},t) = \mathbf{w}(\mathbf{x})\,\mathbf{f}(\mathbf{x},t)$ and $\sigma \sim 10^{-\alpha}$ (α =number of digits in floating point representation) where $\mathbf{w} = O(1)$ is an unknown function which may depend on $\mathbf{f}$ and on the software of the computer [107]. In general, the round-off error is very small and may have, as much as the noise, a positive role, as underlined by Ruelle [27], in selecting the physical probability measure, the so-called *natural measure*, from the set of ergodic invariant measures (see Sect. 1.1.1).

In chaotic systems the effects of a small uncertainty on the evolution law is, for many aspects, similar to those due to imperfect knowledge of initial conditions. This can be understood by the following example. Consider the Lorenz equations [1]

$$\begin{aligned} \frac{dx}{dt} &= 10(y-x) \\ \frac{dy}{dt} &= Rx - y - xz \\ \frac{dz}{dt} &= xy - 8/3z\,. \end{aligned} \tag{3.22}$$

In order to mimic, e.g, an experimental error in the determination of the evolution law we consider a small error, σ, on the parameter R: $R \to R+\sigma$. Let us consider the difference $\Delta\mathbf{x}(t) = \mathbf{x}_M(t) - \mathbf{x}_T(t)$ with, for simplicity, $\Delta\mathbf{x}(0) = 0$, i.e. we assume a perfect knowledge of the initial conditions[2]. From here we use the symbol T to indicate the "true" (reference) trajectories and M the "model" (perturbed) trajectories. One has, with obvious notation:

$$\frac{d\Delta\mathbf{x}}{dt} = \mathbf{f}_\sigma(\mathbf{x}_M) - \mathbf{f}(\mathbf{x}_T) \simeq \frac{\partial \mathbf{f}}{\partial \mathbf{x}}\Delta\mathbf{x} + \frac{\partial \mathbf{f}_\sigma}{\partial R}\sigma\,. \tag{3.23}$$

At time $t=0$ one has $|\Delta\mathbf{x}(0)| = 0$, therefore $|\Delta\mathbf{x}(t)|$ initially grows only by the effect of the second term in (3.23). At later times, when $|\Delta\mathbf{x}(t)| \approx O(\sigma)$ the leading term of (3.23) becomes the first one, and we recover the *first kind predictability problem* for an initial uncertainty $\delta_0 \sim \sigma$. Therefore, apart from an initial (not particularly interesting) growth, which depends strongly on the specific perturbation, the evolution of $< \ln|\Delta\mathbf{x}(t)| >$ follows the usual linear growth with the slope given by λ. Typically the value of the Lyapunov exponent computed by using the "model" dynamics differs from the "true" one by a small amount, i.e. $\lambda_M = \lambda_T + O(\sigma)$ [105].

This scenario is particularly clear looking at the FSLE behavior. We computed $\lambda_{TT}(\delta)$, the FSLE for the true equations (i.e. on two trajectories with slightly different initial conditions), and $\lambda_{TM}(\delta)$, the FSLE computed following the distance between one true trajectory and one model trajectory starting at the same point. These are shown in

[2]Of course in generic cases we have a partial knowledge both on the initial conditions and on the evolution laws

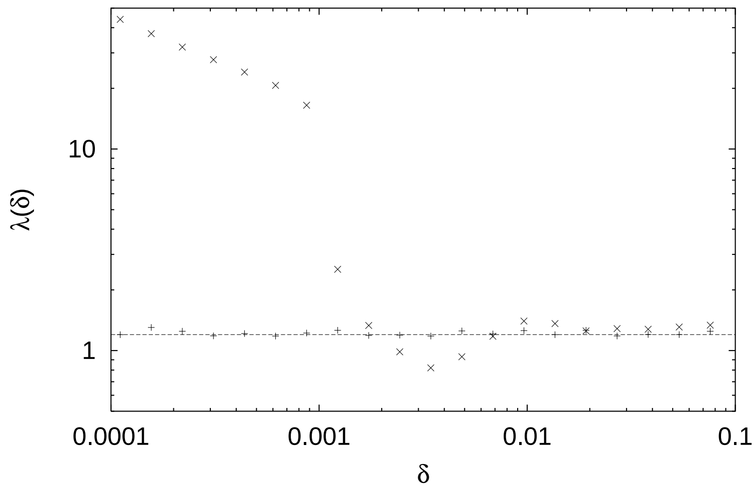

Figure 3.4: Finite Size Lyapunov Exponents $\lambda_{TT}(\delta)$ ($+$) and $\lambda_{TM}(\delta)$ ($\times$) versus δ for the Lorenz model [8] (3.22) with $R = 45$ and $\sigma = 0.001$. The dashed line represents the leading Lyapunov exponent for the unperturbed system ($\lambda \approx 1.2$). The statistics is over 10^4 realizations.

Figure 3.4. The true FSLE $\lambda_{TT}(\delta)$ displays a plateau indicating a chaotic dynamics with leading Lyapunov exponent $\lambda \simeq 1$. Concerning the second kind predictability for very small errors, $\delta < \sigma$, where the growth of the error is dominated by the second term in (3.23), we have $\lambda_{TM}(\delta) > \lambda_{TT}(\delta)$; for $\delta > \sigma$ the second term in (3.23) becomes negligible and we observe the transition to the Lyapunov exponent $\lambda_{TM}(\delta) \simeq \lambda_{TT}(\delta) \simeq \lambda$.

This example shows that it is possible to recover the intrinsic predictability (for $\delta > \sigma$) of a chaotic system even in presence of some uncertainty in the model equations. This is rather clear and intuitive for infinitesimal perturbations. The case of non infinitesimal perturbation is more subtle.

In the following we will consider more complex situations, in which interacting degrees of freedom with different characteristic times are involved. In these cases the correct parameterization of the unresolved modes is crucial for the prediction of large scale behavior [106].

3.3.2 Systems with two scales of motion

Before analyzing in detail the effects of non infinitesimal uncertainties on the evolution laws in some specific models let us clarify our aims. Let us consider a dynamical system which can be written as follows:

$$\begin{aligned} \frac{d\mathbf{x}}{dt} &= \mathbf{f}(\mathbf{x},\mathbf{y}) \\ \frac{d\mathbf{y}}{dt} &= \mathbf{g}(\mathbf{x},\mathbf{y})\,, \end{aligned} \tag{3.24}$$

where $\mathbf{f},\mathbf{x} \in \mathcal{R}^n$ and $\mathbf{g},\mathbf{y} \in \mathcal{R}^m$, in general $n \neq m$. Now, let us suppose that the fast variables, $\mathbf{y}$, cannot be resolved: a typical example are the sub-grid modes in PDE discretizations. In this framework, a natural question is: how must we parameterize the unresolved modes ($\mathbf{y}$) in order to predict the resolved modes ($\mathbf{x}$) ?

As discussed by Lorenz [8], to reproduce – at a qualitative level – a given phenomenology, e.g. his example is the El Niño Southern Oscillation (ENSO) phenomenon, one can drop out the small scale features without negative consequences. But one unavoidably fails in forecasting the ENSO (i.e. the actual trajectory) without taking into account in a suitable way the small scale contributions. In other words reproducing the statistics of some events does not mean to be able to predict them. The best one can hope is to parameterize the small scales in order to recover the intrinsic predictability of the system (i.e. to have $\lambda_{TM}(\delta) \approx \lambda_{TT}(\delta)$ for enough large δ).

An example in which it is relatively simple to devise a model for the fast modes is represented by skew systems, i.e.

$$\begin{aligned} \frac{d\mathbf{x}}{dt} &= \mathbf{f}(\mathbf{x},\mathbf{y}) \\ \frac{d\mathbf{y}}{dt} &= \mathbf{g}(\mathbf{y})\,. \end{aligned} \tag{3.25}$$

In this case, the fast modes ($\mathbf{y}$) do not depend on the slow ones ($\mathbf{x}$). One can expect that in this case, neglecting the fast variables or parameterizing them with a suitable stochastic process, should not drastically affect the prediction of the slow variables [108].

On the other hand, if $\mathbf{y}$ feels some feedback from $\mathbf{x}$, we cannot simply neglect the unresolved modes. In Appendix B we discuss this point in detail. In practice, one has to construct an *effective equation* for the resolved variables:

$$\frac{d\mathbf{x}}{dt} = \mathbf{f}_M(\mathbf{x},\mathbf{y}(\mathbf{x}))\,, \tag{3.26}$$

where the functional form of $\mathbf{y}(\mathbf{x})$ and $\mathbf{f}_M$ are found by phenomenological arguments and/or by numerical studies of the full dynamics. A possibility which is described in Appendix B is to construct $\mathbf{y}(\mathbf{x})$ by mean of conditioned averages. Of course this method is possible only if one knows the full equations of motion.

Let us now come back to the example discussed in Sect. 3.1.1 by reconsidering it from the point of view of *second kind predictability*. If one is interested in forecasting the large scale behavior of the model by using only the slow variables x_k, a natural choice for the effective equations is:

$$\frac{dx_k}{dt} = -x_{k-1}\left(x_{k-2} - x_{k+1}\right) - \nu x_k + F - G_k(\mathbf{x}) \, , \tag{3.27}$$

where $G_k(\mathbf{x})$ represents the parameterization of the fast components in (3.27) (see Appendix B). The FSLE for the true system is shown in Figure 3.5 and displays the two

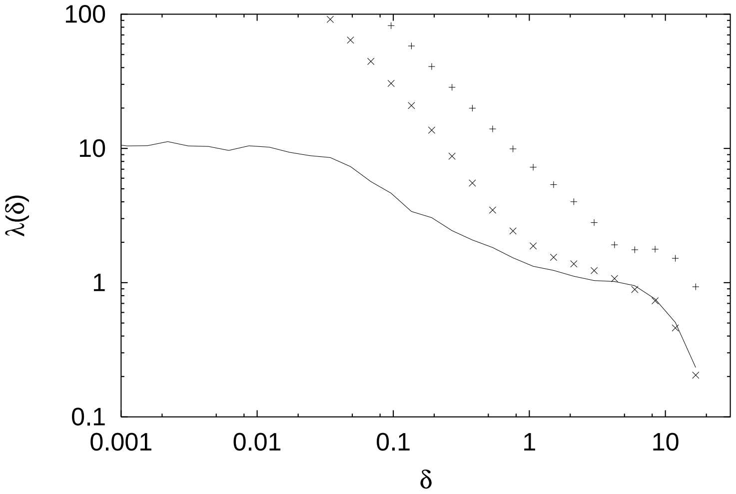

Figure 3.5: Finite Size Lyapunov Exponents for the Lorenz '96 model $\lambda_{TT}(\delta)$ (solid line) and $\lambda_{TM}(\delta)$ versus δ obtained by dropping the fast modes ($+$) and with the parameterization ($\times$) discussed in (3.27) and (3.28). The parameters are as in Figure 3.1. The value of $\nu_e = 4$ is chosen after a numerical integration of the complete equations as discussed in Appendix B.

characteristic plateaus corresponding to the fast component (for $\delta \ll 0.1$) and the slow component for large δ . Figure 3.5 also shows what happens when one simply neglects the fast components $y_{j,k}$ (i.e. $\mathbf{G}(\mathbf{x}) = 0$). At very small δ one has $\lambda_{TM}(\delta) \simeq \delta^{-1}$. This behavior can be understood by noticing that if $\delta \ll \sigma$, the error grows as $d\delta/dt \sim \sigma$ and thus $\lambda_{TM} \sim \sigma/\delta$.

For large errors we observe that, with this rough approximation, we are not able to recover the intrinsic predictability of the original system. More refined parameterizations in terms of stochastic processes with the correct probability distribution function and correlation times do not improve the forecasting ability.

The reason for this failure is the presence of a feedback term in the equations (3.27) which induces strong correlations between the variable x_k and the unresolved coupling $\sum_{j=1}^{J} y_{j,k}$. Therefore, in order to devise a model which is able to make a "good" forecasting of the large scales motion only in terms of the large scale (slow) variables, one has to insert the effect of the fast neglected variables so as to take into account these correlations, at least in a phenomenological way. Following the strategy discussed in Appendix B, we build an effective equation of the type (3.26-3.27) in which the fast modes are substituted by a function of the slow ones which mimics the conditioned average of the former with respect to the latter ones. This average is obtained by a numerical simulation of the full system and the result is:

$$G(\mathbf{x}) = \nu_e x_k \,, \tag{3.28}$$

where ν_e is a numerically determined parameter. Figure 3.5 shows that, although the small scales are not resolved, the large scales predictability is well reproduced, indeed one has $\lambda_{TM}(\delta) \simeq \lambda_{TT}(\delta)$ for large δ.

3.3.3 Eddy viscosity and predictability in a model for turbulence

We now consider a more complex system which mimics the energy cascade in fully developed turbulence. The model is in the class of the so called *Shell Models* introduced some years ago [70] for a dynamical description of small-scale turbulence. For a recent review on Shell Models see [6] (see also Sect. 1.2.2). This model has relatively few degrees of freedom but, at the same time, involves many characteristic scales and times. The velocity field is assumed isotropic and it is decomposed on a finite set of complex velocity components u_n representing the typical turbulent velocity fluctuation on a "shell" of scales $\ell_n = 1/k_n$. In order to reach very high Reynolds number with a moderate number of degrees of freedom, the scales are geometrically spaced as $k_n = k_0 2^n$ $(n = 1, \ldots N)$.

The specific model here considered has the form [109]

$$\frac{du_n}{dt} = i\left(k_{n+1}u^*_{n+1}u_{n+2} - \frac{1}{2}k_n u^*_{n-1}u_{n+1} + \frac{1}{2}k_{n-1}u_{n-2}u_{n-1}\right) - \nu k_n^2 u_n + f_n \,, \tag{3.29}$$

where ν represent the kinematic viscosity and f_n is a forcing term which is restricted only to the first two shells (in order to mimic large scale energy injection).

Without entering in the details, we recall that the Shell Model (3.29) displays an energy cascade *à la* Kolmogorov from large scales (small n) to dissipative scales ($n \sim N$)

with a statistical stationary energy flux. Scaling laws for the average velocity components are observed:

$$\langle |u_n^p| \rangle \simeq k_n^{-\zeta_p} \,, \tag{3.30}$$

with exponents close to the Kolmogorov 1941 values (i.e. $\zeta_p = p/3$), apart from intermittent corrections which are compatible with that measured in turbulent flows [6].

Neglecting this (small) intermittency effects, a dimensional estimate of the characteristic time (eddy turnover time, i.e. the typical time after which $u_n(t)$ is practically independent of $u_n(0)$) for scale n gives

$$\tau_n \simeq \frac{\ell_n}{|u_n|} \simeq k_n^{-2/3} \,. \tag{3.31}$$

The scaling behavior holds up to the Kolmogorov scale $\eta = 1/k_D$, defined as the scale at which the dissipative term in (3.29) becomes relevant. Analogously to the case of turbulence, the Lyapunov exponent of the turbulence can be estimated as the fastest characteristic time τ_D and one obtains exactly the result (3.11), i.e. $\lambda \sim 1/\tau_D \sim Re^{1/2}$, where here the Reynolds number $Re \propto 1/\nu$. It is possible to predict the behavior of the FSLE by observing that the faster scale k_n at which an error of size δ is still active (i.e. below the saturation) is such that $u_n \simeq \delta$. Thus $\lambda(\delta) \sim 1/\tau_n$ and, using Kolmogorov scaling, one obtains [7, 9](see also Sect. 3.1.1)

$$\lambda_{TT}(\delta) \sim \begin{cases} \lambda & \text{for} \quad \delta \leq u_D \\ \delta^{-2} & \text{for} \quad u_D \leq \delta \leq u_0 \end{cases} . \tag{3.32}$$

To be more precise there is an *intermediate range* (due to intermittency) between the two showed in (3.32). For a discussion on this point see [9, 10].

In order to simulate a finite resolution in the model, we consider a modelization of (3.29) in terms of an *eddy viscosity* [110]

$$\frac{du_n}{dt} = i\left(k_{n+1}u_{n+1}^* u_{n+2} - \frac{1}{2}k_n u_{n-1}^* u_{n+1} + \frac{1}{2}k_{n-1}u_{n-2}u_{n-1}\right) - \nu_n^{(e)} k_n^2 u_n + f_n \,, \tag{3.33}$$

where now $n = 1, ..., N_M < N$ and the eddy viscosity, restricted to the last two shells, has the form

$$\nu_n^{(e)} = \kappa \frac{|u_n|}{k_n} \left(\delta_{n,N_M-1} + \delta_{n,N_M}\right) \,, \tag{3.34}$$

κ is a constant of order 1 (see Appendix B). The model equations (3.33) are for the Shell Models the analogous of Large Eddy Simulation (LES) for turbulence. LES is one of the most popular numerical scheme for integrating large scale flows [69]. Thus, although

Shell Models are not realistic models for large scale geophysical flows (being nevertheless a good model for small scale turbulent fluctuations), the study of the effect of truncation in term of eddy viscosity is of general interest. In Figure 3.6 we show $\lambda_{MM}(\delta)$, i.e. the

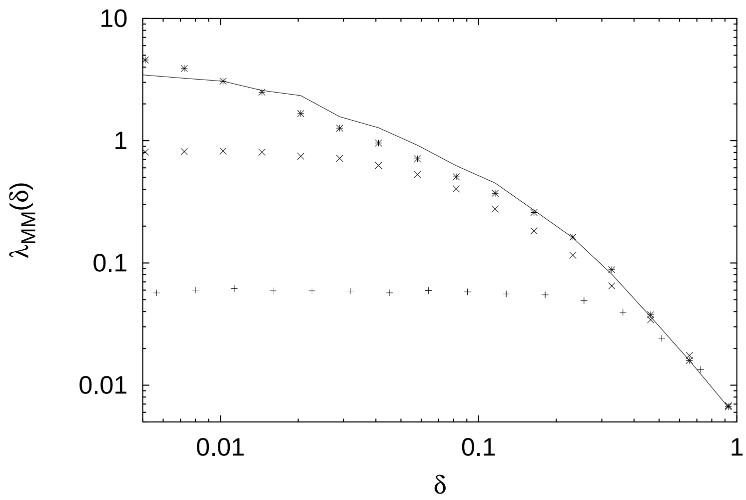

Figure 3.6: The FSLE for the eddy-viscosity shell model (3.33) $\lambda_{MM}(\delta)$ at various resolutions $N_M = 9(+), 15(\times), 20(*)$. For comparison it is drawn the FSLE $\lambda_{TT}(\delta)$ (continuous line). Here $\kappa = 0.4$, $k_0 = 0.05$.

FSLE computed for the model equations (3.33) with $N = 24$ at different resolutions $N_M = 9, 15, 20$. A plateau is detected for small amplitudes of the error δ, corresponding to the leading Lyapunov exponent, which increases with increasing resolution – being proportional to the fastest time-scale – according to $\lambda \sim k_{N_M}^{2/3}$. At larger δ the curves collapse onto the $\lambda_{TT}(\delta)$, showing that large-scale statistics of the model is not affected by the small-scales resolution. The capability of the model to predict satisfactorily the large scales features of the "true" dynamics is not determined by $\lambda_{MM}(\delta)$ but by $\lambda_{TM}(\delta)$, which is shown in Figure 3.7.

Increasing the resolution $N_M = 9, 15, 20$ towards the fully resolved case $N = 24$ the model improves, in agreement with the expectation that λ_{TM} approaches λ_{TT} for a perfect model. At large δ the curves practically coincide, showing that the predictability time for large error sizes (associated with large scales) is independent on the details of small-scale modeling. Better resolved models achieve $\lambda_{TM} \simeq \lambda_{TT}$ for smaller values of the error δ.

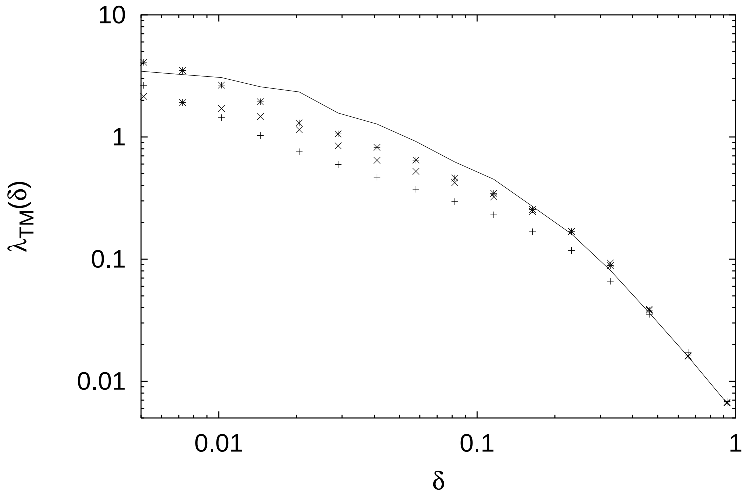

Figure 3.7: The FSLE between the eddy-viscosity shell model and the full shell model $\lambda_{TM}(\delta)$, at various resolutions $N_M = 9(+), 15(\times), 20(*)$. For comparison it is drawn the FSLE $\lambda_{TT}(\delta)$ (continuous line). The total number of shell for the complete model is $N = 24$, with $k_0 = 0.05$, $\nu = 10^{-7}$.

3.4 Final Remarks

The effects of uncertainties of the initial conditions or of the evolution laws on the predictability properties are investigated[3] and quantitatively characterized by means of the Finite Size Lyapunov Exponent. In particular, we have considered systems involving several characteristic scales and times. Regarding the problem of characterizing the predictability with respect to imperfect knowledge of the initial conditions one has that by using the FSLE one can properly characterize the predictability of the large scales features.

As far as uncertainties on evolution equations are concerned, we have shown that in systems where there is a feedback on the small (unresolved) scales by the large (resolved) scales, the dynamics of the former ones cannot be thoroughly discarded, without affecting the ability to forecast the large scales features. For the general case, there are not systematic procedures to construct a "good" model for the small unresolved scales. With the term "good" model we mean a model such that the predictability due to uncertainties on the evolution laws is not worse than the intrinsic predictability of the true system. However, the FSLE analysis has shown that by suitable phenomenological parameterizations of the small scales, e.g. the eddy-viscosity modelization in turbulence, the ability

[3] For the first one we have mainly reviewed previous works, the second one is an original contribution of this thesis

to predict the large scales is basically the same one has in the case of uncertainties of the same size on the initial conditions.

Chapter 4

Dynamics of perturbations in high dimensional systems

In this Chapter we study the dynamics of perturbations in Globally Coupled Maps (GCM) displaying non-trivial collective motion (in particular, irregular dynamics of macroscopic variables such as, e.g., the mean field), and the propagation of initially localized perturbations in CMLs characterized by a velocity for the perturbation propagation greater than that predicted by the linear analysis.

In both cases the Finite Size Lyapunov Exponent turns out to be a good indicator to characterize the systems behaviors. Indeed in GCM, macroscopic motion is typically associated with the emergence of a time scales separation (generated by the dynamics itself) and, therefore, the discussions of the previous Chapter apply. In the second case, the propagation is entirely due to non linear effects which cannot be captured by the linear analysis (specifically by the comoving Lyapunov exponent, see Sect. 2.2.2). We shall show that a suitable generalization of the FSLE to a comoving reference frame is able to predict the value of the velocity of propagation.

4.1 Collective motion in Globally coupled maps

In the last few years the emergence of *non-trivial collective behaviors* in high dimensional systems has gathered much attention [30, 31, 111, 112, 113, 114, 115, 116]. One of the most popular models in this field is an ensemble of globally coupled chaotic elements. Such systems arise naturally in the description of Josephson arrays [117], certain multi-mode laser systems [118], in biological systems such as fish locomotion, oscillatory neural systems (see reference therein Ref. [61]), and the dynamics of vortices in two-dimension.

In this Section we study Globally Coupled Maps (GCM), which are a sort of mean-filed theory-type extension of coupled map lattices (Sect. 1.2.1), i.e. a collection of elements x_n evolving according to the following equation:

$$x_n(t+1) = (1-\epsilon) f_a(x_n(t)) + \frac{\epsilon}{N} \sum_{i=1}^{N} f_a(x_i(t)), \tag{4.1}$$

where N is the total number of elements, t is the discrete time, $f_a(x)$ is a nonlinear function depending on a parameter a and ϵ measures the strength of the coupling.

When the local map is the logistic map[1] $(f_a(x) = ax(1-x))$, varying ϵ and a one can observe the following phenomenology [113]:

a- *Coherent phase*: global synchronization, i.e. all the element assume the same value.

b- *Ordered phase* or *clustering*: partial synchronization, i.e. the elements split into few clusters (k), such that the elements belonging to the same cluster k take an identical value $\tilde{x}_k(t)$

c- *Turbulent phase*: the elements are desynchronized, i.e. they assume different values in an almost random way.

In the phase (b), it has been shown that the number, $\mathcal{C}$, of the possible clusters can be very large with N ($\ln \mathcal{C} \sim \sqrt{N}$) and the dynamics can show a glass-like behavior with the failure of ergodicity [112, 113]. Beyond global synchronization (a) and clustering (b) other type of non-trivial collective motions can appear also in the fully desynchronized phase (c). For instance, Kaneko [30] studied a parameters region where the number of positive Lyapunov exponents is proportional to N; in this region the elements x_n are desynchronized so that one might expect, by the law of large numbers, that the temporal fluctuations of the mean-field

$$h(t) = \frac{1}{N} \sum_{i=1}^{N} f_a(x_i(t)) \tag{4.2}$$

or, equivalently, the fluctuation of the center of mass[2], $m(t) = 1/N \sum_{i=1,N} x_i(t)$, obey a Gaussian statistics, with a mean square deviation $\sigma_N^2 = \langle h^2 \rangle - \langle h \rangle^2$ proportional to N^{-1}. Actually, one observes that the temporal evolution of $h(t)$ displays behaviors ranging from

[1] The phenomenology described in this Section is indeed rather generic and holds also for others local maps.

[2] Indeed, $m(t) = h(t-1)$.

periodic-like motion (plus fluctuations) to chaotic-like (see Sect. 4.1.1). Similar behaviors have been also observed in coupled map lattices with local coupling and certain *Cellular Automata* on d-dimensional lattices for enough high dimension d [111].

Here, we address the problem of *macroscopic chaos*, i.e. the irregular (chaotic-like) behavior of some global variables (e.g. $h(t)$) which evolve with typical times much longer than the characteristic time of the full dynamics (the microscopic dynamics); the latter time is essentially given by the inverse of the first Lyapunov exponent λ_1 of the full (microscopic) dynamics

Macroscopic chaos in high dimensional maps can be viewed, in some sense, as the analogous of *hydro-dynamical chaos* for molecular motion [33]. For a Hamiltonian dynamical system describing the evolution of the molecules of a fluid the microscopic characteristic time is essentially given by the mean collision time. On the other hand, in the hydrodynamic equations – those describing the motion on space and time scales that are very large with respect to the molecular scales – the involved characteristic times are much larger. So one expects that for the full dynamics $\lambda_1 \sim O(10^{11})\,\mathrm{s}^{-1}$, while the first Lyapunov exponent for the hydrodynamic equations (in a chaotic regime) is of order $(10^{-1} - 1)\,\mathrm{s}^{-1}$ (the exact value depending on the geometry of the system, the external forcing, the Reynolds number and so on).

This big difference comes from the *coarse graining* procedure in building the hydrodynamic equations, that is from the very different (temporal and spatial) scales on which one is observing the system in the two cases.

If one is able to write the hydro-dynamical equations, then it is possible to characterize the macroscopic motion by means of the standard techniques of dynamical system theory [2]. However, in this case, it appears the problem of the norm to be used in the definition of the Lyapunov exponents[3]. However, in generic CML there are no systematic methods to build up the macroscopic equations apart from the Perron-Frobenius operator approach [30, 31, 116] (see Sect. 4.1.2), which only works for particular GCM.

In the following we propose a characterization of the macroscopic motion remaining at the microscopic level of description, by means of the Finite Size Lyapunov Exponent we shall define a sort of *macroscopic* Lyapunov exponent for the macroscopic motion.

[3]For finite dimensional systems all the norms are equivalent [40] and there is no ambiguity. This is not true for infinite dimensional systems (as the hydro-dynamical partial differential equations are), so that the Lyapunov exponents can depend on the used norm. See also Chapter 1

4.1.1 Macroscopic Chaos: first naive approaches

We studied mainly systems (4.1) of globally coupled tent maps, i.e. $f_a(x) = a(1/2 - |x - 1/2|)$, where, due to their banded structure (i.e. the elements are grouped in bands which are left unchanged by the dynamics [30]), we can have some control on the attractor of the system (e.g. by taking constant the percentage of elements *per* band when we vary the number of elements, see Sect. 4.1.3). To test the validity of our approach, we have also considered heterogeneous GCM [32, 115], in which the interacting elements are not all identical:

$$x_n(t+1) = (1-\epsilon) f_{a_n}(x_n(t)) + \frac{\epsilon}{N} \sum_{i=1}^{N} f_{a_i}(x_i(t)) \,, \tag{4.3}$$

here the control parameters a_i are quenched variables. We choose $f_{a_i}(x) = 1 - a_i x^2$, with a_i assuming equally spaced values in an interval between a_{min} and a_{max}, equivalently one can take a_i as random variables [32].

At varying ϵ and a in Eq. (4.1) (or a_{min} and a_{max}, in Eq. (4.3)), and by looking at the evolution of a macroscopic variable as, for instance, $m(t)$, one observes different kinds macroscopic behaviors while the microscopic dynamics is almost unchanged.

A possible classification of the observed behaviors is the following:

i) STANDARD CHAOS: the microscopic Lyapunov exponent is positive and the law of large numbers holds: if one plots $m(t)$ versus $m(t-1)$, one observes a spot with size of order $1/\sqrt{N}$ (see Fig. 4.1a).

ii) MACROSCOPIC PERIODICITY: the microscopic Lyapunov exponent is positive and the plot of $m(t)$ versus $m(t-1)$ gives rise to k spots with size of order $1/\sqrt{N}$, for a macroscopic motion of period k (see Fig. 4.1b). There are also less trivial periodic or quasi-periodic motion (e.g. in [115] a case is shown in which the mean-field dynamics evolves on a 2-dimensional torus), see also Fig. 4.1c.

iii) MACROSCOPIC CHAOS: the microscopic Lyapunov exponent is positive and the plot of $m(t)$ versus $m(t-1)$ shows an apparently well structurated function, see Fig. 4.1d-e, that suggests chaotic motion for $m(t)$.

The first hope is that, at a macroscopic level, the system can be described by few global variables, that are able to catch the large scale properties[4]. For instance, Fig. 4.1e seems

[4] I.e. one hopes that the macroscopic motion is driven by a low dimensional dynamics.

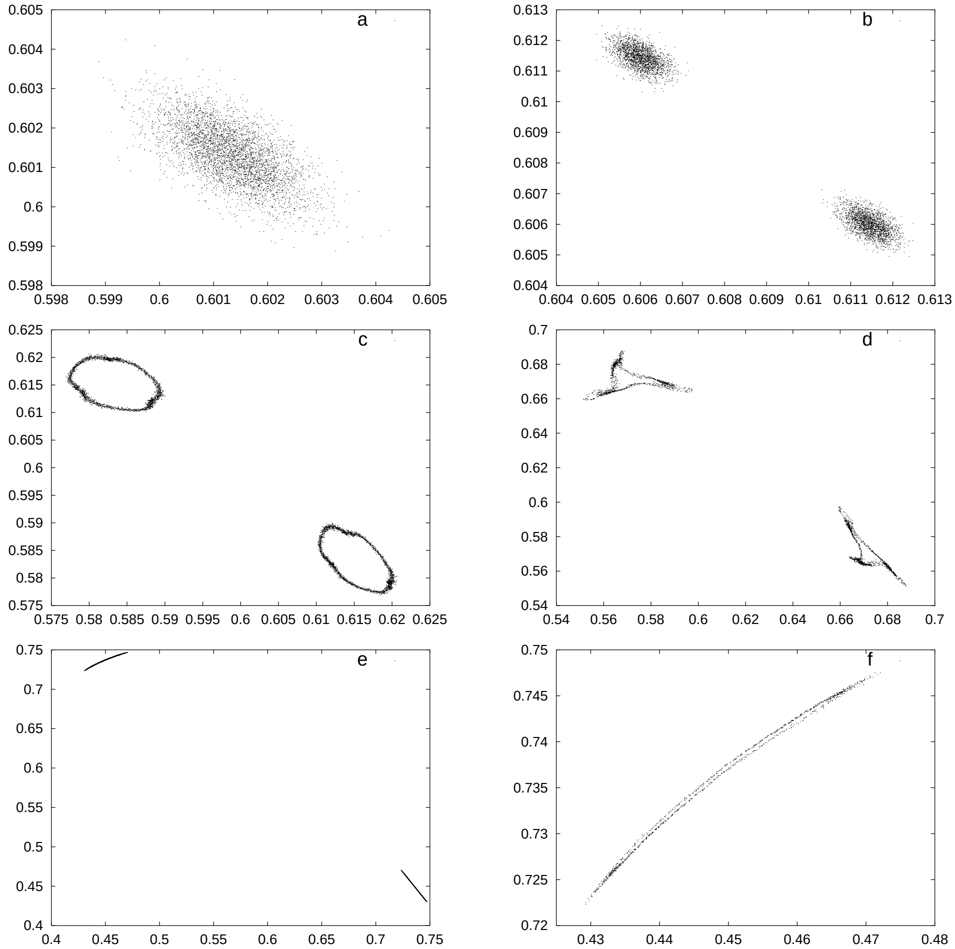

Figure 4.1: First return plot $m(t)$ *versus* $m(t-1)$ for the GCM (4.1) using as local map the tent map for various parameters: (a) $a = 1.8$ $\epsilon = 0.1$, (b) $a = 1.7$ $\epsilon = 0.2$, (c) $a = 1.6$ $\epsilon = 0.2$, (d) $a = 1.8$ $\epsilon = 0.3$, (e) $a = 1.7$ $\epsilon = 0.3$, (f) enlargement of (e). This plots have been obtained using $N = 10^6$ maps.

to suggest such a possibility: the first-return plot for the center of mass evolution appears to generate a one dimensional map. In such a case one can conjecture that

$$m(t+1) = F(m(t)) + \eta_N(t)\,, \tag{4.4}$$

where η_N is a small ($\sim 1/\sqrt{N}$) incoherent fluctuation, vanishing in the limit $N \to \infty$. If the above equation holds, one can define the Lyapunov exponent for dynamical system (4.4) as usual for one dimensional maps (e.g. see Eq. (2.35)). This latter quantity gives information on the sensitivity of the macroscopic dynamics to the initial conditions, so that one may call it *macroscopic* Lyapunov exponent λ_{macro}. However, Eq. (4.4) is not sufficient to describe the macroscopic dynamics [33]: the motion of $m(t)$ seems to be enough high dimensional [30]. In fact, if one looks carefully at the plot of $m(t)$ versus

$m(t-1)$, for large N, one realizes that very fine grained structures exist, see Fig. 4.1f. As a result $m(t)$ alone is not sufficient for a full description of the macroscopic properties of the system. It seems likely that the system evolution at a macroscopic scale is driven by a full set of equations of phenomenological type such as, e.g.,

$$\begin{cases} m(t+1) &= F_1(m(t), \sigma(t), \ldots) + \eta_N^{(1)} \\ \sigma(t+1) &= F_2(m(t), \sigma(t), \ldots) + \eta_N^{(2)} \\ \vdots & \quad \vdots \end{cases} \tag{4.5}$$

where $\sigma^2 = (\sum x_i^2)/N - (\sum x_i/N)^2$, and $\eta_N^{(i)}$ are small fluctuations vanishing as $N \to \infty$. Unfortunately, as far as we know, there is not a systematic approach (even of numerical type) for the building of Eqs. (4.5).

Another naive approach, based on the possible *time scales separation* between the microscopic and the macroscopic dynamics, is the analysis of the microscopic and macroscopic time auto-correlation functions, defined as follows:

$$C^{(i)}_{micro}(\tau) = \frac{\langle x_i(t+\tau)x_i(t)\rangle - \langle x_i\rangle^2}{\langle x_i^2\rangle - \langle x_i\rangle^2}\,, \tag{4.6}$$

$$C_{macro}(\tau) = \frac{\langle m(t+\tau)m(t)\rangle - \langle m\rangle^2}{\langle m^2\rangle - \langle m\rangle^2}\,, \tag{4.7}$$

where $\langle(...)\rangle$ means time average along the trajectory.

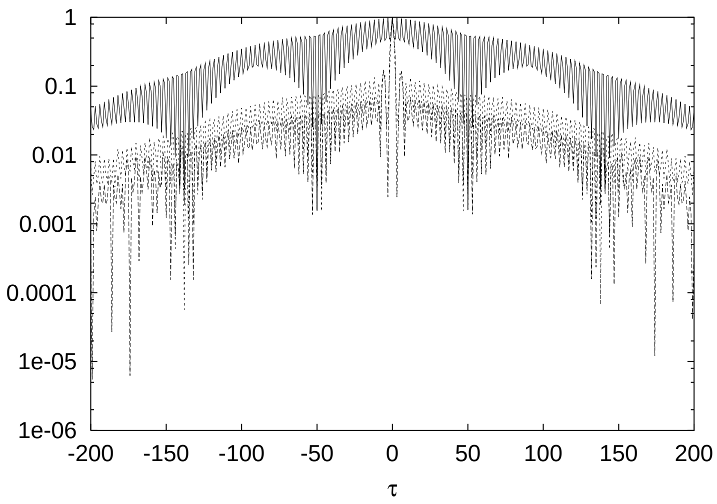

Figure 4.2: Absolute value of the correlation function $C_{macro}(\tau)$ (solid line) compared with the absolute value of the correlation functions for two different $x_i(t)$, $C^i_{micro}(\tau)$, (dashed and dot-dashed lines). The parameters are $a = 1.8$, $\epsilon = 0.3$ and $N = 10^5$.

It is to be noted, at this point, that the system shows a non trivial macroscopic behavior in a parameter region where it is also in a *broken ergodicity phase*, namely the knowledge of the probability distribution of a generic x_n does not permit a good description of the system [33].

Figure 4.2 shows the correlation functions (4.7) in the regime of macroscopic chaos. Due to the aforementioned failure of the ergodicity, different sites have different autocorrelations. Nevertheless, we found that the characteristic decay times of $C^{(i)}_{micro}(\tau)$, τ^i_m, and of $C_{macro}(\tau)$, τ_M, defined by the equations

$$C^i_{micro}(\tau) \sim e^{-\tau/\tau^i_m}, \qquad C_{macro}(\tau) \sim e^{-\tau/\tau_M}\,, \tag{4.8}$$

are not very different; for instance, in the case of Fig. 4.2 one has: $\tau^i_m \approx \tau_M \approx 115$, which are much larger than $1/\lambda_1$ (for the system of fig. 4.2 one has $1/\lambda_1 \approx 4.$). This last fact can be related to the intermittency of the system[5]. In the next Sections we discuss some less naive approaches to the characterization of the macroscopic chaos.

4.1.2 The Perron Frobenius operator approach

Let us now discuss the way in which one can try to characterize the collective dynamics of GCM in terms of the Perron-Frobenius (PF) operator [30, 31, 116] (see Sect. 1.1). At any time t one can wonder about the snapshot density $\rho_t(y)$, defined by the probability density that $x_n(t)$ assumes the value y:

$$\rho_t(y) = \frac{1}{N}\sum_{i=1}^{N} \delta(y - x_i(t))\,. \tag{4.9}$$

Using the fact that, for a mean field coupling as in Eq. (4.1), each x_n interacts with all the other $\{x_i\}$ in the same way, the time evolution of $\rho_t(y)$ can be written in terms of $\rho_{t-1}(y)$, by means of a self-consistent approach:

$$\rho_t(y) = \mathcal{L}^{(1)}\rho_{t-1}(y) = \frac{1}{1-\epsilon}\sum_i \frac{\rho_{t-1}(y_i)}{|f'_a(y_i)|}\,, \tag{4.10}$$

where the sum is on the pre-images given by[6]

$$y_i = f_a^{-1}\left(\frac{y - \epsilon\int f_a(z)\rho_{t-1}(z)dz}{1-\epsilon}\right), \tag{4.11}$$

[5] We have to stress that this behavior of the correlation times has been observed also in the heterogeneous logistic GCM (4.3).

[6] From a conceptual point of view Eqs. (4.10-4.11) are close to the Boltzmann equation for the gases [57]. Indeed, as one can check by a direct inspection, the PF operator $\mathcal{L}^{(N)}$ that rules the evolution of

f_a^{-1} being the inverse function of f_a, for instance, if $f_a(y) = 1 - ay^2$ then $f_a^{-1}(z) = \pm\sqrt{(1-z)/a}$.

For the standard chaos case (see Sect. 4.1.1) where $m(t) = \text{const.} + O(1/\sqrt{N})$, one has that, after long times, $\rho_t(y)$ converges toward a stationary distribution $\rho_\infty(y)$, i.e.:

$$\rho_t(y) \to \rho_\infty(y) \qquad \text{for} \quad t \to \infty\,. \tag{4.12}$$

On the other hand, for a macroscopic periodic behavior, the long time properties of the density $\rho_t(y)$ are described by means of a finite collection of functions of y; e.g. when $m(t)$ asymptotically oscillates among two different values, i.e. $m(2t) = m_e\,,\ m(2t+1) = m_o$, after a transient time one observes $\rho_{2t}(y) = \rho_e(y)\,,\ \rho_{2t+1}(y) = \rho_o(y)$. Finally, in the case of macroscopic chaos $\rho_t(y)$ does not converge toward any finite set of functions of y, but evolves with a nontrivial time behavior.

The above approach has been introduced by K. Kaneko [30], Pikovsky and Kurths [31] and Perez and Cerdeira [116].

Since the evolution equations (4.10 – 4.11) for $\rho_t(y)$ constitute a dynamical system (though of infinite dimension), one can formally compute the first Lyapunov exponent [30]. By so doing, as already noted, one is faced with the mathematical problem of the choice of the norm [40]: in the following, for sake of simplicity, we adopt the L_2 norm.

To practically compute the first Lyapunov exponent, firstly one applies an infinitesimal perturbation $\delta\rho_0(y)$ on $\rho_t(y)$ (with the constraint $\int \delta\rho(y)dy = 0$ in order to satisfy the normalization condition) then one observes the evolution $\delta\rho_n(y)$ of the perturbation. In this way, following standard methods [41], it is possible to estimate the whole set of the Lyapunov exponents $\{\tilde\lambda_i\}$; in particular one has

$$\tilde\lambda_1 = \frac{1}{2}\lim_{T\to\infty}\lim_{\delta\rho_0\to 0}\frac{1}{T}\sum_{n=0}^{T-1}\ln\frac{\int|\delta\rho_{n+1}(y)|^2dy}{\int|\delta\rho_n(y)|^2dy}\,. \tag{4.13}$$

Let us note that $\tilde\lambda_1$ can give interesting *global information* completely different from the microscopic Lyapunov exponent. In the case of standard chaos, or macroscopic periodic

the probability density $\rho_t^{(N)}(y_1, y_2, \ldots, y_N)$ in the whole phase space

$$\rho_t^{(N)}(x_1, x_2, \ldots, x_N) = \mathcal{L}^{(N)}\rho_{t-1}^{(N)}(x_1, x_2, \ldots, x_N)$$

is a linear operator. On the other hand the PF operator $\mathcal{L}^{(1)}$ for the evolution of $\rho_t(y)$, given by Eqs. (4.10 – 4.11), is a nonlinear one [31], since it depends explicitly on $\rho_{t-1}(y)$. In the kinetic theory of gases one has a similar situation: the Liouville equation, for the evolution of the probability density in the whole phase space, is linear, while the Boltzmann equation for the one-body statistics is nonlinear.

behavior, $\tilde{\lambda}_1$ is negative, or zero, while for macroscopic chaos $\tilde{\lambda}_1 > 0$. Let us stress that $\tilde{\lambda}_1$ can be negative even if the first Lyapunov exponent for the dynamical equations (4.1) is positive. Some detailed numerical investigation of Kaneko on GCM show that $\tilde{\lambda}_1$ is positive in the cases of macroscopic chaos [30].

Equations (4.10 – 4.11) hold only in the case of a mean field interaction for homogeneous GCM (4.1) and other particular systems [31], but they are not valid for generic GCM, e.g. for heterogeneous GCM (4.3). Nevertheless, the computation of $\tilde{\lambda}_1$ according to the definition (4.13) remains possible also for generic CML, at least by using a numerical approach[7]. This is accomplished by following the evolution of $\rho_t(y)$, as given by the time development of the histogram of the instantaneous microscopic configuration $(x_1, x_2, \ldots, x_N)$.

Besides the previous important properties of $\tilde{\lambda}_1$, we have to underline a subtle point that rises for its numerical computation when it is not possible to write down the appropriate Eq. (4.10). In this case, one is forced to study the evolution of $||\delta\rho_t(y)||$ making histograms from two instantaneous configurations $\{x_i\}$ and $\{x_i'\}$, obtained by the introduction of a small perturbation on $\{x_i\}$ at $t = 0$. To show where the problem is let us consider the time evolution of $\delta m(t)$ in the case of standard chaos. One can write δm in two different ways:

$$\delta m(t) = \frac{1}{N}\sum_{n=1}^{N} \delta x_n(t)\,; \qquad \delta m(t) = \int y\delta\rho_t(y)dy\,. \tag{4.14}$$

If λ_1 is positive, but $\tilde{\lambda}_1$ is negative, we have both $|\delta x_n(t)| \sim |\delta x_n(0)|\exp(\lambda_1 t)$ and $||\delta\rho_t|| \sim ||\delta\rho_0||\exp(-|\tilde{\lambda}_1|t)$. So that apparently we fall into a contradiction, since from the first of equations (4.14) we obtain

$$|\delta m(t)| \sim e^{\lambda_1 t}\,, \tag{4.15}$$

while from the second of equations (4.14) we have

$$|\delta m(t)| \sim e^{-|\tilde{\lambda}_1|t}\,. \tag{4.16}$$

To understand the origin of the apparent contradiction one has to take into proper account the scales of the perturbations on which these two equations hold. In particular, Eq. (4.15) holds at small scales: $|\delta m| \ll O(1/\sqrt{N})$, while Eq. (4.16) holds for $|\delta m| \gg O(1/\sqrt{N})$.

Basically, for $|\delta m(0)| \ll O(1/\sqrt{N})$ one has an exponential growth driven by the microscopic dynamics up to $|\delta m(0)| \approx O(1/\sqrt{N})$, i.e. the maximum allowed by the laws of

[7] Even if it may result in a very huge and heavy task.

large numbers. In an analogous manner starting from a perturbation $|\delta m(0)| \gg O(1/\sqrt{N})$ one has an exponential decrease up to $O(1/\sqrt{N})$. From the previous example it is clear that if one studies numerically the time evolution of $||\delta\rho_t||$ for large but finite N, at small times (or, more precisely, small $||\delta\rho||$) one observes just the "microscopic" Lyapunov exponent. So one has to introduce some coarse-graining – i.e. to consider non infinitesimal $\delta\rho_0$ – to obtain a macroscopic level description. However, there is a large arbitrariness in choosing a non infinitesimal $\delta\rho_0$.

In order to avoid these difficulties (numerical and conceptual) concerning the one-body description, in the next Section we shall introduce an approach based on the Finite Size Lyapunov Exponent.

4.1.3 "Macroscopic" Lyapunov Exponent

Our hope is that, as in the usual hydro-dynamical description of thermodynamic systems, the variables of systems exhibiting macroscopic chaos can be separated in slow variables (given by $m(t)$, $\sigma(t)$ and so on) and fast variables. We have already seen (Chapter 3) that in presence of two (or many) time scales the Finite Size Lyapunov Exponent is able to give a good characterization of perturbations dynamics on different length scales. In particular, in presence of two temporal scales the FSLE displays a two plateau behavior (e.g. Fig. 3.2). In this respect, the system here studied is particularly interesting because the two temporal scales emerge by the microscopic dynamics itself.

Therefore, one can hope to define the macroscopic Lyapunov exponent λ_{macro} by identifying it with the lower plateau of $\lambda(\delta)$, which is computed looking at $|\delta m(t)|$ (similarly to what we have done for the "slow"component Lyapunov exponent in Sect. 3.1.1). We have evaluated the FSLE both for the homogeneous GCM (4.1), using as local map the tent map, and for the heterogeneous GCM[8] (4.3), for different values of the parameters.

The numerical experiments have been performed as described in Sect. 2.2 but looking only at the evolution of the macroscopic variable which is initialized at the value $|\delta m(t)| = \delta_{min}$. For each realization, the perturbed system is obtained by shifting all the elements of the unperturbed one by δ_{min} (i.e. $x_i'(0) = x_i(0) + \delta_{min}$)[9].

From Figure 4.3a, which shows $\lambda(\delta)$ versus δ in the case with macroscopic chaos,

[8] For heterogeneous map also Kaneko and Shibata [32] have, independently from us, computed the FSLE obtaining results similar to ours [33].

[9] We have also superimposed a small amount of zero mean noise obtaining the same results.

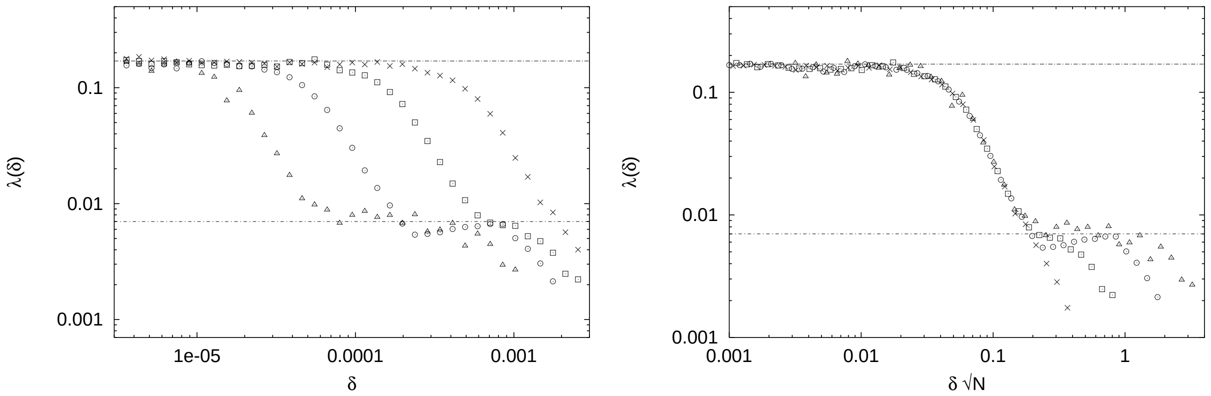

Figure 4.3: $\lambda(\delta)$ versus δ for the system (4.1) with $a = 1.7$, $\epsilon = 0.3$ for $N = 10^4$ ($\times$), $N = 10^5$ ($\Box$), $N = 10^6$ ($\odot$) and $N = 10^7$ ($\triangle$) . The first plateaus corresponds to the microscopic Lyapunov exponent $\lambda_{micro} \approx 0.17$ and the second one to the macroscopic Lyapunov exponent $\lambda_{macro} \approx 0.007$. The average is over $2 \cdot 10^3$ realizations for $N = 10^4$, 10^5, 10^6 and 250 realizations for $N = 10^7$. The system has been initialized in order to leave the attractor unchanged (as explained in the text). (b) The same as figure 5a rescaling the $\delta-$axis with $\sqrt{N}$.

the two expected plateau are evident. At small values of δ ($\delta \leq \delta_1$) one recovers the (microscopic) Lyapunov exponent, $\lambda(\delta) = \lambda_1$; while for $\delta \geq \delta_2$ one has another plateau which can fairly be called "macroscopic" Lyapunov exponent, $\lambda(\delta) = \lambda_{macro}$.

Let us observe that both δ_1 and δ_2 decrease at increasing N. In fact, from Fig. 4.3b, where we report $\lambda(\delta)$ versus $\delta\sqrt{N}$ for different values of N, one can see that both δ_1 and δ_2 scale as $\sim 1/\sqrt{N}$. Incidentally, one can also observe that the macroscopic plateau, being almost non-existent for $N = 10^4$, becomes more and more resolved and extended at increasing N up to $N = 10^7$. From these features we can argue that the macroscopic motion is well defined in the limit $N \to \infty$ and, therefore, we can conjecture that in this limit the microscopic signature in the evolution of $|\delta m(t)|$ completely disappears in favor of the macroscopic behavior.

For standard chaos ($\lambda_{macro} < 0$) one has only the microscopic plateau and then a fast slowing down of $\lambda(\delta)$, as can be seen in Fig. 4.4. Also for periodic or quasi-periodic (i.e. $\lambda_{macro} = 0$), we see only the microscopic plateau followed by a decreasing up to the saturation. This is a consequence of the fact that $\lambda(\delta)$ is not able to distinguish between $\lambda < 0$ and $\lambda = 0$, by definition. Indeed we have computed the FSLE from the doubling times (see Sect. 2.2).

One can wonder if it is possible to compute the macroscopic Lyapunov exponent di-

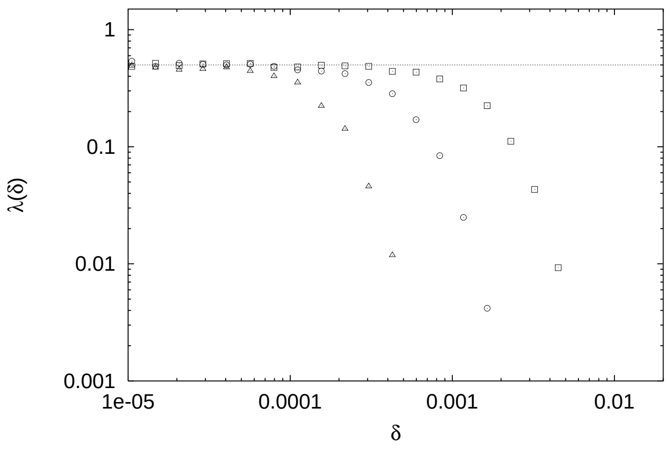

Figure 4.4: $\lambda(\delta)$ versus δ for the system (4.1) with $a = 1.8$, $\epsilon = 0.08$ for $N = 10^4$ ($\square$), $N = 10^5$ ($\odot$) and $N = 10^6$ ($\triangle$). The plateau corresponds to the microscopic Lyapunov exponent $\lambda_{micro} \approx 0.5$. The average is over $2 \cdot 10^3$ realizations.

rectly looking at $\langle \ln |\delta m| \rangle$ versus t. The macroscopic regime is expected to appear as a change of slope at a time t^* such that $|\delta m(t^*)| \approx O(1/\sqrt{N})$. In Fig. 4.5 $\langle \ln |\delta m(t)| \rangle$ is shown as a function of t for the same systems of Fig. 4.3a (with identical initial conditions). One can see that for small values of $\delta m(t)$ one has a well defined exponential growth corresponding to the microscopic Lyapunov exponent. This regime stops at $|\delta m(t)| \sim O(1/\sqrt{N})$ i.e. when the microscopic error growth saturates. At larger values of $\delta m(t)$ one observes a second (macroscopic) slope. One has a clear evidence also from Fig. 4.5 that the macroscopic motion sets in at a scale that is smaller when N is larger, as already established by the analysis of Fig. 4.3. The two estimation for λ_{macro} are in fair quantitative agreement. However, in general, due to intermittency the macroscopic regime can start at different times and with different rates, therefore the naive method in which the averages are performed at fixed delay times can give spurious laws; see Ref. [9, 88] and Sect. 5.2 for a discussion of these effects.

It is important to note that in order to obtain the results shown in Fig. 4.3 and Fig. 4.5 some precautions must be taken in initializing the system. In fact, because of the complex structure of the phase space of this system, one has that different initial conditions can led to different attractors [30]. Therefore, choosing random initial conditions while increasing N, one likely obtains different values for the macroscopic and/or microscopic Lyapunov exponents. In order to maintain the system on the same attractor, we kept fixed the percentage of elements *per* band (see Kaneko [30]), at varying the number of elements N.

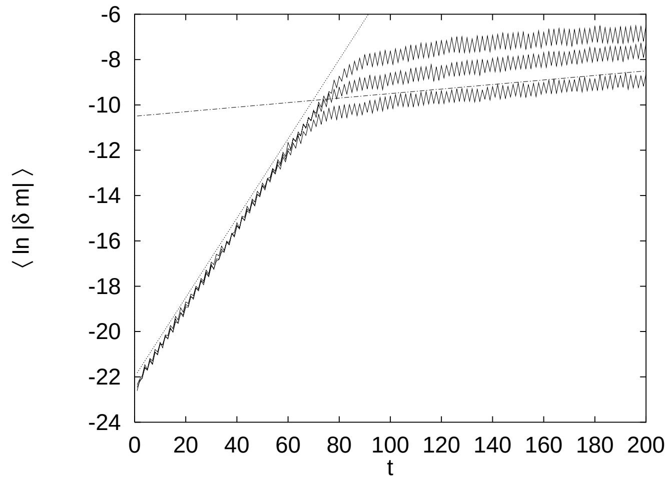

Figure 4.5: $< \ln|\delta m| >$ versus t for the system (4.1) with $a = 1.7$, $\epsilon = 0.3$ and $N = 10^4$ (upper curve), $N = 10^5$ (middle curve), $N = 10^6$ (lower curve) The straight lines correspond to the two exponential growth the microscopic one ($\lambda_{micro} \approx 0.17$) and the macroscopic ($\lambda_{macro} \approx 0.01$). The average is over 500 realizations.

Of course *a priori* there is no deep reason to believe that the above analysis performed only $m(t)$ is enough accurate. Therefore, we performed a similar study looking at two macroscopic variables, $m(t)$ and $\sigma(t)$. Since there is not a natural way to introduce a perturbation on $m(t)$ and $\sigma(t)$, we are forced to follow the method of Wolf et al. [119] for the computation of the Lyapunov exponent from data, but with some modifications. We considered the phase space generated by the variables $m(t)$, $\sigma(t)$ and we looked at the time separation between *analogies* [120] whose initial distance δ_0 is not very small (i.e. in the region of the "macroscopic" plateau in Fig. 4.3a). Following the evolution of the full system we compute the quantity:

$$\Gamma(\tau) = \frac{1}{\mathcal{A}} \sum_{j=1}^{\mathcal{A}} \ln \frac{\Delta(t_j + \tau)}{\Delta(t_j)}, \tag{4.17}$$

where $\Delta(t) = \sqrt{\delta m^2(t) + \delta\sigma^2(t)}$, t_j are the "return" times such that $\Delta(t_j) \in [\delta_0, 2\,\delta_0]$ and $\mathcal{A}$ is the number of analogies[10]. In Fig. 4.6 we show $\Gamma(\tau)$ versus τ. It is remarkable the agreement between the values for the macroscopic Lyapunov exponent obtained with the three different methods.

Finally, let us observe that, from a mathematical point of view, the results discussed

[10]It is important to stress the relevance of the value of δ_0, which must not be too small. Using a δ_0 out of the "macroscopic" (i.e. $\delta_0 < \delta_2$) plateau one may have spurious behavior due to intermittency (see Sect. 5.2).

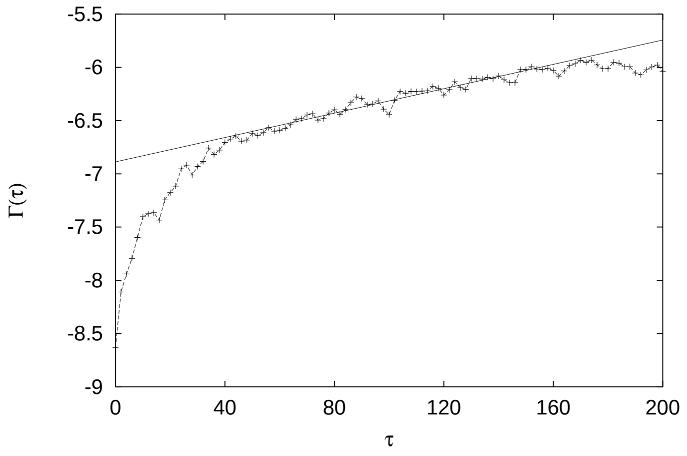

Figure 4.6: $\Gamma(\tau)$ versus τ for the system (4.1) with $a = 1.7$, $\epsilon = 0.3$ and $\mathcal{A} = 250$, the dashed line corresponds to $\lambda_{macro} \approx 0.006$. The distance has been plotted every two time steps to eliminate oscillations given by the switching between bands.

in this Section suggest that one can define the "macroscopic" Lyapunov exponent as:

$$\lambda_{macro} = \lim_{t\to\infty} \lim_{|\delta m(0)|\to 0} \lim_{N\to\infty} \frac{1}{t} \log \frac{|\delta m(t)|}{|\delta m(0)|}, \tag{4.18}$$

i.e. one has first to perform the thermodynamic limit and after the usual limits for the definition of the Lyapunov exponent. We stress that, for systems like GCM, the non-trivial point is in performing the first limit, namely $N \to \infty$, due to the coexistence of many attractors [30] one has to be sure that by changing the number of elements the attractor remains the same.

Finally, it is interesting to mention the case of "single-band" chaos (see Ref. [30]), where one has irregular behavior with some macroscopic coherence, but there is not a separation between the microscopic and the macroscopic scales, i.e. $\lambda_{macro} = \lambda_1$ [33].

4.2 Linear versus Non-linear propagation in extended systems

It is well recognized that chaotic dynamics generates a *flow of information*, i.e.: due to the sensitive dependence on initial conditions one has an information flow from "insignificant" digits towards "significant" ones [2, 4]. The characterization of such an information flow in systems involving many (temporal and spatial) scales (see Chapter 3) and in spatially distributed systems is relevant for the understanding of the phenomenology of spatio-temporal chaos. In particular, in spatially distributed systems one has an information flow both in *bit space* and in *real space* [11] (Sect. 2.1). As a consequence, the predictability time is essentially related to the propagation process and not to the Lyapunov exponent [26]. This point can be easily understood and analyzed in the context of coupled maps on a lattice. If the coupling among the maps is local an initially localized perturbation both grows on site (due to local instability) and propagates through the lattice (due to the coupling). Such kind of problem is particularly relevant in open flows such as pipe flow (Sect. 2.1), where one can have *convective chaos* [21, 80].

In this Section we study the information flow generated by the spatio-temporal evolution of an initially localized perturbation in coupled map lattices (with symmetric and local coupling). The spatial spreading of the perturbation can be well characterized in terms of the spreading velocity and of the comoving Lyapunov exponent [11, 34, 35]. However, as we will see in the following, there exist systems for which such a characterization is not sufficient [34]. In such systems the characterization in terms of comoving-LE essentially fails due to non linear effects, indeed the phenomenon we are going to study seems to be associated to a strong sensitivity to finite perturbation (Sect. 2.3.2). An interesting limiting case is the propagation of finite perturbations in non-chaotic systems such as those studied in Refs. [19, 20] (see Fig. 2.9), for which the linear analysis predicts a zero velocity of propagation.

In order to obtain a quantitative characterization of this "non linear" propagation, we introduce a generalization of the comoving Lyapunov exponent to non infinitesimal perturbation, in particular we define the FSLE in a moving reference frame: the Finite Size Comoving Lyapunov Exponent (FSCLE) [79]. This indicator predicts the correct value of the velocity of propagation both in generic CML (reducing to the usual Comoving-LE) and in the strongly non-linear CML we have studied.

4.2.1 Linear propagation and the Comoving-LE

Consider the following system of CML (2.9):

$$x_i(t+1) = f\left((1-\epsilon)x_i(t) + \frac{\epsilon}{2}(x_{i-1}(t) + x_{i+1}(t))\right) , \quad i = -L/2, \ldots, L/2 \ . \qquad (4.19)$$

We can now consider the dynamics of a perturbation initially localized, i.e. one follows two replicas of the system (4.19) initially differing for the value of the map in one site[11].

[11] What we are going to describe is independent to the details of the initial perturbation and refers to enough localized perturbations.

Indicating with $\{x_i\}$ and $\{y_i\}$ the two configuration, we follow the evolution of $|x_i(t)-y_i(t)|$ with

$$y_i(0) = \begin{cases} x_i(0) + d_0 & \text{for} \quad i = 0 \\ x_i(0) & \text{for} \quad i \neq 0\,. \end{cases} \tag{4.20}$$

In Figure 4.7 a we show a 3D plot of the evolution of $|x_i(t)-y_i(t)|$, using as local map the

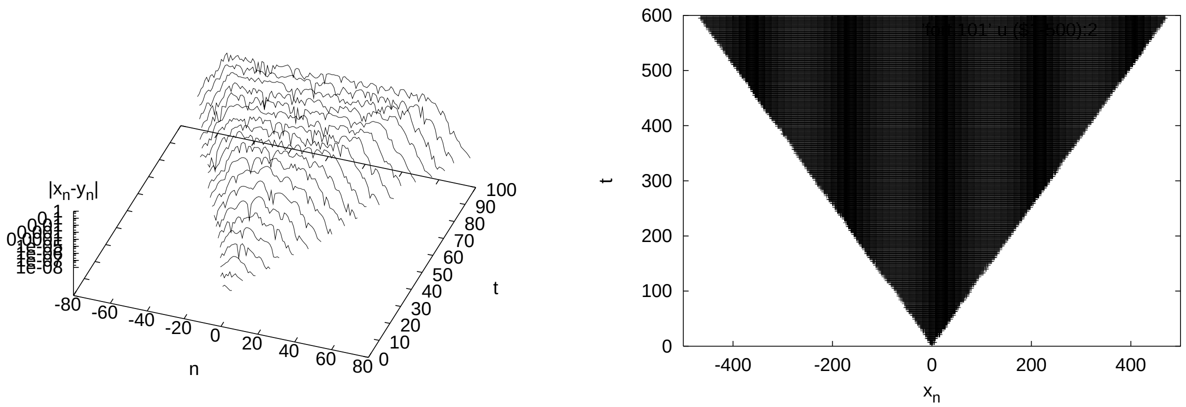

Figure 4.7: Evolution of the difference between two replicas of system 4.19, $|x_n(t) - y_n(t)|$ as function of time, t, and position, n. Initially the perturbation is localized in the middle of the lattice $|x_n(0) - y_n(0)| = d_0\delta_{n,0}$. (a) $|x_n(t) - y_n(t)|$ for a CML with local map the tent map, $f(x) = a(1/2 - |x - 1/2|)$, with $a = 2$, $\epsilon = 2/3$ and $L = 1001$, the initial perturbation has amplitude $d_0 = 10^{-8}$. (b) space-time plot of figure (a), the sites in which $|x_n(t) - y_n(t)| > d_0$ are in black.

tent map, as one can see the perturbation both grows and propagates. The disturbance propagates linearly, i.e. with a finite velocity, originating a sort predictability "horizon" (the boundary between white and black sites in Fig. 4.7b) in space-time. If one wonders which sites are perfectly predictable (or into a given threshold) up to a certain time [26] one obtains a spatio-temporal diagram as shown in Figure 4.7b. One expects a finite velocity of propagation since the coupling is local. Indeed, for nearest neighbors coupling (here adopted) it is possible to show that the velocity of disturbances propagation is less than 1 [34, 91].

Another qualitative feature emerging from Figure 4.7 is a possible connection between the spatio-temporal evolution of a perturbation with *front propagation* into stable or unstable states in spatially extended systems. This issue has been subject of intense study in the last decades [121], since the pioneristic work of Kolmogorov, Petrovsky and Piskunov [62], due to the relevance of spreading fronts for the emergence of spatial structures (patterns) in non-equilibrium systems [52]. In particular, *reaction-diffusion* models has been demonstrated to be appropriate for describing propagation phenomena in many fields including fluid dynamics, combustion, epidemics, chemical reactions, crystal growth [122] and biological aggregation (see Ref. [52] for a complete review).

The prototype equation for reaction diffusion phenomena is (in one-dimension):

$$\frac{\partial \phi(x,t)}{\partial t} = \frac{\partial^2 \phi(x,t)}{\partial x^2} + F(\phi(x,t))\,, \tag{4.21}$$

where $F(\phi) \in C^1[0,1]$ is a function describing the reaction with $F(0) = F(1) = 0$ and $F^{'}(0) > 0$, $F^{'}(1) < 0$. It is possible to show that any sufficiently localized initial profile, $\phi(x, t = 0)$, generates a propagating front joining the unstable ($\phi = 0$) to the stable ($\phi = 1$) state. By means of the linear stability analysis one can show that the front can have any speed V_F larger than a minimum value V_L which depends on $F(\phi)$ at $\phi = 0$ [62, 121].

Usually, velocities larger than V_L require special initial conditions to be realized, so that the "physical" speed is exactly $V_F = V_L$, where V_L indicates the "linear velocity", i.e. predicted by the linear stability theory. Whether it is selected or not depends on the shape of $F(\phi)$ for $\phi > 0$. In particular, it has been shown in [123, 124] that convexity of $F(\phi)$ is sufficient to ensure that $V_F = V_L$. Intuitively, we can say that, if $F'(0) > F'(\phi)$ for all $\phi > 0$, the front is "pulled" by the initial growth of ϕ (i.e. by the infinitesimal edges of the front) and, otherwise, it is "pushed" by the faster growth of finite ϕ [125]. Analogously, for the propagation of fronts (of perturbations) in CML we shall see that the velocity of the front can be obtained by the linear analysis. But in dependence of the local map used also other regimes for which it is necessary to take into account non-linear effects can appear. In the following we briefly summarize the known results about the linear regime.

In order to quantify the perturbation spreading let us introduce the propagating front velocity, V_F. A direct measurement of the velocity V_F can be obtained considering two evolving systems starting as in Eq. (4.20), one can then define the evolving left and right edge of the front, E_- and E_+ respectively, as:

$$\begin{aligned} E_-(t) &= \min\{i \quad \text{such that} \quad |x_i(t) - y_i(t)| \geq \Theta\} \\ E_+(t) &= \max\{i \quad \text{such that} \quad |x_i(t) - y_i(t)| \geq \Theta\} \end{aligned} \tag{4.22}$$

with $i \leq t$ and where Θ is an arbitrary threshold chosen to identify the front. The front velocity is then defined as:

$$V_F^{\pm} = \lim_{t\to\infty} \lim_{L\to\infty} \frac{E_{\pm}(t)}{t} . \tag{4.23}$$

Of course, for symmetric couplings, such as the case here considered, one has $V_F^+ = V_F^- = V_F$. Let us remark that one has to take before the limit of infinite lattices and after $t \to \infty$ in order to avoid boundaries effects. For a generic perturbation, the velocity V_F

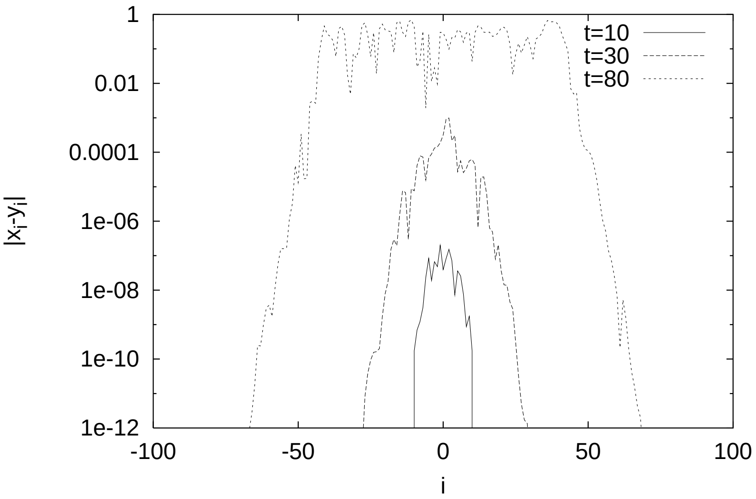

Figure 4.8: Perturbation front ($|x_n(t) - y_n(t)|$) as function of the space index n, at three different times. The local map is the tent map with the same parameter of Figure 4.7. The perturbation was initialized as in Fig. 4.7. Note that the right and left edges are infinitesimal and within the fluctuation exponential.

is independent either on the amplitude of the initial perturbation either on the threshold value. This independence stems from the fact that the propagation velocity is selected by the infinitesimal edge of the front. The front evolves leaving its edge infinitesimal, typically with an exponential profile (see Fig. 4.8), therefore one can obtain a prediction on the front velocity by analyzing the perturbation dynamics in tangent space, i.e.:

$$\delta x_i(t+1) = f'(\tilde{x}_i(t)) \left[(1-\epsilon)\delta x_i(t) + \frac{\epsilon}{2}(\delta x_{i-1}(t) + \delta x_{i+1}(t)) \right] , \tag{4.24}$$

where $f'(\tilde{x}_i(t))$ represents the derivative of the local map computed on $\tilde{x}_i = (1-\epsilon)x_i + \epsilon/2(x_{i-1} + x_{i+1})$. One studies the linearized equation in a reference frame moving with a velocity $v = i/t$. The exponential growth rate in this reference frame is nothing but the comoving Lyapunov exponent, so that the disturbance evolves according to (Sect. 2.2.2):

$$|\delta x_i(t)| \sim |\delta x_0(0)| e^{\lambda(v)t} , \tag{4.25}$$

where $\lambda(v)$ is the maximal comoving Lyapunov exponent. In symmetric CML $\lambda(v)$ is concave [91], so that the equation

$$\lambda(v) = 0 \tag{4.26}$$

has only two solutions corresponding to forward and backward fronts. If we call V_L the solutions of this equation, one expects that $V_F = V_L$. This can be understood immediately realizing that V_L corresponds to observe the front evolution from a reference frame in which the front edge neither grows ($\lambda(v) > 0$) nor decrease ($\lambda(v) < 0$). Therefore, in terms of

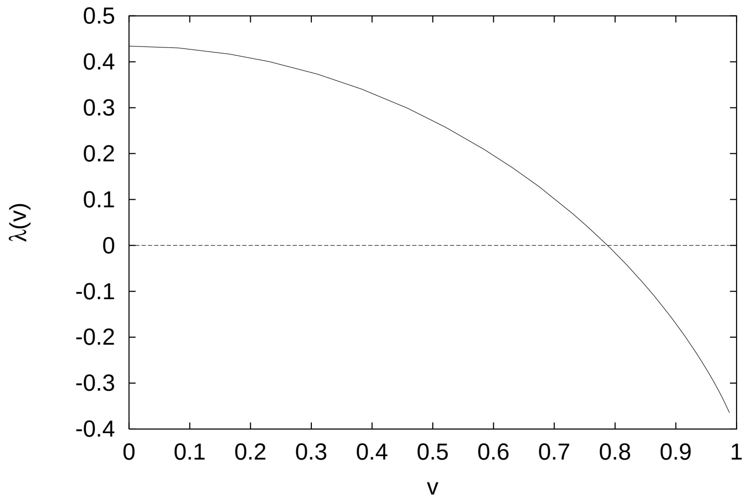

Figure 4.9: $\lambda(v)$ for $v > 0$ for a CML of tent maps with the same parameter of Figure 4.7. The straight line indicates the zero and the intersection between the curve $\lambda(v)$ and 0 is nothing but $V_L \approx 0.75$.

the comoving-LE one obtains a good characterization of the perturbation dynamics in tangent space.

An alternative way to perform the linear analysis is by considering perturbations decaying exponentially in space and defining the so-called *specific* Lyapunov exponent, introduced in Sect. 2.2.1. In the following we briefly recall this approach [34, 91], which is very instructive for understanding the front velocity selection mechanism. The starting point is the linearized equation (4.24), instead of considering an initially localized perturbation, now one chooses a perturbation with an exponential profile, i.e. $\delta x_i(0) \sim e^{-\eta i}$. As seen in Sect. 2.2.1, its temporal evolution depends on η as

$$\delta x_i(t) \sim e^{\lambda(\eta)t - \eta i}\,. \tag{4.27}$$

By using equation (4.22), which defines the front edges, it is easy to realize that the front velocity depends on the η as:

$$V(\eta) = \frac{\mathrm{d}i}{\mathrm{d}t} = \frac{\lambda(\eta)}{\eta} \,. \tag{4.28}$$

For an absolutely unstable system $\lambda(\eta = 0) = \lambda_{max} > 0$, from Eq. (4.28) one has $V(\eta) \to \infty$ for $\eta \to 0$: indeed, a flat front appears to propagate with arbitrary large velocity. For nearest neighbor coupling one has $V(\eta) \to 1$ for $\eta \to \infty$, i.e. for extremely localized perturbations [34].

Now, coming back to a generic localized perturbation one can understand that the front velocity is determined by the η_0 characterizing the leading edge profile, which is selected by the dynamics. Therefore, the front velocity is given by $V_F = V(\eta_0)$.

As seen above the selected front speed is such that a disturbance neither grows nor decreases at V_L, i.e. $\lambda(V_L) = 0$, which can be expressed in terms of $\lambda(\eta)$ and η by recalling that they are related to $\lambda(v)$ through a Legendre transformation Eq. (2.24) [91, 94]. So that the derivative of $V(\eta)$ is connected to the comoving Lyapunov exponent through the relation:

$$\frac{dV}{d\eta} = \frac{1}{\eta}\left(\frac{d\lambda}{d\eta} - \frac{\lambda}{\eta}\right) = -\frac{\lambda(v)}{\eta^2} \,. \tag{4.29}$$

Using $\lambda(V_L) = 0$, one can see that $dV/d\eta = 0$ at a value η_0 for which $v(\eta_0) = V_L$, and since $\lambda(v)$ is convex (being a Legendre transform), this is the unique minimum of $V(\eta)$. Finally, one has

$$V_L = \frac{\lambda(\eta_0)}{\eta_0} = \left.\frac{d\lambda(\eta)}{d\eta}\right|_{\eta=\eta_0} \,. \tag{4.30}$$

Thus for an infinitesimal perturbation, the selected velocity is the lowest possible speed. This justifies the use of the term “linear velocity” for V_L.

Recalling that for closed systems, $\lambda(v)$ is always a decreasing function (limiting us to $v \geq 0$ for symmetry reasons) and that $\lambda(v = 0) = \lambda_{max}$[28], from Eq. (4.30) one has that V_L is defined if and only if the system is absolutely unstable, i.e. $\lambda(0) > 0$.

Let us conclude this Section by noting that besides the strong analogies between front propagation in reaction-diffusion systems and disturbance propagation in CML, the very nature of the front here studied is indeed different. Here the front does not separate two different phases, e.g. one stable and the other unstable: the system is chaotic (and thus unstable) on both sides of the front.

4.2.2 Non Linear propagation and the Finite Size Comoving-LE

We now analyze the propagation of localized perturbations in CML which are very sensitive to finite perturbations, i.e. for which $\lambda(\delta) \geq \lambda$ for some $\delta > 0$ (see Sect. 2.3.2). Inside this class one can find both chaotic (absolutely unstable) maps and non-chaotic (absolutely stable) maps. We have investigated coupled map lattice whose dynamics is ruled by: the generalized shift map (2.39), i.e. $f(x) = \beta x \mod 1$, which generates a chaotic CML; the circle map

$$f(x) = \alpha + x \mod 1\,, \tag{4.31}$$

which, even if marginally stable, is sensitive (due to the modulo function) to finite perturbations, see Eq. (2.43), and can generate propagating fronts [34]. Finally, one can consider stable maps[12] [19, 20], e.g., such as that defined in Eq. (2.44). It is worth remembering that even if CMLs with the local dynamics given Eq. (2.44) are stable (i.e. $\lambda < 0$ for any value of the coupling) and the asymptotic evolution of the CML is confined on a periodic attractor, these maps generate very complex (disordered) transients the duration of which diverges exponentially with the number of elements composing the system [19, 20].

In Figures 4.10a,b we show the space-time evolution of an initially localized perturbation for a lattice of coupled shift maps.

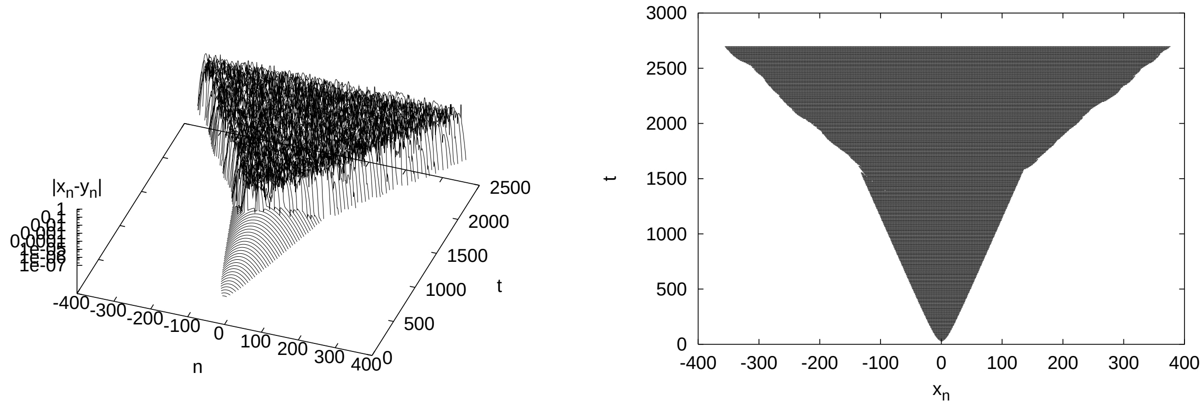

Figure 4.10: (a) Evolution of the difference between two replicas of system (4.19) by using a local map the shift map (2.39) with $\beta = 1.01$, $\epsilon = 1/3$ and $L = 1001$. Initially the perturbation is localized in the middle of the lattice $|x_n(0) - y_n(0)| = d_0 \delta_{n,0}$ with $d_0 = 10^{-8}$. (b) Space-time plot of figure (a), the sites in which $|x_n(t) - y_n(t)| > d_0$ are in black.

[12]Work in this direction is in progress.

It is rather evident the presence of two different mechanisms which drive the front propagation:

- At short times, until the core of the perturbation front is infinitesimal, the linear analysis of the previous Section applies. The front velocity is given by the linear velocity, V_L, given by $\lambda(V_L) = 0$.

- At large times, the front velocity exceeds the linear prediction (Fig. 4.10b: $V_F > V_L$). This is the signature of the failure of the linear analysis in characterizing the spreading process. Looking carefully at Fig. 4.10a and comparing with Fig. 4.7a, one can see that this new stage of the propagation starts when the core of the front reaches values high enough for the non linear instabilities to become dominant (see also Fig. 2.9).

Of course, the first regime (the linear one) is visible only if we initialize the two replicas with a very small disturbance and if we choose the threshold of visualization (Fig. 4.10b) small enough. Otherwise, as soon as the perturbation starts to be finite in some sites, the linear regime disappears.

Analogous computations for the circle map (4.31) or the stable map (2.44) show a propagation with velocity $V_F > 0$ while the linear analysis predict $V_L = 0$ [34, 35].

Intuitively, if one would be able to quantify the stability properties of finite amplitude perturbations in a moving frame of reference, one can hope to predict the front velocity, V_F, as the velocity for which these perturbations are stable.

In order to quantify the stability properties of perturbation fronts we introduce the Finite Size Comoving Lyapunov Exponent, i.e. we generalize the FSLE to a moving frame of reference [79]. The basic idea is the following. Consider two replicas $\{x_i\}$ and $\{y_i\}$ initially differing only in one site (i.e. $|x_i(0) - y_i(0)| = \delta_{min}\, \delta_{i,0}$) then we follow the evolution of the perturbation measuring it with the following norm:

$$||\delta x(t)||_v \equiv |x_{0+v\,t}(t) - y_{0+v\,t}(t)| \,. \tag{4.32}$$

In other words we measure the distance between the two replicas along the line $i = vt$. Then, we use the FSLE algorithm described in Sect. 2.3, i.e. we define a set of thresholds $\delta_n = \delta_0 r^n$ $(n = 1, \dots, N)$ and measure the time $\tau(\delta_n, r)$ which needs to go from $||\delta x(t)||_v = \delta_n$ to $||\delta x(t)||_v \geq \delta_{n+1}$ until the last threshold is reached. After we reinitialize one of the replicas with a perturbation on the site $i = 0$ and so on. Finally we define the Finite Size Comoving Lyapunov Exponent according to:

$$\lambda(\delta, v) = \frac{1}{\langle \tau(\delta, r)\rangle_e} \left\langle \log\left(\frac{\tilde{\delta}_{n+1}}{\tilde{\delta}_n}\right)\right\rangle_e \,, \tag{4.33}$$

where the dependence on the velocity v comes from the norm (4.32). Note that we have used Eq. (2.32) to take into account the discreteness of the dynamics. Therefore, $\lambda(\delta, v)$ quantifies the rate of divergence of the perturbation of size δ in a frame of reference moving with velocity v. With arguments similar to that used for the usual FSLE, we expect that in the limit of very small perturbation (where the linear analysis applies) the FSCLE recovers the Comoving-LE, i.e.

$$\lim_{\delta\to 0} \lambda(\delta, v) = \lambda(v)\,, \tag{4.34}$$

and, of course, for $v = 0$ one has the usual FSLE. Actually there are finite time effects which prevents the limit (4.34) to be attained [82, 126]. This problem is due to the fact that the perturbation grows through the chosen thresholds in finite time and the coupling between nearest neighbor sites must be taken into account in order to measure the correct Lyapunov exponent. In Appendix C we show the way in which one can take into account such corrections.

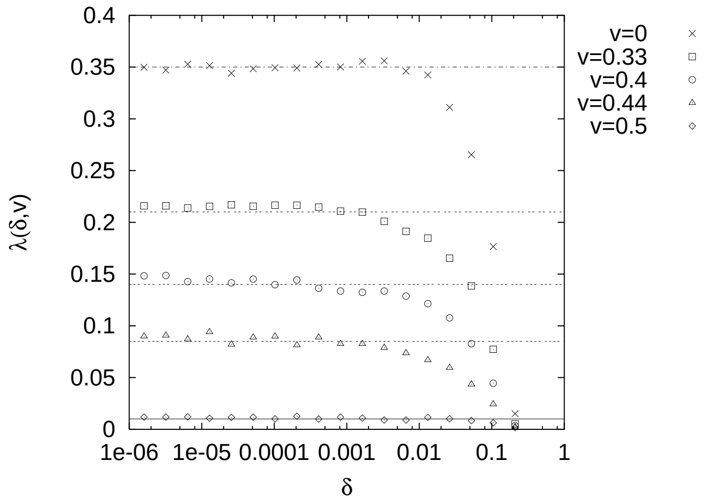

Figure 4.11: $\lambda(\delta, v)$ versus δ for a lattice of coupled logistic maps with $a = 4$, $\epsilon = 2/3$ and $L = 20^4$. The straight lines indicate the values of the comoving-LE ($\lambda(v)$). In the legend on the right the symbols for identifying the different velocities are shown. The statistics is over 10^4 doubling experiments.

In Figure 4.11 we show the FSCLE for a lattice of coupled logistic maps, where one expects the propagation to be dominated by the linear regime. In this system the linear analysis works and we obtain that $\lambda(\delta, v) = \lambda(v)$ up to a certain δ and after drops down analogously to the case $v = 0$ (i.e. the FSLE). This result constitutes a test of consistency of the proposed analysis and, moreover, it is useful for making a comparison with Figure 4.12a,b, where we show the FSCLE for a CML of generalized shift maps. Indeed, by

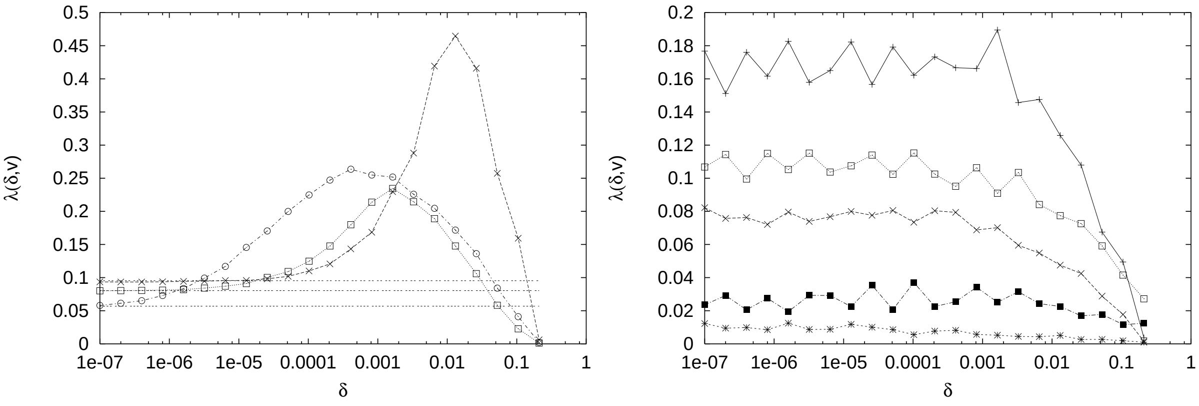

Figure 4.12: (a) $\lambda(\delta, v)$ versus δ for the shift map with $\beta = 1.1$ and $\epsilon = 1/3$, (from up to down) for $v = 0$, $v = 0.10$ and $v = 0.16$, the straight lines correspond to $\lambda(v)$. (b) the same of (a) in for $v > V_L$, in particular from the top $v = .25$, $v = .286$, $v = .30$, $v = .33$, $v = .341$. We have used a lattice from $L = 10^4$ up to $L = 10^5$, namely by approaching V_F one has to increase the lattice size in order to avoid boundaries effects (in this range $\lambda(v) < 0$ and, therefore, the non linear propagation can start after a while). The statistics is over $2\,10^3$ doubling times.

comparing Fig. 4.12a, with Fig. 4.11, it is well evident that the stability properties of the two systems are rather different. In fact, as expected from the analysis of the single map (Sect. 2.3.2), there exist a range of δ values for which $\lambda(\delta, v = 0) > \lambda(v = 0)$. For $v < V_L$ one has $\lambda(\delta, v) = \lambda(v)$ up to a certain δ^* after which it starts to exceed the comoving-LE value, denoting the beginning of the non linear regime which is characterize by being more sensitive to finite perturbations. Moreover, we note that δ^* decreases as $v \to V_L$. At $v = V_L$, where $\lambda(V_L) = 0$, the FSCLE is still positive ($\lambda(\delta, V_L) > 0$) and it goes to zero at V_F, as shown in Figure 4.13. It is worth underlining in this range of velocities ($V_L < v < V_F$) the comoving-LE is negative indicating an exponential decrease of the front. This difference stems from the fact that the above effects cannot be predicted by looking at the dynamics in tangent space. For $v > V_F$ one has $\lambda(\delta, v) = 0$, indeed with the definition of the FSCLE here adopted negative exponents appear to be 0. The fluctuations, which are visible in Fig. 4.12a-b, are essentially due to poor statistics. Indeed, this method requires very large lattices (and consequently large CPU-times) since one has to avoid boundaries effects. In figure 4.13 we show the dependence of $\max_\delta\{\lambda(\delta, v)\}$ on

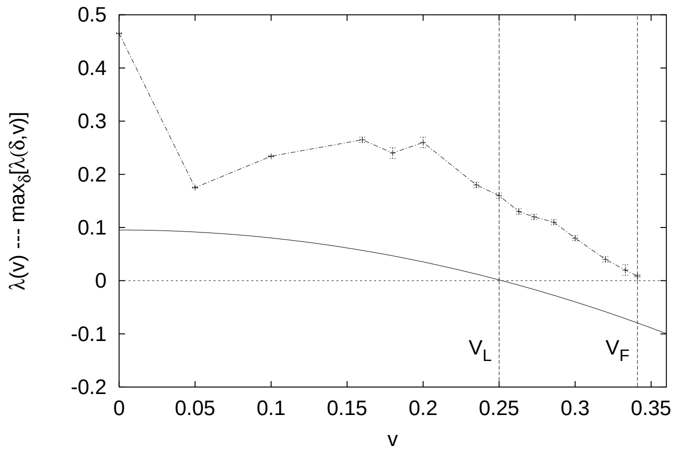

Figure 4.13: $\max_\delta \lambda(\delta, v)$ (dashed line with points) versus v for the shift map with $\beta = 1.1$ and $\epsilon = 1/3$, compared with $\lambda(v)$ (continuous line). The two vertical lines indicates the linear velocity $V_L \approx 0.250...$ and the directly measured (4.23) front velocity $V_F \approx 0.342$. Note that $\max_\delta \lambda(\delta, v)$ approaches zero exactly at V_F.

v, as expected it goes to zero exactly at the measured front speed V_F. We note that for $v < V_L$ there is a non-monotone behavior, this is probably due to the complex interplay of linear and nonlinear effects. For $v > V_L$, the region where we are interested in, the behavior is more smooth and monotone decreasing on v. Similar results hold for the circle map: also in this case the FSCLE predicts correctly the front velocities. Test on the stable maps are currently at working.

From the above results, it is clear that the proposed indicator seems to be the proper one to quantitatively characterize the relevant features of the non linear propagation of localized perturbations.

4.2.3 Remarks on the non linear propagation

In this Section we discuss some analogies among the propagation phenomena in CML, reaction diffusion systems [62, 52] and Cellular Automata (CA) [63].

As seen in Sect. 4.2.1, front propagation in reaction diffusion systems (the evolution of which is ruled by Eq. (4.21)) is entirely determined by the shape of the function $F(\phi)$. In particular, the front is pulled by the leading edges if $F^{'}(\phi) < F^{'}(0)$ for $\phi > 0$ or pushed by the nonlinear core of the front if for some $\phi > 0$ one has $F^{'}(\phi) > F^{'}(0)$. The velocity selection mechanism can be understood studying the stability properties of the traveling solutions of Eq. (4.21), essentially one has that the selected speed is the minimal velocity leading to a stable front [62, 121].

In CML apart the qualitative observation that one needs a strong sensitivity to finite perturbations there is not a direct link between the front propagation behavior and the shape of the map which rules the local dynamics of CML. This is due to the fact that in CML the analogous of the field ϕ is the difference between the values of maps on the same site, i.e.:

$$\phi(x,t) \rightarrow |x_i(t) - y_i(t)|$$

where i indicates the discretization of the space. In this situation one can think to write the equation in tangent space and thus consider directly the equation for the difference (i.e. ϕ). However, the equation in tangent space only refers to infinitesimal differences and, therefore, one cannot characterize the non-linear propagation phenomenon.

Intuitively one can think that the FSLE, $\lambda(\delta)$, plays a role analogous to that of $F(\phi)$. Indeed, in all cases $\lambda(\delta) \leq \lambda(0)$ with $\lambda(0) > 0$ (i.e. absolutely unstable) one has propagation with a velocity which is predicted by the linear analysis: $V_F = V_L$, given by the zero of the CLE. This situation is similar to that we have called front "pulled" by the leading edge. Differently, the case $\lambda(\delta) \geq \lambda(0)$ seems to be the analogous of the front "pushed" by the non linear part of the front. Indeed in all cases in which this condition was fulfilled we had measured $V_F > V_L$. This behavior tells us that if one is not interested in computing the front velocity but only in understanding if in some systems the propagation is dominated by the non linear regime one can limit himself in computing the FSLE and looking at its behavior as a function of δ: if the condition $\lambda(\delta) \geq \lambda(0)$ holds in a certain range of scales, δ, one has a propagation in which the "pushing" mechanism is dominant on the "pulling" one.

An example of how an inspection of the FSLE behavior can give some insight on the propagation front phenomenology we have studied the behavior of $\lambda(\delta)$ for the shift map at varying the non linear parameter β. In Fig 4.14 we show $\max_\delta\{\lambda(\delta) - \log(\beta)\}$ (being $\log(\beta) = \lambda(\delta = 0)$, i.e. we have subtracted the to the FSLE the value of the maximal Lyapunov exponent). As it is possible to see for $\beta \approx 1.3$ there is a sharp decreasing of the difference between the peak of the FSLE and the Lyapunov exponent, indicating a slowing down of the non linear effects. Therefore one expects the front velocity V_F to be much larger of the linear prediction V_L at small β and to become close to V_L as β approaches the value discussed above. By observing Fig. 4.14 one can see that this expectation is indeed verified.

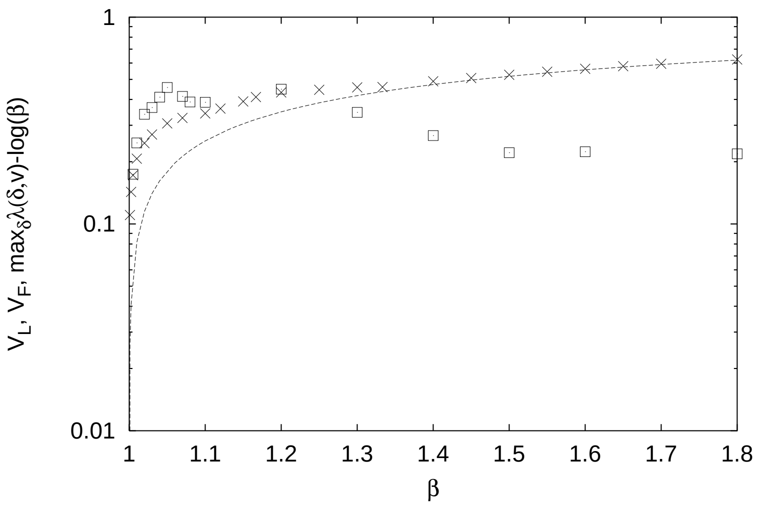

Figure 4.14: Propagation velocity as a function of the non-linear parameter β for the shift coupled maps with $\epsilon = 1/3$. The full line show the prediction of the comoving Lyapunov exponent (V_L), the crosses are the measured velocities V_F and the boxes are $\max_\delta\{\lambda(\delta, v)\} - \ln\beta$

Let us conclude this Section by noting, as suggested in Ref. [34], that the features of the non linear propagation studied in CML closely resembles the *damage spreading* analysis in *Cellular Automata* (CA) [63]. Indeed, in this systems which have time, space and configuration space discrete one can only have (for finite systems) periodic behaviors. However, before reaching this regime, in dependence of the number of elements and for particular rules [63] one can observe highly non trivial behaviors resembling some features of spatio-temporal chaos. In CA *a priori* the concept of Lyapunov exponent makes no sense since it is impossible to look at the tangent space equation due to the discreteness of the mapping. However, in literature one usually speaks of chaotic CA when a defect introduced in one copy of two identical CA starts to propagate infecting all sites [63]. Indeed some authors use the spreading velocity of defects as a "definition" of Lyapunov exponent [63, 127] For several regards this situation is very close to that we have observed in our CML systems. In particular, we have seen that even in absence of local instabilities, i.e. when the local map is stable or marginally stable, one can have propagation of an initially localized disturbance. We have understood this phenomena as an effect of the sensitivity to finite perturbation: even if the systems is stable with respect to infinitesimal perturbations ($\lambda \leq 0$) a finite perturbation $\delta > 0$ initially localized amplifies and propagates due to the coupling.

In Fig. 4.15 we show the $\max_\delta\{\lambda(\delta)\}$ and V_F for the circle map at varying the coupling parameter. These two quantities seem to be related in some (unknown) way (work in this direction is in progress). This is a possible indication that the behavior of CA can be mapped in the behavior of marginally stable (or stable) maps. In Ref. [20] some analogies in this direction was already discussed. However, much work has to be done to understand this issue. A further correspondence between the two systems can be given following the

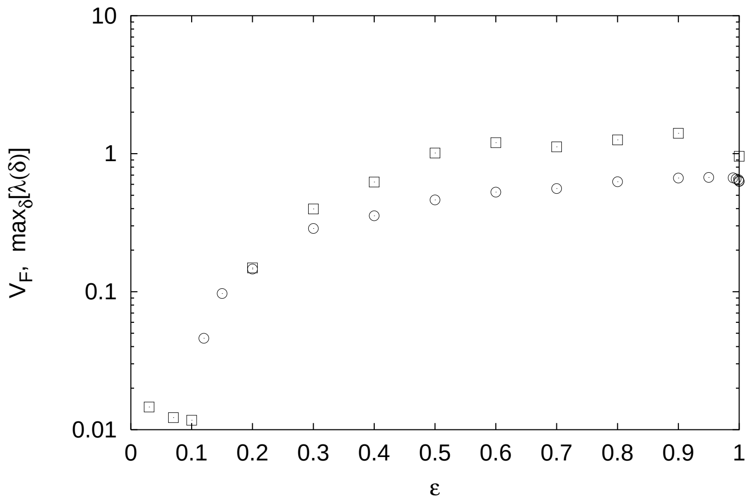

Figure 4.15: Comparison between the measured front velocities, V_F (circles), and $\max_\delta\{\lambda(\delta, 0)\}$ (boxes), for the circle map (4.31) with $\alpha = (1 - (\sqrt{5}) - 1)/2)/2$ at varying the coupling parameter ϵ. We had used lattices of $L = 5\,10^4$ sites. The statistics is over $2\,10^3$ doubling experiments.

Boolean derivatives approach, proposed by Bagnoli et al. [127], which defines a sort of first Lyapunov exponent for CA. In some sense one can think that these Boolean derivatives are a generalization of the FSLE. Indeed Bagnoli et al. [127] have shown that a finite damage spreading velocity is linked with a positive Lyapunov exponent (defined in terms of such Boolean derivatives).

Chapter 5

Transport and dispersion in non-ideal systems

In this Chapter we investigate dispersion properties of passive particles advected by a given two-dimensional incompressible velocity field confined in bounded domains. Dispersion phenomena are indeed natural candidates for the application of the scale dependent analysis developed in this thesis, in particular in non-ideal systems (i.e. systems which cannot reach an asymptotic regime, e.g. in confined flows).

The analysis in terms of the Finite Size Lyapunov Exponent for the Lagrangian dynamics of passive particles allows us to understand the dispersion mechanisms acting on different length scales. In particular, at very small scales one can investigate possible chaotic behaviors (*Chaotic Advection* [85, 86, 87]), which, even in flow with simple Eulerian structure, may generate complex Lagrangian trajectories. We apply the FSLE analysis both to simple models and to Lagrangian experimental data in a convective flow, where we find a clear evidence of chaotic behavior, i.e. a positive Lagrangian Lyapunov exponent.

For sake of completeness in the first Section we briefly recall the practical and theoretical problems involved in dispersion phenomena and recall standard tools for their investigation.

5.1 Dispersion properties of Lagrangian tracers

Transport processes play a crucial role in many natural phenomena [128], e.g.: particle transport in plasma physics and in geophysical flows. The most natural framework for investigating such phenomena is to adopt a Lagrangian viewpoint in which the particles are advected by a given Eulerian velocity field, $\boldsymbol{u}(\boldsymbol{x}, t)$, according to the ODE

$$\frac{d\boldsymbol{x}}{dt} = \boldsymbol{u}(\boldsymbol{x}, t) = \boldsymbol{v}(t)\,, \tag{5.1}$$

where, by definition, $\boldsymbol{v}(t)$ is the Lagrangian particle velocity. We neglect the molecular diffusion (see next section), and we only consider incompressible velocity fields, $\boldsymbol{\nabla} \cdot \boldsymbol{v} = 0$.

Despite the apparent simplicity of (5.1), the problem of relating the Eulerian properties of $\boldsymbol{u}$ with the Lagrangian properties of the trajectories $\boldsymbol{x}(t)$ is a very difficult task [129]. In the last decades the scenario has become even more complex by the recognition of the ubiquity of *Lagrangian chaos – chaotic advection* – [39, 85, 86, 87]. Even very simple Eulerian fields can generate very complex Lagrangian trajectories practically indistinguishable from those obtained in a turbulent flow.

In two-dimensional incompressible flows in absence of molecular diffusion, the emergence of Lagrangian Chaos can be understood as follows. The equations describing these flows are formally those of a two degrees of freedom Hamiltonian system [37, 39] where the Hamilton function is the stream function ψ:

$$\frac{\mathrm{d}x(t)}{\mathrm{d}t} = \frac{\partial\psi(x,y,t)}{\partial y}\,, \quad \frac{\mathrm{d}y(t)}{\mathrm{d}t} = -\frac{\partial\psi(x,y,t)}{\partial x}\,. \tag{5.2}$$

If ψ is time-dependent the equations (5.2) are non-autonomous and, in general, non-integrable, then chaotic trajectories may exist [39, 85, 86].

However, despite these difficulties, the study of relative dispersion of two particles can give some insight on the link between Eulerian and Lagrangian properties at different length-scales. Indeed, the evolution of the separation $\boldsymbol{R}(t) = \boldsymbol{x}^{(2)}(t) - \boldsymbol{x}^{(1)}(t)$ between two tracers is given by

$$\frac{d\boldsymbol{R}}{dt} = \boldsymbol{v}^{(2)}(t) - \boldsymbol{v}^{(1)}(t) = \boldsymbol{u}(\boldsymbol{x}^{(1)}(t) + \boldsymbol{R}(t), t) - \boldsymbol{u}(\boldsymbol{x}^{(1)}(t), t) \tag{5.3}$$

and thus depends on the velocity difference at scale $R = |\boldsymbol{R}|$. It is obvious from (5.3) that the Eulerian velocity components of typical scale much larger than R will not contribute to the evolution of $\boldsymbol{R}$. Since, in incompressible flows, separation $\boldsymbol{R}$ typically grows in time [130] from the evolution of the relative separation one can, in principle, extract the contributions of all the components of the velocity field. For these reasons, we prefer to study (two particles) relative dispersion (i.e. $R(t) = \langle ||\boldsymbol{x}^{(1)}(t) - \boldsymbol{x}^{(2)}(t)||^2\rangle$) instead of (one particle) absolute dispersion (i.e. $\langle ||\boldsymbol{x}(t) - \boldsymbol{x}(0)||^2\rangle$). For spatially infinite systems, without mean drift asymptotically there is no difference, while for flows in bounded domains (of typical size L_B) relative dispersion is, for many aspects, more interesting than the absolute one, which is dominated by the sweeping induced by large scale flow.

There are very few general results on the link between Eulerian and Lagrangian properties essentially related to the asymptotic ones. Let us suppose that the Eulerian velocity field is characterized by two typical length-scales: the (small) scale l_u below which the velocity is smooth, and a (large) scale L_0 representing the size of the largest structures (usually influenced by the boundaries, so that in many situation $L_0 \approx L_B$) present in the flow. In most non turbulent flows it will turn out that $l_u \sim L_0$. At very small separations, $R \ll l_u$, we have that the velocity difference in (5.3) can be reasonably approximated by a linear expansion in R, which in most time-dependent flows leads to an exponential growth of the distance between, initially close, particles, which is the signature of *Lagrangian chaos* [87]:

$$\langle \ln R(t) \rangle \simeq \ln R(0) + \lambda t \,, \tag{5.4}$$

the average is taken over many couples starting at a distance $R(0)$. The coefficient λ is the Lagrangian Lyapunov exponent of the system [39]. The rigorous definition of the Lyapunov exponent imposes to take the two limits $R(0) \to 0$ and then $t \to \infty$: in physical terms these limits amount to the requirement that the separation has not to exceed the scale l_u but for very long times (see Sect. 1.1.2). This is a very strict condition, rarely accomplished in real flows, rendering often infeasible the experimental observation of the behavior (5.4).

On the opposite limit, for very long times and for separations $R \gg L_0$, the two particles $\boldsymbol{x}^{(1)}(t)$ and $\boldsymbol{x}^{(2)}(t)$ are advected by two velocities which are practically uncorrelated. We thus expect normal diffusion, i.e. $\langle R^2(t) \rangle \simeq 2D\,t$, where D is the diffusion coefficient.

5.1.1 Ideal Systems: asymptotic tools and behaviors

At the foundation of the study of dispersion phenomena it is the understanding of the mechanisms which lead to transport enhancement as a fluid is driven farther from the motionless state. The reason of the enhancement is that transport is affected by the trajectories of individual fluids elements, or tracers, which, as seen in the previous section, can be quite complex even in simple laminar flows due to Lagrangian Chaos.

In general, dispersion of passive tracers in a given velocity field is the result, usually highly nontrivial, of two different contributions:

- molecular diffusion always present and affecting the *microscopic* scales;
- advection due to Eulerian field which influences larger scales and, in turbulent flows, involves a large number of different scales.

However, in presence of Lagrangian Chaos, one can have rather fast transport even without molecular diffusion[1].

Taking into account molecular diffusion, the motion of a test particle (the tracer) is described by the following Langevin equation:

$$\frac{d\boldsymbol{x}}{dt} = \boldsymbol{u}(\boldsymbol{x}, t) + \boldsymbol{\eta}(t) \,, \tag{5.5}$$

where $\boldsymbol{\eta}(t)$ is a Gaussian white noise with zero mean and

$$< \eta_i(t)\eta_j(t^{'}) >= 2D_0\delta_{ij}\delta(t - t^{'}) \,, \tag{5.6}$$

being D_0 the (bare) molecular diffusivity.

Denoting $\Theta(\boldsymbol{y}, t) = \langle\delta(\boldsymbol{x}(t) - \boldsymbol{y})$ the tracers' concentration, one has that the concentration evolves according to the Fokker-Planck equation [44] associated to the Langevin dynamics (5.6), i.e.:

$$\partial_t\Theta + (\boldsymbol{u}\cdot\boldsymbol{\nabla})\,\Theta = D_0\,\Delta\Theta \,. \tag{5.7}$$

For an Eulerian velocity field periodic in space, or anyway defined in infinite domains, the long-time, large-distance behavior of the diffusion process is described by the *eddy-diffusivity tensor* [132] D^E_{ij}:

$$D^E_{ij} = \lim_{t\to\infty}\frac{1}{2t}\langle(x_i(t) - \langle x_i\rangle)(x_j(t) - \langle x_j\rangle)\rangle \,, \tag{5.8}$$

where $\mathbf{x}(t)$ is the position of the the tracer at time t, $i, j = 1, \cdots, d$ (being d the spatial dimension), and the average is taken over the initial positions or, equivalently, over an ensemble of test particles. The tensor D^E_{ij} describes the long-time, large-distance behavior of $\langle\Theta\rangle$, i.e. the concentration field locally averaged over a volume of linear distance much larger than the typical length l_u of the velocity field, according to the diffusion equation

$$\partial_t\langle\Theta\rangle = \sum_{i,j=1}^{d} D^E_{ij}\,\frac{\partial^2}{\partial x_i\partial x_j}\langle\Theta\rangle + O\left(|\nabla^2\langle\Theta\rangle|^2\right) \,. \tag{5.9}$$

[1] For this reason one usually neglect the molecular diffusion, even if in some cases the interplay between diffusion and advection can leads to non-trivial effects if the diffusion have some correlation [131].

If D^E_{ij} is finite this means that, for very large times, one has a standard diffusion process. However, there exist also cases of *anomalous diffusion* in which the particles' spreading does not behave linearly with time but with a power law $t^{2\nu}$ with $\nu \neq 1/2$. In general, transport anomalies are the signature of strong correlation in the Lagrangian dynamics, even at large time and space scales [133]. In incompressible velocity fields there exist theorems[2] ensuring an asymptotic standard diffusion in dependence of the infrared spectral properties of the velocity field [134]. Sometimes chaotic advection may generate anomalous diffusive behaviors [135, 136, 137].

For spatial infinite domains and periodic Eulerian fields the *multiscale technique* [138], known as *homogenization* in mathematical literature, constitutes a powerful tool for studying standard diffusion and, with some precautions, also the anomalous situations [139]. The idea at the basis of this technique is to study the *macro-dynamics* dynamics (at long times and large scales) of the passive scalar field.

On the other hand we have to stress that the diffusivity tensor (5.8) is mathematically well defined only in the limit of infinite times, which, physically speaking, corresponds to cases in which the characteristic length l_u of the velocity field is much smaller than the size L_B of the domain. However, the case when l_u and L_B are not well separated is rather common in many geophysical problems, e.g. spreading of pollutants in Mediterranean or Baltic sea [140], and in plasma physics [141]. Therefore it is important to introduce other characterizations of the diffusion properties which can be used also in such non ideal cases.

5.2 Non-asymptotic dispersion

The characterization of dispersion in non-ideal systems, e.g., systems with no sharp scale-separation between the domain size (L_B) and the Eulerian characteristic length (l_u) cannot be achieved in terms of the asymptotic concepts and tools above discussed. We show now that the Finite Size Lyapunov Exponent is a natural candidate for characterizing the dispersion properties in such systems [88, 89, 142, 90].

In order to introduce the FSLE analysis for dispersion let us start with a simple example. Consider the relative dispersion of a cloud of N test particles in a smooth, spatially periodic velocity field with characteristic length l_u. We assume the Lagrangian

[2] Rigorously proved for spatially periodic or random velocity fields.

motion to be chaotic, i.e. $\lambda > 0$. Denoting with $R^2(t)$ the square of the typical radius of the cloud

$$R^2(t) = \langle |\mathbf{x}_i(t) - \langle \mathbf{x}_i(t) \rangle|^2 \rangle \,, \tag{5.10}$$

being $\langle \mathbf{x}_i(t) \rangle = 1/N \sum_{i=1,N} \mathbf{x}_i(t)$. In particular, we expect the following regimes to hold

$$\overline{R^2(t)} \simeq \begin{cases} R^2(0) \exp(L(2)t) & \text{if } \overline{R^2(t)}^{1/2} \ll l_u \\ 2Dt & \text{if } \overline{R^2(t)}^{1/2} \gg l_u \end{cases} \,, \tag{5.11}$$

where $L(2) \geq 2\lambda$ is the generalized Lyapunov exponent of order 2 [24], D is the diffusion coefficient and the over-bar denotes the average over initial conditions. From Equation (5.11) one has two different regimes in the spreading phenomenon: one related to Lagrangian chaos at very small size of the cloud and one related to diffusion at larger scales.

Another way to investigate the dispersion is in terms of the Finite Size Lyapunov Exponent $\lambda(\delta)$ (see Sect. 2.3), computed following the growth of the radius of the passive cloud. For δ non infinitesimal, $\lambda(\delta)$ depends on the details of the nonlinear mechanisms of expansion and in the case of standard diffusion one expects $\lambda(\delta) \sim \delta^{-2}$. The Lagrangian Lyapunov exponent λ is obtained as usual by

$$\lambda = \lim_{\delta \to 0} \frac{1}{\tau(\delta)} \log r \,, \tag{5.12}$$

physically, this limit corresponds to $\delta \ll l_u$. In Refs. [141, 144] related approaches have been proposed for computing diffusion coefficients in nontrivial cases.

From the previous results one has the following scale dependent scenario [88]:

$$\lambda(\delta) \sim \begin{cases} \lambda & \text{if } \delta \ll l_u \\ D/\delta^2 & \text{if } \delta \gg l_u \end{cases} \,, \tag{5.13}$$

one could naively conclude, matching the behaviors at $\delta \sim l_u$, that $D \sim \lambda l_u^2$. This is not always true, since one can have a rather large range for the crossover due to the fact that nontrivial correlations can be present in the Lagrangian dynamics [145].

Moreover, in presence of boundaries, i.e. in closed domains (of size L_B), one has that the tracers' cloud saturates on scales $\delta \sim O(L_B)$. For a large class of systems we have found that on scales of the order of the domain size $\lambda(\delta)$ follows the following universal behavior [88]

$$\lambda(\delta) = \frac{D(\delta)}{\delta^2} \propto \frac{1}{\tau_R} \frac{(\delta_{max} - \delta)}{\delta} \,, \tag{5.14}$$

where δ_{max} is the saturation distance, which corresponds to having a uniform distribution of the tracers in the basin, and τ_R is a quantity having the dimension of a time. Eq. 5.14 can be easily obtained by assuming that particles' distribution relaxes exponentially (with a relaxation time τ_R) to the uniform distribution. This condition is indeed generally accomplished. In the language of dynamical systems theory corresponds to assuming that the second eigenvalue of the Perron-Frobenius operator is inside the unit circle [38] (see also Sect. 1.1). In Appendix D we describe the computation of (5.14) in a simple example.

In system with the Eulerian characteristic length of the same order of the domain size ($l_u \approx L_B$), we do not expect to observe any diffusive regime. In these cases we will observe only the exponential (5.12) and the saturation one (5.14).

Therefore by studying $\lambda(\delta)$ one can characterize all the spreading behaviors at different length scales, also when the diffusive regime does not take place [89, 90].

Another case in which the behavior of $\lambda(\delta)$ as a function of δ is essentially understood is dispersion of tracers in three dimensional fully developed turbulence [142]. For sake of simplicity we ignore intermittency effects. There are then three different regimes:

1. $\delta \ll \ell_D =$ Kolmogorov length : $\lambda(\delta) \sim \lambda$;
2. $\ell_D \ll \delta \ll \ell_E =$ typical size of the energy containing eddies: from the Richardson law [143] $\overline{R^2(t)} \sim t^3$ one has $\lambda(\delta) \sim \delta^{-2/3}$;
3. $\delta \gg \ell_E$: usual diffusion behavior $\lambda(\delta) \sim \delta^{-2}$.

In Ref. [142] it is presented a detailed study of this problem including intermittency effects. One might wonder that the proposal to introduce the FSLE is just another way to look at $\overline{R^2(t)}$ as a function of t. This is true only in limiting cases, when the different characteristic lengths are well separated and intermittency is weak. Indeed, the method of working at fixed scale δ allows us to extract the physical information at that spatial scale avoiding unpleasant troubles of the method of averaging at a fixed delay time t. For instance, if one has intermittency, and this is rather usual, $R^2(t)$ as a function of t can appear very different in each realization leading to spurious behavior for the average at fixed times $\overline{R^2(t)}$. In order to show the way in which this can happen we discuss now a very simple example. Since at small scales (say $l \ll l_u$) one typically has an exponential growth of $R(t)$, due to Lagrangian Chaos, and, at large scale a diffusive behavior, one can

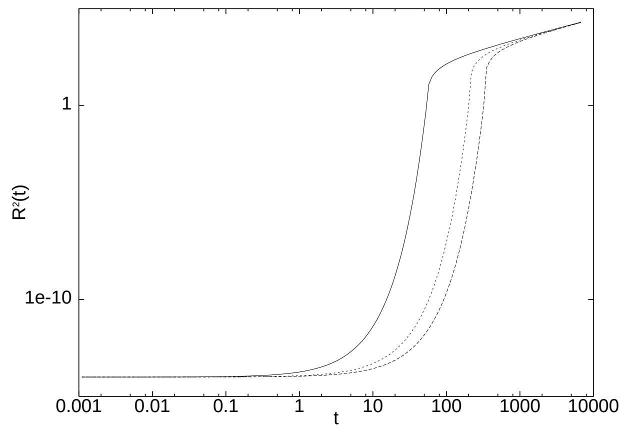

(a)

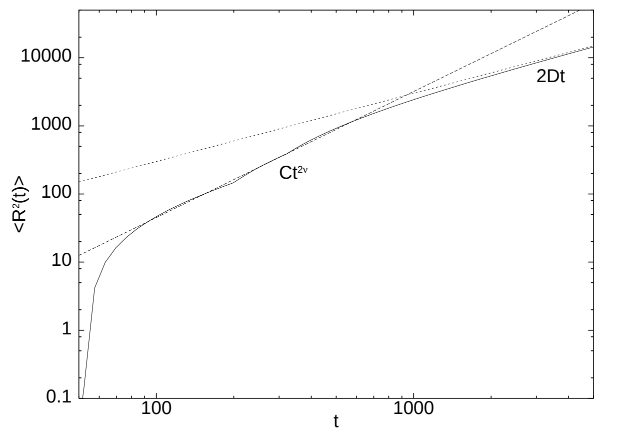

(b)

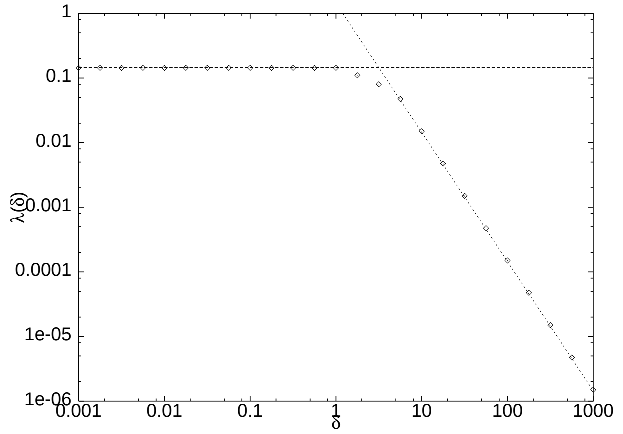

(c)

Figure 5.1: a- Three realizations of $R^2(t)$ as a function of t built as follows: $R^2(t) = \delta_0^2 \exp(2\gamma t)$ if $R^2(t) < 1$ and $R^2(t) = 2D(t - t_*)$ with $\gamma = 0.08, 0.05, 0.3$ and $\delta_0 = 10^{-7}$, $D = 1.5$. b- $\langle R^2(t) \rangle$ as function of t averaged on the three realizations shown in (a). The apparent anomalous regime and the diffusive one are shown. c- $\lambda(\delta)$ vs δ, with Lyapunov and diffusive regimes.

mimic $R(t)$ as follows:

$$R^2(t) = \begin{cases} \delta_0^2 e^{2\gamma t} & R(t) < l_u \\ 2D(t - t_*) & R(t) > l_u \,, \end{cases} \tag{5.15}$$

where t_* is such that $R(t)$ is continuous.

In Fig. 5.1a we show three different realizations of (5.15) with different (γ) exponential rates of growth (intermittency). By averaging at fixed times one has a rather odd behavior of the average $\overline{R^2(t)}$ without any physical meaning. In Figure 5.1b it is shown $\overline{R^2(t)}$ versus time t: at large times we recover the diffusive behavior but at intermediate times appears a "spurious" *anomalous* regime which is only due to superposition of exponential and diffusive contributions by different samples at the same time. On the other hand by averaging at fixed scales one has a unambiguous result (see Figure 5.1c).

Of course the interesting situations are those where the characteristic lengths (l_u, L_B) are not very different, i.e. where the scaling regime for $\overline{R^2(t)}$ is not well evident. In the following we shall present some numerical examples to show how the FSLE applied to dispersion phenomena works and conclude the Chapter by presenting the results of the computation of the FSLE in Lagrangian experimental data.

5.3 Numerical Examples

Before presenting the numerical experiments we briefly recall the numerical method adopted. All the systems here discussed are chaotic. We choose a trajectory having a chaotic behavior, i.e. we avoid to choose particles inside regular islands [37, 39]. Then we place $N-1$ particles around the chosen one, generating a cloud of initial size $R(0) = \delta_{min}$ with $R(0)$ (5.10). Then we apply the FSLE algorithm (see Sect. 2.3) following the growth of the cloud radius $R(t)$ measuring the doubling times for thresholds $\delta_n = \delta_0 r^n$ with $\delta_0 \gg \delta_{min}$ as already described. Of course, we repeat this procedure reconstructing the passive cloud around the last position reached by the reference chaotic tracer at the end of the previous expansion. Then we average over many expansion experiments as prescribed by Eqs. (2.31-2.32).

In the numerical experiments we observed the regimes described in the previous section: exponential regime, i.e. $\lambda(\delta) = \lambda$, and diffusion-like regime i.e. $\lambda(\delta) = D/\delta^2$, at least if the size L_B of the basin is enough large. Moreover, we have found that the behavior at large scale δ is well described by Eq. (5.14).

5.3.1 A model for transport in Rayleigh-Bénard convection

Rayleigh-Bénard convection is a well known example of flow [146]. It is observed in viscous fluids subject to the gravitational field and to a temperature gradient opposing to it. In the two-dimensional time periodic regime, the flow pattern is constituted by a set of cells with counter-rotating rolls. This regime appears for large aspect ratio (the ratio between the height and the width of the vessel containing the fluid) and in a certain range of Rayleigh number $\mathcal{R}a$, which is the main control parameter for such phenomenon [69]. One can study such flow by solving the full dynamical equations or by using a

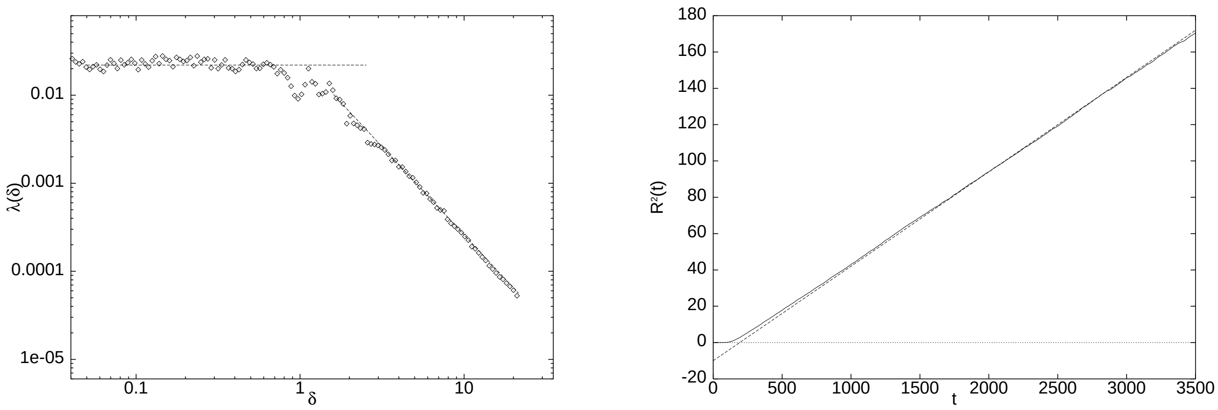

Figure 5.2: Lagrangian motion given by the Rayleigh-Bénard convection model with: $A = 0.2$, $B = 0.4$, $\omega = 0.4$, $k = 1.0$, $a = \pi$, the number of realizations is $\mathcal{N} = 2000$ and the series of thresholds is $\delta_n = \delta_0 r^n$ with $\delta_0 = 10^{-4}$ and $r = 1.05$. a)$\lambda(\delta)$ vs δ, the horizontal line indicates the Lyapunov exponent $\lambda = 0.022$, the dashed line is $D\delta^{-2}$ with $D = 0.26$. b)$\overline{R^2(t)}$ as function of t, the line is $2D\,t$ with $D = 0.26$.

simple kinematic model, i.e. by studying the Lagrangian dynamics induced by a stream function sharing the relevant features of the flow. Since here we are not interested on the dynamical mechanisms but only on the effects of the flow patterns on the diffusion we study a simple kinematic model originally introduced by Solomon and Gollub [147] to describe chaotic advection in the time-periodic Rayleigh-Bénard convection, which is defined by the following stream function:

$$\psi(x, y, t) = \frac{A}{k} \sin\left\{k\left[x + B\sin(\omega t)\right]\right\} W(y)\,, \tag{5.16}$$

where $W(y)$ is a function that satisfies rigid boundary conditions on the surfaces $y = 0$ and $y = a$ (we use $W(y) = \sin(\pi y/a)$). The direction y is identified with the vertical direction and the two surfaces $y = a$ and $y = 0$ are the top and bottom surfaces of the convection cell. The time dependent term $B\sin(\omega t)$ represents lateral oscillations of the roll pattern which mimic the even oscillatory instability [147].

The equation of motion are obtained by (5.2 and 5.16) Trajectories starting near the roll separatrices usually have a positive Lyapunov exponent and display diffusion in the x-direction. It is remarkable that, in spite of the simplicity of this model, the numerical results are in nice agreement with the experimental data on Rayleigh-Bénard convection [147].

Defining a passive cloud in the x-direction (i.e. a segment) and performing the expansion experiment, we have that, until δ is below a fraction of the dimension of the cell, $\lambda(\delta) = \lambda$ (Figure 5.2a). For larger values of δ one recovers standard diffusion $\lambda(\delta) = D/\delta^2$, with good quantitative agreement with the value of the diffusion coefficient evaluated by the standard technique, i.e. using $\overline{R^2(t)}$ as a function of time t (compare Figure 5.2a with Figure 5.2b).

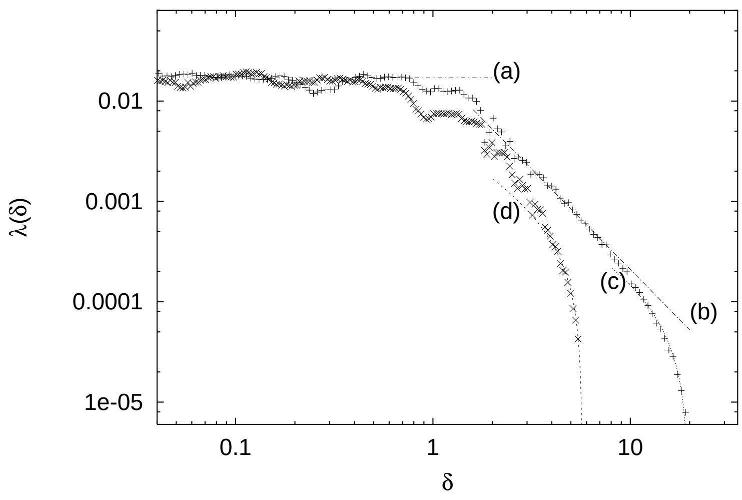

Figure 5.3: $\lambda(\delta)$ vs δ for the same model and parameters of Fig. 5.2, but in a closed domain with 6 (crosses) and 12 (diamonds) convective cells. The lines are respectively: (a) Lyapunov regime with $\lambda = 0.017$; (b) diffusive regime with $D = 0.021$; (c) saturation regime with $\delta_{max} = 19.7$; (d) saturation regime with $\delta_{max} = 5.7$.

To confine the motion of tracers in a closed domain, i.e. $x \in [-L_B, L_B]$, we must slightly modify the stream function (5.16). A possibility is to modulate the oscillating term in such a way that for $|x| = L_B$ the amplitude of the oscillation goes to zero, i.e. $B \to B\sin(\pi x/L_B)$ with $L_B = 2\pi n/k$ (n is the number of convective cells). In this way the motion is confined in $[-L_B, L_B]$.

In Figure 5.3 we show $\lambda(\delta)$ for two values of L_B. If L_B is large enough one can well see the three regimes, the exponential one, the diffusive one and the saturation given by equation (5.14). Decreasing L_B the range of the diffusive regime decreases, and for small values of L_B it disappears completely.

5.3.2 Point vortices in a disk

As second example, we consider the two-dimensional time-dependent flow generated by the motion of N point vortices in a disk [85]. For a unitary disk the positions of the vortices $(x_i = r_i \cos\theta_i, y_i = r_i \sin\theta_i)$, with circulation Γ_i, evolve according to the Hamiltonian dynamics

$$\dot{x}_i = \frac{1}{\Gamma_i}\frac{\partial H}{\partial y_i}, \quad \dot{y}_i = -\frac{1}{\Gamma_i}\frac{\partial H}{\partial x_i}, \tag{5.17}$$

where the Hamiltonian is [148]

$$H = -\frac{1}{4\pi}\sum_{i>j}\Gamma_i\Gamma_j \log\left[\frac{r_i^2 + r_j^2 - 2r_i r_j\cos(\theta_i - \theta_j)}{1 + r_i^2 r_j^2 - 2r_i r_j \cos(\theta_i - \theta_j)}\right] + \frac{1}{4\pi}\sum_{i=1}^{N}\Gamma_i^2 \log(1 - r_i^2). \tag{5.18}$$

Passive tracers evolve according to (5.2) with ψ given by

$$\psi(x,y) = -\frac{1}{4\pi}\sum_{i}^{N}\Gamma_i \log\left[\frac{r^2 + r_i^2 - 2rr_i\cos(\theta - \theta_i)}{1 + r^2 r_i^2 - 2rr_i\cos(\theta - \theta_i)}\right], \tag{5.19}$$

where $(x = r\cos\theta, y = r\sin\theta)$ denote the tracer position.

Figure 5.4a shows the relative dispersion, $\overline{R^2(t)}$, as a function of time in a system with 4 vortices. Apparently there is an intermediate regime of anomalous diffusion. On the other hand from Figure 5.4b one can see rather clearly that, with the method of working at fixed scale, only two regimes survive: the exponential and saturation one. Comparing Figure 5.4a and Figure 5.4b one understands that the mechanism described in Sect. 5.2 drives to a spurious anomalous diffusion. We stress the fact that these misleading behaviors are due to the superposition of different regimes and that the method of working at fixed scale has the advantage to eliminate this trouble. The absence of the diffusive range $\lambda(\delta) \sim \delta^{-2}$ is due to the fact that the characteristic length of the velocity field, which is of the order of the typical distance between two close vortices, is not much smaller than the size of the basin (see the discussion in Sect. 5.2 and 5.4.1).

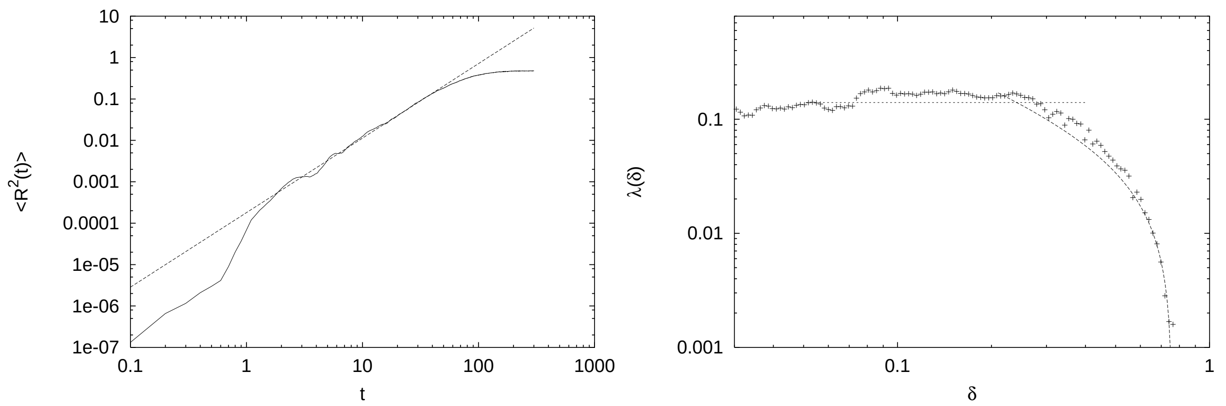

Figure 5.4: $\overline{R^2(t)}$ for the four vortex system with $\Gamma_1 = \Gamma_2 = -\Gamma_3 = -\Gamma_4 = 1$. The threshold parameter is $r = 1.03$ and $\delta_0 = 10^{-4}$, the dashed line is the power law $\overline{R^2(t)} \sim t^{1.8}$. The number of realizations is $\mathcal{N} = 2000$.

5.4 Experimental study of Lagrangian dynamics in a convective flow

The experimental configuration we have used constrains the fluid motion to be essentially two-dimensional in wide range for the parameters variability. The convection is generated in a rectangular tank (filled with water) by a linear heat source. The tank is $L = 15.0\,cm$ wide, $10.4\,cm$ deep and $H = 6.0\,cm$ height. The upper and lower surfaces are kept at constant temperature and the side walls can be considered as adiabatic (see Ref. [90] for further details).

The Eulerian features of the flow are controlled by 3 non-dimensional parameters [146]: the Rayleigh number $\mathcal{R}a = (g\beta Q H^3)/(\alpha\nu\kappa)$, the Prandtl number $\mathcal{P}r = \nu/\kappa$ and the aspect ratio $A = H/L$, where g is the gravitational acceleration, β the thermal expansion coefficient, α the thermal conductivity, ν the kinematic viscosity, κ the thermal diffusivity, Q the heat flux per unit length of the linear source, H the height of the tank, and L its width. Essentially we vary the heat flux Q furnished to the system (see Table 5.1).

The flow consists of two main counter-rotating rolls divided by an ascending thermal plume above the heat source [149]. The upper end of the plume oscillates horizontally almost periodically with a frequency depending on the Rayleigh number. Lagrangian trajectories generated by a large number of small ($50\,\mu m$ in diameter), non-buoyant particles are identified on the middle vertical plane by the Particle Tracking Velocimentry technique (PTV) [149].

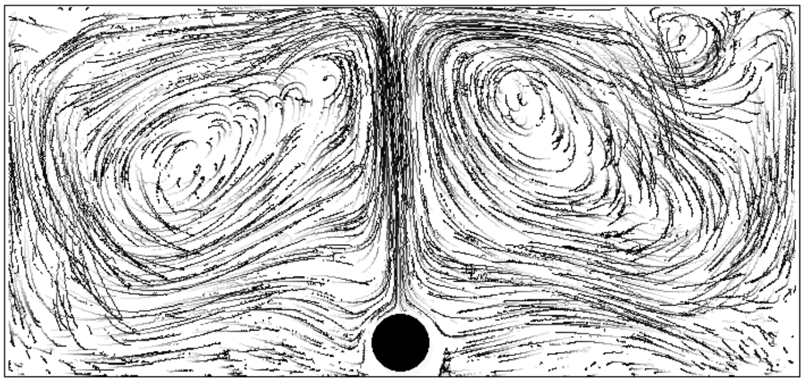

Figure 5.5: Snapshot of some trajectories obtained by the PTV algorithm, on the bottom the black circle indicates the heat source.

Figure 5.5 shows an example of the long living Lagrangian trajectories obtained as output of the PTV analysis. Acquisitions last for 2700 s: during this period 22500 frames are digitized. Typically 900 particles are simultaneously tracked for each frame. Experiments have been performed for 6 different values of the heat flux supplied through the linear source. The values of the physical parameters for the runs are reported in Table 5.1.

$P(W/s)$	$\nu(10^{-7}m^2/s)$	$\kappa(10^{-7}m^2/s)$	$\alpha(10^{-4}m^3/K)$	$\mathcal{R}a$	$\mathcal{P}r$
1.00	8.850	1.441	2.593	$6.87\ 10^7$	6.14
3.50	8.870	1.440	2.583	$2.39\ 10^8$	6.16
8.25	8.720	1.444	2.652	$5.96\ 10^8$	6.04
12.20	9.440	1.429	2.329	$7.20\ 10^8$	6.61
22.4	8.380	1.452	2.815	$1.74\ 10^9$	5.77
29.20	8.560	1.447	2.729	$2.17\ 10^9$	5.92

Table 5.1: Parameters related to the analyzed runs. Q is the heat flux injected into the system, ν the kinematic viscosity, κ the thermal diffusivity and α the thermal dilatation factor.

We directly investigate the "chaoticity" of the Lagrangian motion by looking at the separation growth of initially close trajectories with the FSLE.

5.4.1 Finite size Lyapunov exponent from Lagrangian data

Since the convective pattern in the experiment is essentially a two-dimensional, time dependent flow even at very high Rayleigh numbers, we expect chaotic Lagrangian motion

[86, 87]. We used the FSLE analysis for the experimental trajectories in order to probe the separation growth at different scales: from the Lyapunov exponential regime (5.12) up to the saturation regime (5.14). For all the results presented here below we use as unit length the height of the cell, H, and as unit time the diffusive time $t_\kappa = H^2/\kappa$.

We report the results for 6 runs at different Rayleigh numbers (see Table 5.1). The FSLE analysis on the experimental data has been done as follows. Fixed a set of thresholds $\delta_n = \delta_0 r^n$ $(n = 0, \ldots, N)$, for each time t_0 a new couple is considered whenever we find two particles (not yet forming a couple) at distance $R(t_0) \le \delta_0$. The separation growth between these particle is then followed for times $t > t_0$ and the "doubling times", $\tau(\delta_n, r)$, at scale δ_n as described (Sect. 2.3). Since trajectories are sampled at discrete times, the average over for computing $\lambda(\delta)$ is done following (2.32). In order to increase the statistics at large separations δ (indeed trajectories cannot be followed for the whole experiments, see Ref. [90]) , we computed the FSLE for different values of the smallest scale δ_0 ($\delta_0 = .067\,H$, $.1\,H$, $.13\,H$) and $r = 1.2$ for all the analysis.

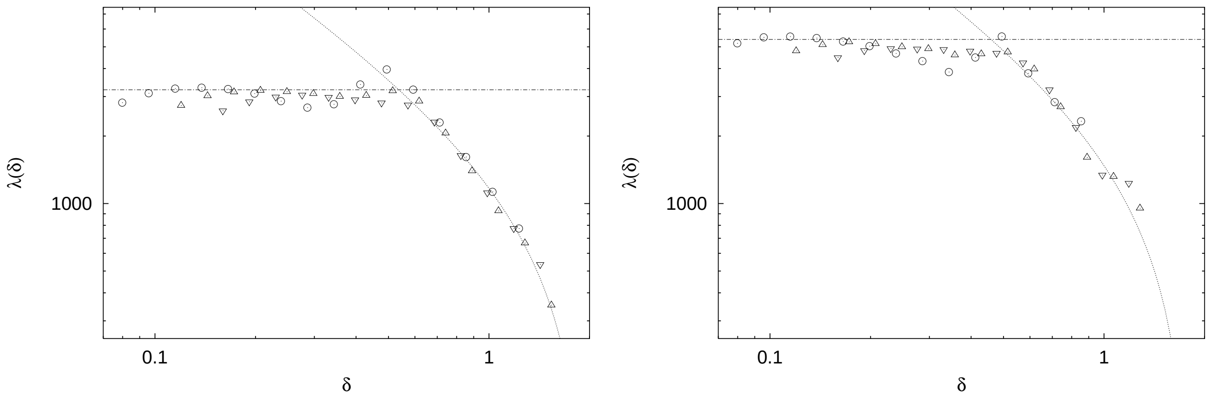

Figure 5.6: (a) $\lambda(\delta)$ versus δ for different initial thresholds $\delta_0 = .067\,H$, $.1\,H$, $.13\,H$ at $\mathcal{R}a = 2.392\,10^8$, the straight line is the Lyapunov exponent $\lambda = 3100 \pm 2001/t_\kappa$ while the other curve is the saturation regime Eq. (5.14) with $\tau_R = 8.0\,10^{-4}\,t_\kappa$ and $\delta_{max} = 1.9\,H$, (b) is the same of Fig. (a) for $\mathcal{R}a = 5.96\,10^8$ one has $\lambda = 5400 \pm 6001/t_\kappa$, while $\tau_R = 5.0\,10^{-4}\,t_\kappa$ and $\delta_{max} = 1.8\,H$

Figure 5.6 shows the FSLE computed for two different Rayleigh numbers ($\mathcal{R}a = 2.39\,10^8$ and $\mathcal{R}a = 5.96\,10^8$). We observe the collapse of $\lambda(\delta)$ to a plateau at small values of δ which gives the Lyapunov exponent λ and so we have a clear evidence that the motion is chaotic.

For larger separation $\lambda(\delta)$ drops to smaller values, indicating a slowing down in the separation growth. This is quantitatively well described by the saturation behavior (5.14), confirming that $\lambda(\delta)$ is a very good indicator for the characterization of particles dispersion. The collapse of the curves at different δ_0 confirms that sufficient high statistics is reached even at large scales and the fluctuations among different δ_0 curves can be taken as an estimation of the error for $\lambda(\delta)$.

The characteristic Eulerian scale l_u can be estimated by the end of the exponential regime (plateau $\lambda(\delta) \simeq \lambda$) after which the non linear effects start to dominate. We find $l_u \simeq 0.5H$, indeed not too far from the saturation value. From the general discussion of Section 5.2 we do not expect the intermediate diffusive regime as Fig 5.6 confirms.

The fit of Figure 5.6 with the saturation regime (5.14) allows us to estimate the saturation scale $\delta_{max} \simeq 1.9\,H$ and the relaxation time $\tau_R \simeq 8.0\,10^{-4} t_\kappa$. We observe that both $1/\lambda$ (an estimation of the small scale mixing time) and τ_R are much smaller than the diffusive time t_κ. This means that diffusion plays marginal role in the dispersion of Lagrangian tracers in the convective cell. In addition, we observe that the characteristic scales l_u and δ_{max} seems to be independent on the Rayleigh number.

In addition, in order to explore the dependence of the Lagrangian statistics on the Eulerian characteristics, we have performed the FSLE analysis for Rayleigh number which varies over more than one order of magnitude (see Table 5.4). We found a power law dependence of the Lagrangian Lyapunov exponent on $\mathcal{R}a$ [90]

$$\lambda \sim \mathcal{R}a^{1/2} \,. \tag{5.20}$$

We have understood such power law behavior in terms of a simple dimensional argument, for details see Ref. [90].

These results show that the FSLE analysis is indeed very powerful in quantifying dispersion properties and, moreover, can be very useful in experimental studies. In fact for this flow the usual relative dispersion analysis at fixed time delays is unsatisfactory (see Ref. [90]).

5.5 Discussions and Remarks

In the study of relative dispersion of Lagrangian tracers one has to tackle situations in which the asymptotic behavior is never attained. This may happen in presence of many characteristic Eulerian scales or, what is typical of real systems, in presence of boundaries.

It is worth to stress that such kind of systems are very common in geophysical flows (see [140] and reference therein), and also in plasma physics [141]. Therefore a close understanding of non-asymptotic transport properties can give important information about these natural phenomena.

To face these problems, in recent years, there have been proposed several different approaches. We remind the symbolic dynamics [150, 151] and the chaotic scattering [73] approaches, the exit time description for transport in semi-enclosed basins [140], symplectic maps [152], open flows [153] and in plasma physics [141].

In this Chapter we have discussed the applications of the Finite Size Lyapunov Exponent, $\lambda(\delta)$. We want to stress that this approach is complementary to the traditional one, in which one looks at the average size of the clouds of tracers as function of time. For values of δ much smaller than the smallest Eulerian characteristic length, one has that $\lambda(\delta)$ coincides with the maximum Lagrangian Lyapunov Exponent. For larger δ the shape of $\lambda(\delta)$ depends on the detailed mechanisms of spreading, i.e. the structure of the advecting velocity field and/or the presence of boundaries. The diffusive regime corresponds to $\lambda(\delta) \simeq D/\delta^2$. If δ gets close to its saturation value, i.e. the characteristic size of the basin, the universal shape of $\lambda(\delta)$ can be obtained on the basis of dynamical system theory.

A remarkable advantage of working at fixed scale (instead of at fixed time as in the traditional approach) is its ability to avoid misleading results, for instance apparent anomalous scaling over a certain time interval.

Conclusions

The aim of this thesis is the investigation and characterization of some aspects of dynamical systems connected with the *predictability problem* which cannot be described by standard concepts and tools such as, e.g., the Lyapunov exponents or the Kolmogorov-Sinai entropy.

The usual Lyapunov exponents are mathematically well defined in the limit of infinitesimal perturbations and infinite time; however, these limits are typically not accomplished in realistic settings. The main outcome of our research in this direction is the development of the *Finite Size Lyapunov Exponent*, $\lambda(\delta)$, as a tool for systematically exploring the evolution of perturbations at different scales. Unlike the Lyapunov exponent, $\lambda(\delta)$ contains direct information about the predictability time for a perturbation of a certain size. Moreover, by analyzing the details of the dependence of $\lambda(\delta)$ on δ, one is able to detect the presence of different dynamical mechanisms driving the perturbations evolution (e.g. the presence of different characteristic times, or anomalous behaviors like that studied in Sect. 2.3.2 and 4.2). The results obtained in this thesis are summarized below.

In real world systems, one is often faced with the presence of many characteristic scales, each of which evolving with its own characteristic time (e.g. turbulence in geophysical flows). In such a situation, when one has to devise numerical models, e.g. for weather forecast, he has to reduce the number of degrees of freedom. Since one is typically interested in modeling and forecasting the large slow evolving scales, one usually constructs a parameterization of the fast evolving scales in order to take into account their dynamical effects on the resolved degrees of freedom. This introduces an uncertainty (usually not small) on the "true" equations of motion of the system, which affects our ability to predict the large (slow evolving) scales. By means of the FSLE we have shown the way in which it is possible characterize quantitatively the predictability time of the large scales. In addition, it allows us to evaluate to what extent the parameterization used is good, i.e. if the model equation recovers the intrinsic predictability of the systems (that due to uncertainties on the initial conditions) on large scales.

The Finite Size Lyapunov Exponent is very powerful in detecting the presence of different characteristic times. This is particularly interesting when *a priori* we do not know the presence of different times in the dynamics. In this direction we have studied the coherent dynamics of globally coupled maps showing *macroscopic chaos*: a sort of hydrodynamical-like irregular behavior of some global observable (i.e. the center of mass). While the usual Lyapunov exponent only characterizes the microscopic motion, with the Finite Size Lyapunov Exponent we were able to characterize *macroscopic behaviors*. Indeed, at small scales we found the usual (microscopic) Lyapunov exponent, while at larger scales we were able to define a sort of *macroscopic Lyapunov exponent* which can be much smaller than the microscopic one. In this way we obtain a quantitative characterization of the chaotic motion at hydrodynamical level remaining at a kinetic level of description. This is very important since, in such systems, there are not systematic methods to write an equation of motion at a macroscopic level.

In extended systems, where the spatial development is as important as the temporal evolution, one has to characterize not only the way in which a perturbation grows, but also the way in which it propagates in space. The propagation of infinitesimal perturbations can be fully characterized via linear stability analysis. In particular, the propagation velocity of infinitesimal disturbances can be easily identified by looking at the velocity dependent Lyapunov exponent (the *comoving* Lyapunov exponent). Moreover, in most systems the linear analysis can be applied even when the perturbation is no longer infinitesimal: indeed, for generic systems, the propagation speed is determined by the spatial regions in which the perturbation is infinitesimal. However, in certain systems, finite perturbations can propagate with velocities higher than that given by the linear analysis. By generalizing the Finite Size Lyapunov Exponent to a comoving frame of reference, we were able to identify a *marginal stability criterion* able to capture linear as well as nonlinear propagation phenomena. Indeed, when the perturbation is infinitesimal, the FSLE on a comoving reference frame is nothing but the comoving Lyapunov exponent, but, as soon as the perturbation enters in the non linear regime of its evolution, it is able to capture the relevant non linear mechanisms which drive the perturbation propagation.

As a final application of the Finite Size Lyapunov Exponent, we have studied the problem of characterizing the two-particles dispersion properties of Lagrangian tracers in flows confined in bounded domains. We have considered the case of time-periodic velocity fields for which one expects the Lagrangian motion to be chaotic. The presence of boundaries inhibits the possibility to use asymptotic tools and concepts for characterizing the dispersion properties. However, by using the FSLE analysis, we were able to achieve a good description of such properties: at small (compared with the characteristic length of the velocity field) particles pair separation we recovered the Lagrangian Lyapunov exponent. At large scale, if the particles diffuse (this situation is usually accomplished when the characteristic length of the velocity field is much larger than the domain size) one has $\lambda(\delta) \sim \delta^{-2}$. Finally, at scales comparable with the domain size, we found a characteristic δ-dependence for $\lambda(\delta)$. These results have also been confirmed by an experimental study of Lagrangian motion in a convective flow.

In high dimensional systems, one has a *plethora* of different phenomena, we believe that the application of the scale-dependent analysis discussed in this thesis to other complex dynamical systems could help in understanding many features of such systems. It is worth remarking that a scale-dependent description of high dimensional systems can be also performed by using other quantities, e.g., one can define the ε-entropy or an attractor dimension depending on the observation scale. The combined study of these quantities is a promising tool for applications also in time series analysis.

List of Publications

1. V. Artale, G. Boffetta, A. Celani, M. Cencini and A. Vulpiani
   Dispersion of passive tracers in closed basins: Beyond the diffusion coefficient,
   Physics of Fluids **9**, 3162 (1997).

2. M. Cencini, M. Falcioni, D. Vergni and A. Vulpiani
   Macroscopic chaos in globally coupled maps
   Physica D **130**, 58 (1999).

3. *M. Cencini, G. Lacorata, A. Vulpiani and E. Zambianchi,
   Mixing in a Meandering Jet: a Markovian Approximation
   To appear *Journal of Physical Oceanography*, 1999

4. G. Boffetta, A. Celani, M. Cencini, G. Lacorata and A. Vulpiani
   Predictability in systems with an uncertainty in the evolution equation
   To appear *Journal of Physics A: mathematical and general*, 1999

5. *P. Castiglione, M. Cencini, A. Vulpiani and E. Zambianchi
   Transport in finite size systems in geophysics: an exit time approach,
   To appear on *Chaos*, 1999

6. G. Boffetta, A. Celani, M. Cencini, G. Lacorata and A. Vulpiani
   Non Asymptotic Properties of Transport and Mixing
   To appear on *Chaos*, 2000

7. *L. Biferale, M. Cencini, D. Vergni and A. Vulpiani
   Exit time of turbulent signals: a way to detect the intermediate dissipative range
   To appear on *Physical Review E: Rapid Communications*, 1999

8. G. Boffetta, M. Cencini, S. Espa and G. Querzoli

Experimental evidence of chaotic advection in a convective flow
Europhysics Letters, **48**, 629 (1999)

9. G. Boffetta, M. Cencini, S. Espa and G. Querzoli
Chaotic advection and relative dispersion in an experimental convective flow
Physics of Fluids, Submitted 1999

10. M. Cencini and A. Torcini
A generalized marginal stability criteria for perturbation propagation in extended systems
In preparation, 1999

11. M. Cencini, M. Falcioni, H. Kantz, E. Olbrich and A. Vulpiani
Chaos or Noise — Sense and Nonsense of a Distinction
In preparation, 1999

12. *M. Abel, L. Biferale, M. Cencini, M. Falcioni, D. Vergni and A. Vulpiani
Exit time approach to (ϵ, τ)-entropy
Submitted on *Physical Review Letters*, 1999

* The publications marked with * are not discussed in this thesis because their subjects are not directly related to the guidelines of the thesis.

Appendix A

Technical remarks on the FSLE

In this Appendix we discuss in detail the average on the "doubling" time statistics as prescribed by eqs. (2.31) and (2.32). To understand this point we focus on the case of infinitesimal perturbations, i.e. how one recovers the usual Lyapunov exponent in the limit $\delta \to 0$. We start by showing a subdle point.

Naively one can think that if he knows the doubling time $\tau(x, r)$ as function of the point x (which indivituates the reference trajectory) and the natural measure, i.e. $\rho_\mu(x)$ (having assumed differentiability), one can compute the Lyapunov exponent as (we consider the case of maps for simplicity):

$$\lambda = \left\langle \frac{1}{\tau(x,r)} \log \frac{\delta(\tau(x,r))}{\delta(0)} \right\rangle_{\rho_\mu} = \int dx \rho_\mu(x) \frac{1}{\tau(x,r)} \log \frac{\delta(\tau(x,r))}{\delta(x(0))} \tag{A.1}$$

where $\delta(\tau(x,r))$ is the perturbation size reached when the $|\delta x| \geq \delta$, being the time discrete this size will be in general a fluctuating quantity (see Sect. 2.3.1). As we shall see with a simple example this argument fails.

A simple example

Consider the following map of the unit intervall (see Fig. A.1):

$$f(x) = \begin{cases} 2x & \text{if } x \in [0, 1/2] \\ x - 1 & \text{if } x \in [1/2, 1] \end{cases} . \tag{A.2}$$

This map has an expanding region $[0, 1/2]$, where a perturbation doubles its size in one time step, and a marginally stable region $[1/2, 1]$, where a perturbation remains of the same size. By means of the Perron-Frobenius operator (1.5), one can easily compute

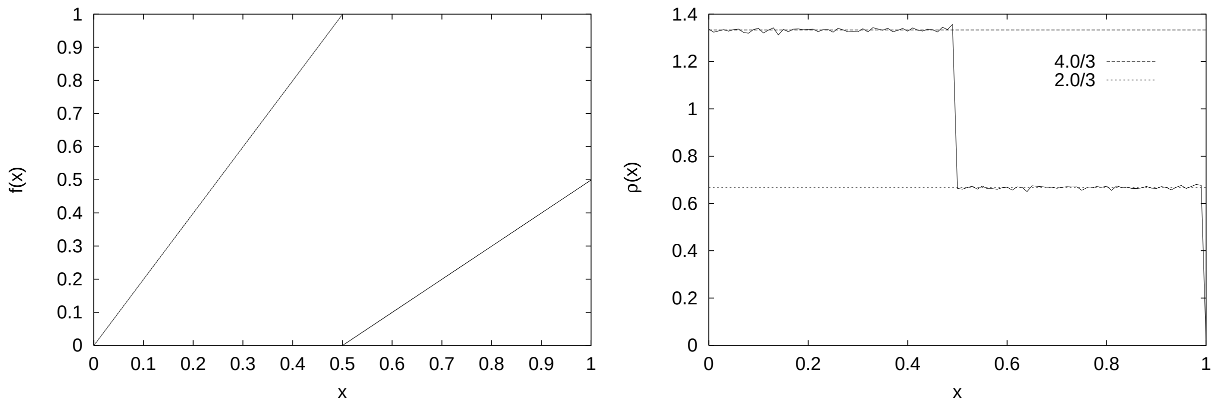

Figure A.1: Plot of the map (A.2) and of the invariant density (A.3)

the invariant probability density $\rho_\mu(x)$ (see Fig. A.1):

$$\rho_\mu(x) = \begin{cases} \frac{4}{3} & \text{if } x \in [0,1/2] \\ \\ \frac{2}{3} & \text{if } x \in [1/2,1] \end{cases} . \tag{A.3}$$

The maximum Lyapunov exponent can be easily computed as:

$$\lambda = \int \mathrm{d}x \rho_\mu(x) \log|f^{'}(x)| = \frac{2}{3}\log(2) = .46209... \tag{A.4}$$

Let us now verify if by studying the doubling time and the average (A.1) we recover the Lyapunov exponent (A.4). Given a perturbation of size δ (very small) on a "reference" trajectory starting at x. The *doubling time* $\tau(x,2)$, i.e. the time the perturbation takes to double its value, depends on the position of the "reference" trajectory as follows:

$$\tau(x,2) = \begin{cases} 1 & \text{if } x \in [0,1/2] \\ 2 & \text{if } x \in [1/2,1] . \end{cases} \tag{A.5}$$

Indeed, if the reference trajectory is in $[0,1/2]$ it doubles in one time step, otherwise if it is in $[1/2,1]$ it remains of the same size in the next steps and the reference point is mapped in the interval $[0,1/2]$ after which doubles in one step. By performing the average of the inverse of the Lyapunov exponent on the invariant measure (A.1) one has:

$$\left\langle \frac{1}{\tau(x,2)} \right\rangle_{\rho_\mu} = \int \mathrm{d}x \rho_\mu(x) \frac{1}{\tau(x,2)} = \frac{2}{3} + \frac{1}{6} = \frac{5}{6} \tag{A.6}$$

which gives a "Lyapunov exponent" equal to :

$$\tilde{\lambda} = \left\langle \frac{1}{\tau(x,2)} \right\rangle_{\rho_\mu} \log(2) = \frac{5}{6}\log(2) \neq \lambda \tag{A.7}$$

which is different from the true value (A.4).

To understand this result one has to consider the wayin which the FSLE algortim works. The subdle point is that, actually, by looking at the points where the perturbation doubles its value we do not sample the *natural measure* as we will see in the following.

Let us initialize a perturbation δ_{min}, follow its growth untill it reaches the value δ, and compute compute the probability distribution function, $\rho_d(x)$, of the points, x, at which the perturbation doubles (of course at each doubling one makes a rescaling of the perturbation at size δ). This distribution is uniform in the interval $[0, 1]$ (i.e. very different from the invariant distribution $\rho_\mu(x)$ (A.5), compare Fig. A.1 with Fig. A.2). The shape of this PDF can be understood by the following simple argument: a perturbation doubles only when the reference trajectory is in the region $[0, 1/2]$, so that the preimages of the points at which one has the doubling are uniformly distributed in this interval. The one step iterates of this distribution (which is $\rho_d(x)$) is nothing but the uniform distribution in $[0, 1]$. Now, averaging the doubling times as in Eq. (2.32) one has:

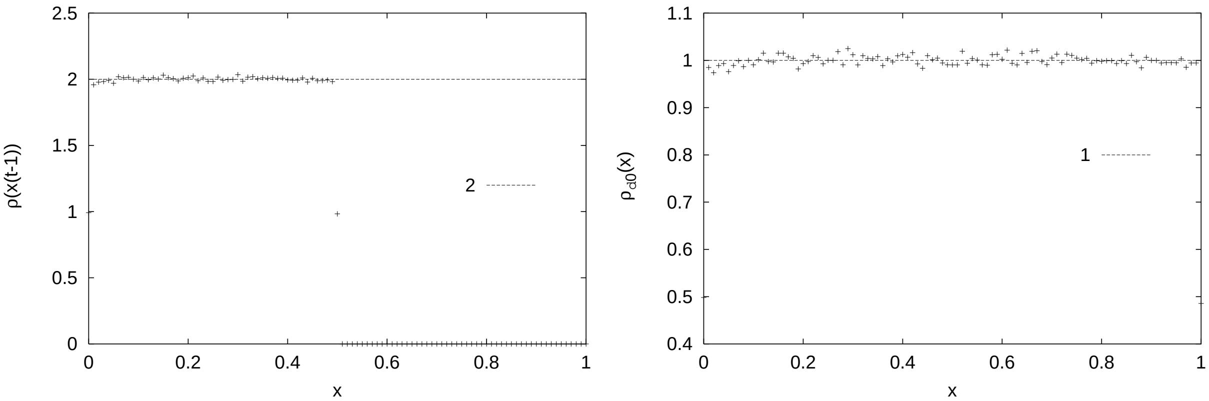

Figure A.2: Plot of $\rho_d(x)$ (right) and the PDF of the preimages (left) for the same map of Fig. A.1.

$$< \tau(x, 2) >_e = \int \mathrm{d}x \rho_d(x) \tau(x, 2) = \frac{1}{2} 1 + \frac{1}{2} 2 = \frac{3}{2}, \tag{A.8}$$

and hence the Lyapunov exponent is:

$$\lambda_{FSLE} = \frac{1}{< \tau(x, 2) >_e} \log(2) = \frac{2}{3} \log(2) = \lambda \tag{A.9}$$

which is equal to the maximum Lyapunov exponent (A.4). We have used the symbol λ_{FSLE} to evidenziate that this is the Lyapunov exponent computed by following the FSLE algorithm.

This simple example shows that actually the doubling times statistics as prescribed by the FSLE algorithm (i.e. starting from $\delta_{min} \ll \delta$) not only allows the perturbation to be oriented along the maximum expanding direction but also selects a measure (i.e. $\rho_d(x)$) which turns out to be the proper measure over which one has to perform the average of the doubling times.

Meaning of the measure $\rho_d(x)$

To better understand this point, we can rewrite (A.1) in another form (valid for infinitesimal perturbation, i.e. we are in tangent space):

$$\lambda = \int dx \rho_\mu(x) \frac{1}{\tau(x,r)} \sum_{i=0}^{\tau(x,r)-1} \frac{d}{dF^{(t)}(x)} \log(|F^{'}(F^{(t)}(x))|)\,, \tag{A.10}$$

which has to be compared with

$$\lambda = \int dx \rho_\mu(x) \log |F^{'}(x)|\,. \tag{A.11}$$

One easily recognizes that these two equation are equal only when $\tau(x,r) = T$ for all x, i.e. $\tau(x,r)$ has to be independent of the position, e.g. for the shif map and the tent map.

However, in generic situations (when there are expanding and contracting regions), the time $\tau(x,r)$ is a function of x. When this is the case the correct average is (2.32), which can be written as:

$$\lambda = \frac{\int dx \rho_d(x) \sum_{i=0}^{\tau(x,r)-1} \log(|F^{'}(F^{(t)}(x))|)}{\int dx \rho_d(x) \tau(x,r)} \tag{A.12}$$

where, for the moment, $\rho_d(x)$ is an unknown function: it is the measure selected by the doubling condition[1].

In order to understand what measure is $\rho_d(x)$, we recall that the invariant density, $\rho_\mu(x)$, is the solution of the Perron-Frobenius equation (see Sect. 1.1):

$$\rho_{t+1}(x) = \int dy \rho_t(y) \delta(x - F(y))\,. \tag{A.13}$$

An error doubling experiment corresponds to the following situation: each point (x) is iterated until the perturbation has reached r times the initial value, i.e. for $\tau(x,r)$ steps. Therefore the point visited by the doubling experiments are distributed with a density

[1] Looking at (A.12) it is easy to realize that when $\tau(x,r)$ does not depend on x, one has $\rho_d(x) = \rho_\mu(x)$, i.e. to the natural measure.

different from the natural one. In particular, let us introduce the following generalization of the Perron-Frobenious equation:

$$
\begin{aligned}
\rho_{R+1}(x) &= \int dy\, \rho_R(y)\delta(x - F^{\tau(y,r)-1}(y)) \\
\tau(x,r) &= \inf_T \left\{ \sum_{i=0}^{T-1} \log(|F'(F^{(t)}(x))|) \le \log(r) \right\}
\end{aligned}
\tag{A.14}
$$

where R labels the R-iteration error-doubling experiments.

Now it is clear that starting from $\delta_{min} \ll \delta_0$ for a given r means that you are iterating Eq. (A.14) many times, that is to say that you have reached an "invariant" (under doubling experiment distribution) $\rho_d(x)$. Let us note that by using the second algorithm for computing the FSLE (see Sect. 2.3.1) each time the last threshold is reached the perturbation is rescaled to δ_{min}, the integration period untill δ_0 is reached corresponds to iterates many times Eq. (A.14). This ensures to reach the correct measure over which the doubling times are averaged[2]

[2] As a confirmation of this stament one can perform the FSLE computation making from one doubling experiment to another a long integration during which the doubling times are not computed and after which the perturbation is setted to δ_{min}. Preoceeding in this way we have found (figure not shown) that the FSLE does not change. The reasons is that in the integration from δ_{min} up to δ_0, if $\delta_{min} \ll \delta_0$, the correct measure $\rho_d(x)$ is recovered.

Appendix B

Parameterization of small scales

Typically a realistic problem (e.g. turbulence) involves many interacting degrees of freedom with different characteristic times. Let us indicate with $\mathbf{z}$ the state of the system under consideration, with an evolution law:

$$\frac{\mathrm{d}\mathbf{z}}{\mathrm{d}t} = \mathbf{F}(\mathbf{z}) \,, \quad \mathbf{F}, \mathbf{z} \in \mathcal{R}^N \,. \tag{B.1}$$

The dynamical variables $\mathbf{z}$ can be split in two sets:

$$\mathbf{z} = (\mathbf{x}, \mathbf{y}) \,, \tag{B.2}$$

where $\mathbf{x} \in \mathcal{R}^n$ and $\mathbf{y} \in \mathcal{R}^m$ $(N = n + m)$, being respectively $\mathbf{x}$ and $\mathbf{y}$ the "slow" and "fast" variables. The distinction between slow and fast variables is often largely arbitrary.

The evolution equation (B.1) is divided into two blocks, the first one containing the dynamics of the slow variables, the second one associated with the dynamics of the fast variables

$$\begin{cases} \dfrac{d\mathbf{x}}{dt} = \mathbf{F_1}(\mathbf{x}) + \mathbf{F_2}(\mathbf{x}, \mathbf{y}) \\ \dfrac{d\mathbf{y}}{dt} = \tilde{\mathbf{F}}_1(\mathbf{x}, \mathbf{y}) + \tilde{\mathbf{F}}_2(\mathbf{y}) \,. \end{cases} \tag{B.3}$$

If one is interested only in the slow variables it is necessary to write an "effective" equation for $\mathbf{x}$. As far as we know there is only one case for which it is simple to find the effective equations for $\mathbf{x}$. If the characteristic times of the fast variables are much smaller than those ones of the $\mathbf{x}$ (adiabatic limit), one can write:

$$\mathbf{y} = < \mathbf{y} > + \boldsymbol{\eta}(t) \,, \tag{B.4}$$

where $\boldsymbol{\eta}$ is a Wiener process, i.e. a zero mean Gaussian process with

$$< \eta_i(t)\eta_j(t') > = < \delta y_i^2 > \delta_{ij}\delta(t-t') \,. \tag{B.5}$$

Therefore one obtains for the slow variables:

$$\frac{\mathrm{d}\mathbf{x}}{\mathrm{d}t} = \mathbf{F_1}(\mathbf{x}) + \delta\mathbf{F_1}(\mathbf{x}) + \delta\mathbf{W}(\mathbf{x}, \boldsymbol{\eta}) \,, \tag{B.6}$$

where

$$\delta\mathbf{F_1}(\mathbf{x}) = \mathbf{F_2}(\mathbf{x}, \langle\mathbf{y}\rangle) + \delta\mathbf{F_2} \,,$$

being $\delta F_{2,j} = 1/2\sum_i \partial^2 F_{2,j}/\partial y_j^2 < \delta y_i^2 >$ and

$$\delta W_i = \sum_i \partial F_{2,j}/\partial y_j|_{<\mathbf{y}>} \eta_i(t) \,.$$

Basically the slow variables $\mathbf{x}$ obey to a non linear Langevin equation.

Here the role of the fast degrees of freedom becomes relatively simple: they give small changes to the drift $\mathbf{F_1} \to \mathbf{F_1} + \delta\mathbf{F_1}$ and a noise term $\delta\mathbf{W}(\mathbf{x}, \boldsymbol{\eta})$. We remark that the validity of the above argument is rather limited. Even if one has a large time scale separation, the statistics of the fast variables can be very far from the Gaussian distribution. In particular, in system with feedback ($\tilde{\mathbf{F}}_1 \neq 0$) one cannot model the fast variable $\mathbf{y}$ independently of the resolved $\mathbf{x}$.

In the generic situation the construction of the effective equation for $\mathbf{x}$ requires to follow phenomenological arguments which depend on the physical mechanism of the particular problem. For example, for the Lorenz '96 model discussed in Sect. 3.1.1, where $F_{2,k}(\mathbf{x}, \mathbf{y}) = \sum_{j=1,J} y_{j,k}$, we use the following procedure for the parameterization of the fast variables and the building of the effective equation for $\mathbf{x}$. Instead of assuming (B.4) we mimic the fast variables in terms of the slow ones:

$$\mathbf{y}(t) = \mathbf{g}(\mathbf{x}(t)) = <\mathbf{y}|\mathbf{x}(t)> + \eta(t) \tag{B.7}$$

where $< \,|\mathbf{x} >$ stands for the conditional average and $\eta(t)$ is a noise term. Inserting (B.7) into the first of (B.3) one obtains

$$\frac{\mathrm{d}\mathbf{x}}{\mathrm{d}t} = \mathbf{F}_1(\mathbf{x}) + \mathbf{F}_2(\mathbf{x}, \mathbf{y}) = \mathbf{F}_1(\mathbf{x}) + \mathbf{F}_2(\mathbf{x}, <\mathbf{y}|\mathbf{x}>) + \delta\mathbf{F}_2(\mathbf{x}) \,, \tag{B.8}$$

where

$$\delta F_{2,i} = \sum_{j,k} \left.\frac{\partial^2 F_{2,i}}{\partial y_j \partial y_k}\right|_{y=<y|x>} \langle \eta_j \eta_k \rangle \,. \tag{B.9}$$

In the Lorenz '96 model (3.3), because of the linear coupling between the different scales, the terms $\delta\mathbf{F}_2$ are absent and one has a close model for the large scale variables

$$\frac{\mathrm{d}\mathbf{x}}{\mathrm{d}t} = \mathbf{F_1}(\mathbf{x}) + \mathbf{F_2}(\mathbf{x}, <\mathbf{y}|\mathbf{x}>) \,. \tag{B.10}$$

The ansatz (B.7) is well verified in the numerical simulations. We have computed the $\lambda_{TM}(\delta)$ by using a best fit for $\mathbf{F_2}$ and we have obtained a good reproduction of the $\lambda_{TT}(\delta)$ for large δ. In the Lorenz '96 model (3.3), where the coupling between slow and fast variables is practically linear, one has that $F_{2,k}(\mathbf{x}, <\mathbf{y}|\mathbf{x}>) = \sum_{j=1,J} <y_{j,k}|x_k> \simeq \nu_e x_k$.

Now we will discuss the case of the Shell Model parameterization which pertains to the general issue of the subgrid-scale modelization. The literature on this field and the related problems (e.g. closure in fully developed turbulence) is enormous and we do not pretend to discuss here in details this field. Let us only recall the basic idea introduced over a century ago by Boussinesq, and later developed further by Taylor, Prandtl and Heisenberg – to cite some of the most famous ones– for fully developed turbulence [53]. In a nutshell the idea is to mimic the energy flux from the large to the small scales (in our terms from slow to fast variables) by an effective dissipation: the effect of the small scales on the large ones can be modeled as an enhanced molecular viscosity.

By simple dimensional arguments one can argue that the effects of small scales can be replaced by an effective viscosity at scales r, given by

$$\nu^{(e)} \sim r\delta v(r) \,, \tag{B.11}$$

where $\delta v(r)$ is the velocity fluctuation on the scale r.

The above argument for the Shell Model (3.29) gives [110]:

$$\nu_n^{(e)} = \kappa \frac{|u_n|}{k_n} \,, \tag{B.12}$$

where $\kappa \sim O(1)$ is an empirical constant. From Eq. (B.11) one could naively think to use dimensional argument *à la* Kolmogorov to set a constant eddy viscosity $\nu_n^{(e)} \sim k_n^{-4/3}$. In this way one forgets the dynamics and this can cause numerical blow up. More sophisticated arguments that do not include the dynamics lead to similar problems.

Let us remark that the parameterization (B.12) is not exactly identical to those obtained by closure approaches where the eddy viscosity is given in terms of averaged quantities. In our case this would mean to write $\langle u_n^2 \rangle^{1/2}$ instead of $|u_n|$ in (B.12).

After this discussion it is easy to recognize that the parameterization in terms of conditional averages introduced for the Lorenz '96 model [8] is, *a posteriori*, an eddy viscosity model.

Appendix C

Finite time correction to the FSCLE

In numerical computation of the Lyapunov exponents one is forced to use a finite time approximation for a infinite time limit Eqs. (1.8)-(1.15). Of course, this is not a big problem if the rate of convergence to the asymptotic value is very fast, and this is typically the case in low dimensional systems. However, also in low dimensional systems one can have a slow convergence to the asymptotic value, e.g., it could need a long time to have the alignment along the direction of maximal expansion if the initial perturbation it is not well prepared. This problem becomes more and more dramatic once one consider high dimensional systems. Indeed, due to the huge dimensionality the time to align along the direction of maximal expansion could be very slow [6, 82, 126].

In particular, this would lead to corrections to the finite time estimate of the Lyapunov exponent. For example, Goldhirsh et al. [126] were able to demonstrate (by studying a set of differential equation for the eigenvalue and the eigenvectors of the stability matrix) that the convergence of the finite time estimate of the Lyapunov exponents, $\lambda_i(t)$, to the asymptotic value(i.e. $\lambda_i(t) \to \lambda_i$ when $t \to \infty$) could be indeed very slow. They found

$$\lambda_i(t) = \lambda_i + \frac{B_i + \xi_i(t)}{t}, \tag{C.1}$$

where B_i is a constant and $\xi_i(t)$ a noisy term, with zero average and relatively small amplitudes.

In the case of the CML here studied, we have the same kind of problem, and if possible, it is also more dramatic. Indeed, we compute the Lyapunov exponent through the $\delta \to 0$ limit of $\lambda(\delta, v)$ (see Eq. (4.34)), i.e. we do not use the evolution in tangent space but the full non linear equations. Due to the near-neighbor coupling, however, it is possible to take into account the finite time corrections. In the following we show how this can be carried out. We show only the case of maps with constant slope, e.g. the shift map. The generalization to more general case is rather difficult and involves a lot of calculations which we do not want to discuss here[1]. In addition, we show only the case at $v = 0$, the generalization to non zero velocities is rather straightforward.

The disturbances we treat are extremely localized ones Eq.(4.20) we perturb only one site (e.g. in the middle of the lattice). Let us consider the shift map,

$$f(x) = \beta\, x \mod 1\,,$$

and the CML defined by Eq. (4.19) with the a perturbation at time $t = 0$ given by Eq.(4.20). The maximum Lyapunov exponent of the system is known and is equal to:

$$\lambda = \ln \beta\,. \tag{C.2}$$

The equation of motion in tangent space are the following:

$$\delta x_i(t+1) = \beta\left[(1-\epsilon)\delta x_i(t) + \frac{\epsilon}{2}(\delta x_{i-1}(t) + \delta x_{i+1}(t))\right]\,, \tag{C.3}$$

so that the firsts iterates of Eq. (C.3) go as follow:

t=1

$$\begin{aligned}
\delta x_0(1) &= \beta\, d_0(1-\epsilon) \\
\delta x_{\pm 1}(1) &= \beta\, d_0 \frac{\epsilon}{2} \\
\delta x_{\neq 0,\pm 1}(1) &= 0
\end{aligned} \tag{C.4}$$

t=2

$$\begin{aligned}
\delta x_0(2) &= \beta^2\, d_0 \left[(1-\epsilon) + 2\left(\frac{\epsilon}{2}\right)^2\right] \\
\delta x_{\pm 1}(2) &= \beta^2\, d_0 \epsilon(1-\epsilon) \\
\delta x_{\pm 2}(2) &= \beta^2 \left(\frac{\epsilon}{2}\right)^2 \\
\delta x_{\neq 0,\pm 1,\pm 2}(2) &= 0
\end{aligned} \tag{C.5}$$

t=3

$$\begin{aligned}
\delta x_0(3) &= \beta^3\, d_0(1-\epsilon)\left[(1-\epsilon) + 2\left(\frac{\epsilon}{2}\right)^2\right] + \epsilon^2(1-\epsilon) \\
\vdots &= \vdots \\
\vdots &= \vdots
\end{aligned} \tag{C.6}$$

[1]Moreover, for our purposes of recovering the $\delta \to 0$ limit it is not compulsory the computation of such corrections, indeed we use the FSCLE just to treat the case of non linear propagation

The finite time Lyapunov exponent computed at these three times is:

$$\begin{aligned}
\lambda(t=1) &= \ln\left(\frac{\delta x_0(1)}{\delta x_0(0)}\right) = \ln\beta + \ln(1-\epsilon) \\
\lambda(t=2) &= \frac{1}{2}\ln\left(\frac{\delta x_0(2)}{\delta x_0(0)}\right) = \ln\beta + \frac{1}{2}\ln\left[(1-\epsilon) + 2\left(\frac{\epsilon}{2}\right)^2\right] \\
\vdots &= \vdots
\end{aligned} \tag{C.7}$$

from these equations, one can see that $\lambda(t) - \lambda = \lambda(t) - \ln\beta \to 0$ as $t \to \infty$. At the moment we are studying if it is possible to find some iterative procedure to carry out the long times behavior of $\lambda(t)$. However, by performing a numerical evaluation of $\lambda(t)$, directly iterating Eq. (C.3) we have obtained a situation similar to that found by Goldhirsh et al. [126], see Eq. (C.1). In Fig. C.1 we show $-(\lambda(t) - \ln\beta)$, we found that

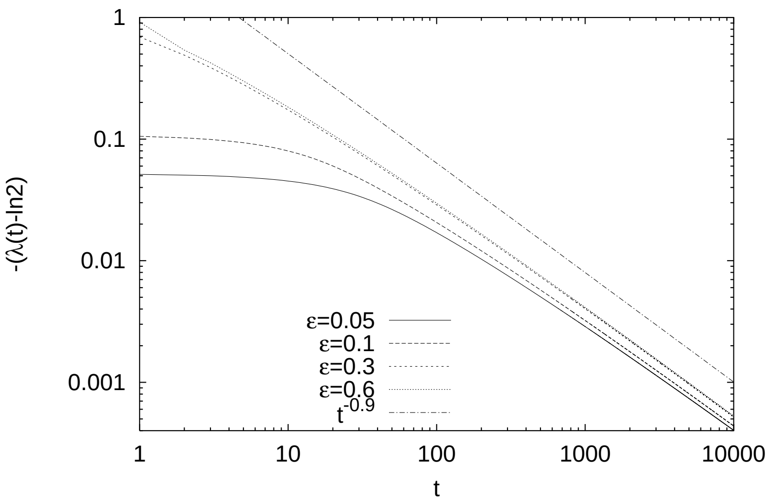

Figure C.1: $-(\lambda(t) - \ln\beta)$ as a function of t for $\beta = 2$ and different values of the coupling, from the bottom $\epsilon = 0.05, 0.1, 0.33, 0.6$. We also show the slope $t^{-0.9}$ for comparison.

the corrections can be well approximated (for large t) as:

$$\lambda(t) - \ln\beta = \frac{c(\epsilon)}{t^{0.9}} \tag{C.8}$$

where $c(\epsilon)$ is a constant[2] depending on the coupling.

Coming back to the problem of recovering λ in the limit $\delta \to 0$ of $\lambda(\delta)$, the procedure we have used is to iterate together with the two replicas for the computation of $\lambda(\delta)$

[2]Form Fig. C.1 one is tempted to say that $c(\epsilon) \to const$ at increasing the coupling, however much numerical and analytical studies are necessary to give a definite answer.

(see Sect. 2.3.1) also Eq. (C.3). In this way we have at each iteration the value of the corrections (C.4)–(C.7). Now one has simply to modify the average procedure (2.32) in:

$$\lambda(\delta) = \frac{1}{\langle \tau(\delta, r)\rangle_e} \left\langle \ln\left(\frac{||\delta \mathbf{x}(t+\tau(\delta_n, r))||}{\delta x(t)}\right) - \ln\left(\frac{|\delta \mathbf{x}^T(t+\tau(\delta_n, r))|}{\delta x^T(t)}\right) + \ln\beta \right\rangle_e . \quad \text{(C.9)}$$

where we have used the notation δx^T to indicate the perturbation in tangent space, the sign $-$ is because the corrections are negative. In this way we have obtained Fig. 4.12. Of course, the case of maps with non constant slope is much more difficult and computationally much heavy.

Let us conclude by observing that the finite time corrections (see Eqs. (C.1–C.8)) do not constitute just a mere technical point. Indeed, in the study of a realistic predictability problem one has to take into account such problem in order to properly characterize the limit of our predictability. In particular, the argument which has led to the formula (2.2) holds only if $\lambda(t) \approx \lambda_{max}$, otherwise Eq. (2.2) modifies in:

$$T_p \sim T_R + \frac{1}{\lambda} \ln \frac{\Delta}{\delta_0}, \quad \text{(C.10)}$$

where T_R roughly corresponds to the time[3] we need to have $\lambda(t) \approx \lambda_{max}$ Hence, in realistic situations and especially in high-dimensional systems the mechanism of transfer of the error $\delta \mathbf{x}$ through the degrees of freedom, which determines T_R, could be more important than the rate of divergence of nearby trajectories. Therefore, studies such that performed in Ref. [126] could be very important. In this perspective, the behavior (C.8) we found deserves future investigations, e.g. in more complex systems.

[3]This time may be connected with the time the tangent vector needs to relax on the time dependent eigenvector $\mathbf{e}_1(t)$ of the stability matrix, corresponding to the maximum Lyapunov exponent λ_{max}.

Appendix D

Derivation of Eq. (5.14) in a simple system

In this Appendix we present the derivation of the asymptotic behavior of $\lambda(\delta)$ for δ near to the saturation (5.14).

Let us first consider the simple case of a one dimensional Brownian motion in the domain $[-L_B, L_B]$, with reflecting boundary conditions. The evolution of the probability density p is ruled by the Fokker-Planck equation [44]

$$\frac{\partial p}{\partial t} = \frac{1}{2} D \frac{\partial^2 p}{\partial x^2} \tag{D.1}$$

with the Neumann boundary conditions

$$\frac{\partial p}{\partial x}(\pm L_B) = 0\,. \tag{D.2}$$

The general solution of (D.1) is

$$p(x,t) = \sum_{k=-\infty}^{\infty} \hat{p}(k,0) e^{ikx} e^{-t/\tau_k} + c.c\,, \tag{D.3}$$

where

$$\tau_k = \left(\frac{D}{2} \frac{\pi^2}{L_B^2} k^2 \right)^{-1}\,. \tag{D.4}$$

At large times p approaches the uniform solution $p_0 = 1/2L_B$. Writing p as $p(x,t) = p_0 + \delta p(x,t)$ we have, for $t \gg \tau_1$,

$$\delta p \sim \exp(-t/\tau_1)\,. \tag{D.5}$$

The asymptotic behavior for the relative dispersion $D(t)$ is

$$D(t) = \frac{1}{2} \int (x - x')^2 p(x,t) p(x',t)\, dx\, dx'\,. \tag{D.6}$$

For $t \gg \tau_1$ using (D.5) we obtain

$$D(t) \sim \frac{1}{2}\left(\frac{L^2}{3} - Ae^{-t/\tau_1}\right) \tag{D.7}$$

where $A \ll L_B^2/3$. Therefore for $\delta(t) = D(t)^{1/2}$ one has

$$\delta(t) \sim \frac{1}{\sqrt{2}}\left(\frac{L_B}{\sqrt{3}} - \frac{\sqrt{3}A}{2L_B}e^{-t/\tau 1}\right) . \tag{D.8}$$

The saturation value of δ is $\delta_{max} = L_B/\sqrt{3}$, so for $t \gg \tau_1$, or equivalently for $(\delta_{max}-\delta)/\delta \ll 1$, we expect

$$\frac{d}{dt}\ln\delta = \lambda(\delta) = \frac{1}{\tau_1}\frac{\delta_{max}-\delta}{\delta} \tag{D.9}$$

which is Eq. (5.14).

Let us remark that in the previous argument for $\lambda(\delta)$ for $\delta \simeq \delta_{max}$ the crucial point is the exponential relaxation to the asymptotic uniform distribution. In a generic deterministic chaotic system it is not possible to prove this property in a rigorous way. Nevertheless one can expect that this request is fulfilled at least in non-pathological cases. In the terminology of chaotic systems the exponential relaxation to asymptotic distribution corresponds to have the second eigenvalue α of the Perron-Frobenius operator inside the unitary circle; now the relaxation time is $\tau_1 = -\ln|\alpha|$ [3, 38].

Bibliography

[1] E.N. Lorenz, "Deterministic non-periodic flow", *J. Atmos. Sci.* **20**, 130 (1963).

[2] J.P. Eckmann & D. Ruelle, "Ergodic theory of chaos and strange attractors", *Rev. of Mod. Phys.* **57**, 617 (1985).

[3] E. Ott, *Chaos in dynamical systems*, (Cambridge University Press, 1993)

[4] R. Shaw, "Strange attractors, chaotic behavior and information flow", *Z. Naturf.* **36a**, 80 (1981).

[5] A.N. Kolmogorov, "New metric invariant of transitive dynamical systems and automorphism of Lebesgue spaces", *Dokl. Akad. Nauk SSSR* **119**, 861 (1958).

[6] T. Bohr, M.H. Jensen, G. Paladin & A. Vulpiani, *Dynamical systems approach to turbulence*, (Cambridge University Press, Cambridge, UK, 1998).

[7] E.N. Lorenz, "The predictability of a flow which possesses many scales of motion", *Tellus* **21**, 3 (1969).

[8] E.N. Lorenz, "Predictability - a problem partly solved", *Proc. Seminar on predictability,* p. 1, (Reading, U.K., ECMRWF, 1996); E.N. Lorenz & K.A. Emanuel, "Optimal sites for supplementary weather observations: simulation with a small model", *J. Atm. Sci.* **55**, 399 (1998).

[9] E. Aurell, G. Boffetta, A. Crisanti, G. Paladin & A. Vulpiani, "Growth of Non-infinitesimal Perturbations in Turbulence", *Phys. Rev. Lett.* **77**, 1262 (1996).

[10] E. Aurell, G. Boffetta, A. Crisanti, G. Paladin & A. Vulpiani, "Predictability in the large: an extension of the concept of Lyapunov exponent", *J. Phys.* **A30**, 1 (1997).

[11] P. Grassberger, "Information content and predictability of lumped and distributed dynamical systems", *Phisica Scripta* **40**, 346 (1989).

[12] S. Lepri, A. Politi & A. Torcini "Chronotropic Lyapunov Analysis: (I) a comprehensive characterization of 1D systems", *J. Stat. Phys.* **82**, 1429 (1996); "Chronotropic Lyapunov Analysis: (II) Towards a Unified Approach", *J. Stat. Phys.* **88**, 31 (1997).

[13] C.E. Shannon, “A mathematical theory of communication” *The Bell System Technical J.* **27**, 623 (1948); C.E. Shannon & W. Weaver, *The Mathematical Theory of Communication*, (University of Illinois Press, 1993).

[14] A.N. Kolmogorov, “Three approaches to the quantitative definition of information”, *Prob. Info. Trans.* **1**, 1 (1965); G.J. Chaitin, *Algorithmic information theory*, 3rd edition, (Cambridge University Press, Cambridge, UK, 1990).

[15] J. Ford, “How Random is a Coin Tossing?”, *Physics Today* **36**, 40 (1983).

[16] P. Grassberger, “Toward a quantitative theory of self-generated complexity”, *Int. J. Theor. Phys.* **25**, 907 (1986).

[17] P. Gaspard & X.J. Wang, “Noise, chaos, and (ϵ, τ)- entropy per unit time”, *Phys. Rep.* **235**, 291 (1993).

[18] R. Badii & A. Politi, *Complexity. Hierarchical structures and scaling in physics*, (Cambridge University Press, Cambridge, UK, 1997).

[19] J.P. Crutchfield & K. Kaneko, “Are attractors relevant for turbulence?”, *Phys. Rev. Lett.* **60**, 2715 (1988).

[20] A. Politi, R. Livi, G.L. Oppo & R. Kapral, “Unpredictable Behavior in Stable Systems”, *Europhys. Lett.* **22**, 571 (1993).

[21] D. Vergni, M. Falcioni & A. Vulpiani, “Spatial complex behavior in non-chaotic flow systems”, *Phys. Rev. E* **56**, 6170 (1997); “Characterization of the spatial complex behavior and transition to chaos in flow systems”, *Physica* **D125**, 65 (1999).

[22] S. Laplace, *Essai philosophique sur les probabilités*, (Courcier, Paris, 1814).

[23] R. Benzi, G. Paladin, G. Parisi & A. Vulpiani, “Characterization of intermittency in chaotic systems”, *J. Phys.* **A18**, 2157 (1985).

[24] G. Paladin & A. Vulpiani, “Anomalous scaling laws in multifractal objects”, *Phys. Rep.* **156**, 147 (1987).

[25] A. Crisanti, M.H. Jensen, G. Paladin & A. Vulpiani, “Intermittency and predictability in turbulence”, *Phys. Rev. Lett.* **70**, 166 (1993).

[26] G. Paladin & A. Vulpiani, “Predictability in spatially extended systems”, *J. Phys.* **A27**, 4911 (1994).

[27] D. Ruelle, “Microscopic fluctuations and turbulence”, *Phys. Lett* **A72**, 81 (1979).

[28] R.J. Deissler & K. Kaneko, “Velocity-dependent Lyapunov exponents as a measure of chaos for open-flow systems”, *Phys. Lett.* **A119**, 397 (1987).

[29] U. Dressler & J.D. Farmer, "Generalized Lyapunov exponents corresponding to higher derivatives", *Physica* **D59**, 365 (1992).

[30] K. Kaneko, "Globally coupled chaos violates the law of large numbers but not the central-limit theorem", *Phys. Rev. Lett.* **65**, 1391 (1990); "Remarks on the mean field dynamics of networks of chaotic elements" *Physica* **D86**, 158 (1995).

[31] A.S. Pikovsky & J. Kurths, "Do globally coupled maps really violate the law of large numbers?", *Phys. Rev. Lett.* **72**, 1644 (1994); "Collective behavior in ensembles of globally coupled maps", *Physica* **D76**, 411 (1994).

[32] T. Shibata & K. Kaneko. "Collective Chaos", *Phys. Rev. Lett.* **81**, 4116 (1998).

[33] M. Cencini, M. Falcioni, D. Vergni & A. Vulpiani, "Macroscopic chaos in globally coupled maps", *Physica* **D130**, 58 (1999).

[34] A. Torcini, P. Grassberger & A. Politi, "Error propagation in extended chaotic systems", *J. Phys.* **A27**, 4533 (1995).

[35] A. Politi & A. Torcini, "Linear and Non-Linear mechanisms of Information propagation", *Europhys. Lett.* **28**, 545 (1994).

[36] G. Boffetta, P. Giuliani, G. Paladin & A. Vulpiani, "An extension of the Lyapunov analysis for the predictability problem", *J. Atmos. Sci.* **55**, 3409 (1998).

[37] J. Gugkenheimer & P. Holmes, *Nonlinear Oscillations, Dynamical Systems, and Bifurcations of Vector Fields*, (Springer, Berlin, 1986)

[38] C. Beck & F. Schlögl, *Thermodynamics of chaotic systems* (Cambridge University Press, 1993).

[39] A.J. Lichtenberg & M.A. Lieberman, *Regular and Chaotic Dynamics*, 2nd Edition, (Springer-Verlag, Berlin, 1992).

[40] A. Kolmogorov & S. Fomine, *Eléments de la théorie des functions et de l' analyse functionnelle*, Chap. III. (Editions MIR, Moscow, 1976)

[41] G. Benettin, L. Galgani, A. Giorgilli & J.M. Strelcyn, "Lyapunov characteristic exponents for smooth dynamical systems and for Hamiltonian systems: a method for computing all of them", *Meccanica* **15**, 9 (1980).

[42] V.I. Oseledec, "A multiplicative ergodic theorem: Lyapunov characteristic numbers for dynamical systems", *Trans. Mosc. Math. Soc.* **19**, 197 (1968).

[43] G. Paladin & A. Vulpiani, "Intermittency in chaotic systems and Renyi entropies", *J. Phys.* **A19**, 997 (1986).

[44] W. Feller, *An Introduction to Probability theory and its Applications, Vol. I*, (Wiley, New York, 1968).

[45] B. Mandelbrot, *The Fractal Geometry of Nature*, (W.H. Freeman, 1982).

[46] P. Grassberger & I. Procaccia, "Characterization of strange attractors", *Phys. Rev. Lett.* **50**, 346 (1983); "Measuring the strangeness of strange attractors", *Physica* **D9**, 189 (1983).

[47] G. Parisi & U. Frisch, "On the singularity structure of fully developed turbulence", in *Turbulence and predictability of geophysical fluid dynamics*, ed. by M. Ghil, R. Benzi and G. Parisi, p. 84 (North-Holland, Amsterdam, 1985)

[48] R. Benzi, G. Paladin, G. Parisi & A. Vulpiani, "On the multifractal nature of fully developed turbulence and chaotic systems", *J. Phys.* **A17**, 3521 (1984).

[49] A.I. Khinchin, *Mathematical foundations of information theory*, (Dover, New York, 1957).

[50] J.L. Kaplan & J.A. Yorke, "Pre turbulence: a regime observed in a fluid model of Lorenz", *Comm. Math. Phys.* **67**, 93 (1979); "Chaotic behavior of multidimensional difference equations", *Lect. Notes in Math.* **730**, 228 (1986).

[51] Y.B. Pesin, "Lyapunov characteristic exponent and ergodic properties of smooth dynamical systems with an invariant measure", *Sov. Math. Dokl.* **17**, 196 (1976).

[52] M.C. Cross & P.H. Hohenberg, "Pattern formation outside of equilibrium", *Rev. Mod. Phys.* **65**, 851 (1993).

[53] U. Frisch, *Turbulence: the legacy of A. N. Kolmogorov*, (Cambridge University Press, Cambridge, UK, 1995).

[54] R. Kapral, "Chemical waves and coupled map lattices", in *Theory and applications of coupled map lattices*, ed. K. Kaneko, p. 135, (John Wiley and Sons, 1993)

[55] S. Ciliberto & P. Bigazzi, "Spatiotemporal intermittency in Rayleigh-Bénard convection", *Phys. Rev. Lett.* **60**, 286 (1988); S. Ciliberto & M.A. Rubio, "Local oscillations, traveling waves, and chaos in Rayleigh-Bénard convection", *Phys. Rev. Lett.* **58**, 2652 (1987).

[56] J.P. Gollub & H.L. Swinney, "Onset of turbulence in a rotating fluid", *Phys. Rev. Lett.* **35**, 927 (1975); *Hydrodynamic Instabilities and Transition to Turbulence*, (Springer Verlag, Berlin, 1981).

[57] A.J. Kreuzer, *Non-equilibrium thermodynamics and its statistical foundations*, (Clarendon Press, Oxford 1981).

[58] D. Ruelle, "Large volume limit of the distribution of characteristic exponents in turbulence", *Commun. Math. Phys.* **87**, 287 (1982).

[59] L.A. Bunimovich & G. Sinai, "Statistical mechanics of coupled map lattices", in *Theory and applications of coupled map lattices*, ed. K. Kaneko, p. 169, (John Wiley and Sons, 1993).

[60] K. Kaneko, "Period-doubling of kink-antikink patterns, quasi-periodicity in antiferro-like structures and spatial intermittency in coupled map lattices —toward a prelude to a field theory of chaos", *Prog. Theor. Phys.* **72**, 480 (1984).

[61] K. Kaneko, "The coupled map lattice", in *Theory and applications of coupled map lattices*, ed. K. Kaneko, p. 1, (John Wiley and Sons, 1993).

[62] A.N. Kolmogorov, I. Petrovsky & N. Piskunov, "Study of the diffusion equation with growth of the quantity of matter and its application to a biology problem", *Bull. Univ. Moscow, Ser. Int.* **A1**, 1 (1937).

[63] S. Wolfram, *Theory and applications of Cellular Automata*, (World Scientific, Singapore, 1986).

[64] P. Collet & J.P. Eckmann, "The definition and measurement of the topological entropy per unit volume in parabolic PDE's", *Nonlinearity* **12**, 451 (1999); "Extensive properties of the complex Ginzburg-Landau equation", preprint (1999).

[65] H. Kantz & T. Schreiber, *Nonlinear time series analysis*, (Cambridge University Press, Cambridge, UK, 1997).

[66] E. Olbrich, R. Hegger & H. Kantz, "Analyzing local observations of weakly coupled maps", *Phys. Lett.* **A244**, 538 (1998).

[67] A. Politi & A. Witt, "Fractal Dimension of Space-Time Chaos", *Phys. Rev. Lett.* **82**, 3034 (1999).

[68] P. Grassberger & T. Schreiber, "Does mesoscopic disorder imply microscopic chaos?", preprint, chao-dyn/9909021 (1999).

[69] M. Lesieur, *Turbulence in Fluids*, 2nd Ed. (Kluwer Academic Publishers, London, 1990).

[70] M. Yamada & K. Okitani, "Lyapunov spectrum of a model of two dimensional turbulence", *Phys. Rev. Lett.* **60**, 983 (1987);"Temporal intermittency in the energy cascade processes and local Lyapunov analysis in fully developed model turbulence", *Prog. Theor. Phys.* **81**, 329 (1989).

[71] C.E. Leith & R.H. Kraichnan, "Predictability of turbulent flows", *J. Atmos. Sci.* **29**, 1041 (1972); D.K. Lilly, *Dynamic Meteorology*, ed. P. Morel, (Riedel, Boston, 1973).

[72] J.M. Burgers, *The Nonlinear Diffusion Equation*, (D. Reidel Publishing Company, Dordrec, 1974).

[73] G. Károlyi & T. Tél, "Chaotic tracer scattering and fractal basin boundaries in a blinking vortex-sink system",*Phys. Rep.* **290**, 125 (1997).

[74] S. Bleher, E. Ott & C. Grebogi, "Routes to chaotic scattering", *Phys. Rev. Lett.* **63**, 919 (1989); Special issue on Chaotic Scattering, *Chaos* **3** n. 4, E. Ott & T. Tél eds. (1993).

[75] U. Feudel & A.S. Pikovsky, "Characterizing strange non-chaotic attractors", *Chaos* **5**, 253 (1995); U. Feudel, J. Kurths & A.S. Pikovsky, "Strange non-chaotic attractors in a quasi-periodically forced circle map", *Physica* **D88**, 176 (1995).

[76] H. Chaté & P. Manneville, "Transition to turbulence via spatio-temporal intermittency", *Phys. Rev. Lett.* **58**, 112 (1987).

[77] A. Crisanti, G. Paladin & A. Vulpiani, *Products of Random Matrices*, (Springer Verlag, Berlin, 1993).

[78] G. Giacomelli & A. Politi "Spatio-temporal chaos and localization", *Europhys. Lett.* **15**, 387 (1991).

[79] M. Cencini & A. Torcini, in preparation (1999).

[80] I.S. Arason, A.V. Gaponov-Grekhov & M. Rabinovich, "The onset and spatial development of turbulence in flow systems", *Physica* **D33**, 1 (1988); I.S. Arason, A.V. Gaponov-Grekhov, M. Rabinovich & I.P. Starobinets, " Strange attractors and the spatial development of turbulence in flow systems", *Sov. Phys. JEPT* **63(5)**, 1000 (1986)

[81] A.S. Pikovsky, "Spatial development of Chaos in non-linear media", *Phys. Lett.* **A137**, 121 (1989).

[82] A. Pikovsky, "Local Lyapunov exponents for spatiotemporal chaos", *Chaos* **3**, 225 (1993).

[83] D. Ruelle & F. Takens, "On the nature of Turbulence", *Commun. Math. Phys.* **20**, 167 (1971).

[84] A. Monin, *Weather prediction as a problem in physics*, (MIT Press, 1973).

[85] H. Aref, "Integrable, chaotic, and turbulent vortex motions in two dimensional flows", *Ann. Rev. Fluid Mech.* **15**, 345 (1983); "Stirring by chaotic advection", *J. Fluid Mech.* **143**, 1 (1984).

[86] J.M. Ottino, *The Kinematics of Mixing: Stretching, Chaos and Transport*, (Cambridge University Press, 1989).

[87] A. Crisanti, M. Falcioni, G. Paladin & A. Vulpiani, "Lagrangian Chaos: Transport, Mixing and Diffusion in Fluids", *La Rivista del Nuovo Cimento* **14**, 1 (1991).

[88] V. Artale, G. Boffetta, A. Celani, M. Cencini & A. Vulpiani, "Dispersion of passive tracers in closed basins: Beyond the diffusion coefficient", *Phys. Fluids A* **9**, 3162 (1997).

[89] G. Boffetta, A. Celani, M. Cencini, G. Lacorata & A. Vulpiani, "Transport and Mixing in non-ideal systems", *Chaos* To appear (2000).

[90] G. Boffetta, M. Cencini, S. Espa & G. Querzoli, "Experimental evidence of Chaotic Advection in a convective flow" *Europhys. Lett.* **48**, 629 (1999); "Chaotic advection and relative dispersion in an experimental convective flow", *Phys. Fluids* Submitted (1999).

[91] A. Politi & A. Torcini, "Periodic orbits in coupled Hénon maps: Lyapunov and multifractal analysis", *Chaos* **2**, 293 (1992).

[92] A.S. Pikovsky & J. Kurths, "Roughening interfaces in the dynamics of perturbations of spatiotemporal chaos",*Phys. Rev. E* **49**, 898 (1994); A.S. Pikovsky & A. Politi, "Dynamic localization of Lyapunov vectors in space-time chaos", *Nonlinearity* **11**, 1049 (1998).

[93] M. Kardar, G. Parisi & Y.C. Zhang, "Dynamic scaling of growing interfaces", *Phys. Rev. Lett.* **56**, 889 (1986).

[94] T. Bohr & D. Rand, "A mechanism for localized turbulence", *Physica* **D52**, 532 (1987).

[95] G. Boffetta, A. Celani, A. Crisanti & A. Vulpiani, "Predictability in Two Dimensional Decaying Turbulence", *Phys. of Fluids* **A9**, 724 (1997).

[96] H. Kantz & T. Letz, "Quasi-chaos and quasi-regularity- the breakdown of linear stability analysis", preprint, (1999).

[97] A.N. Kolmogorov, "On the Shannon theory of information transmission in the case of continuous signals", *IRE Trans. Inf. Theory* **1**, 102 (1956).

[98] C.E. Shannon, in *Information and Decision processes* ed. R. Machol, p.93, (McGraw-Hill, New York, 1960).

[99] A. Cohen & I. Procaccia, "Computing the Kolmogorov entropy from a chaotic signal", *Phys. Rev. A* **31**, 1872 (1985).

[100] M. Abel, L. Biferale, M. Cencini, M. Falcioni, D. Vergni and A. Vulpiani, "Exit time approach to (ϵ, τ)-entropy", *Phys. Rev. Lett.* Submitted (1999).

[101] G. Paladin, M. Serva & A. Vulpiani, "Complexity in dynamical systems with noise", *Phys. Rev. Lett.* **74**, 66 (1995); V. Loreto, G. Paladin & A. Vulpiani, "On the concept of complexity for random dynamical systems", *Phys. Rev. E* **53**, 2087 (1996).

[102] M. Cencini, M. Falcioni, H. Kantz, E. Olbrich & A. Vulpiani, "Chaos or Noise — Sense and Nonsense of a Distinction", in preparation (1999).

[103] E. Aurell, G. Boffetta, A. Crisanti, G. Paladin & A. Vulpiani, "Predictability in systems with many characteristic times: the case of turbulence", *Phys. Rev. E* **53**, 2337 (1996).

[104] G. Berkooz, "An observation probability density equations, or, when simulations reproduce statistics?". *Nonlinearity* **7** 313 (1994).

[105] A. Crisanti, M. Falcioni, & A. Vulpiani, "On the effects of an uncertainty on the evolution law in dynamical systems", *Physica* **A160**, 482 (1989).

[106] G. Boffetta, A. Celani, M. Cencini, G. Lacorata & A. Vulpiani, "The predictability problem in systems with an uncertainty in the evolution law", To appear *J. Phys. A* (1999).

[107] D.E. Knuth, *The Art of Computer Programming*, vol. 2, (Addison-Wesley, Reading, MA, 1969).

[108] G. Boffetta, G. Paladin & A. Vulpiani, "Strong Chaos without Butterfly Effect in Dynamical Systems with Feedback", *J. Phys.* **A29**, 2291 (1996).

[109] V.S. L'vov, E. Podivilov, A. Pomyalov, I. Procaccia & D. Vandembroucq, "Improved shell model of turbulence", *Phys. Rev. E* **58**, 1811 (1998).

[110] R. Benzi, L. Biferale, S. Succi & F. Toschi, "Intermittency and eddy-viscosities in dynamical models of turbulence", *Phys. Fluids* **11**, 1221 (1998).

[111] H. Chatè & P. Manneville, "Collective behaviors in spatially extended systems with local interactions and synchronous updating", *Prog. Theor. Phys.* **87**, 1 (1992).

[112] A. Crisanti, M. Falcioni & A. Vulpiani, "Broken ergodicity and glassy behavior in a deterministic chaotic map", *Phys. Rev. Lett.* **76**, 612 (1996).

[113] K. Kaneko, " Chaotic but regular posi-nega switch among coded attractors by cluster-size variation", *Phys. Rev. Lett.* **63**, 219 (1989); "Clustering, coding, switching, hierarchical ordering, and control in a network of chaotic elements" *Physica* **D41**, 38 (1990); "Globally coupled chaos violates the law of large numbers", *Phys. Rev. Lett.* **65**, 1391 (1990).

[114] T. Konishi & K. Kaneko, "Clustered motion in symplectic coupled maps system", *Jour. Phys.* **A25**, 6283 (1992).

[115] T. Shibata & K. Kaneko, "Heterogeneity induced order in globally coupled systems", *Europhys. Lett.* **38**, 417, (1997).

[116] G. Perez & H.A. Cerdeira, "Instabilities and non statistical behavior in globally coupled systems", *Phys. Rev. A* **46**, 7492 (1992).

[117] A.T. Winfree, *The Geometry of Biological Times*, (Springer-Verlag, New York, 1980).

[118] C. Bracikowaki, R. Roy, "Chaos in multimode solid-state laser system", *Chaos* **1**, 49 (1991); T. Arecchi, "Rate processes in nonlinear optical dynamics with many attractors", *Chaos* **1**, 357 (1991)

[119] A. Wolf, J.B. Swift, H.L. Swinney & J.A. Vastano, "Determining Lyapunov exponents from a time series", *Physica* **D16** 285 (1985).

[120] E.N. Lorenz, "Atmospheric predictability as revealed by naturally occurring analogies", *J. Atmos. Sci.* **26**, 636 (1969).

[121] W. van Saarloos, "Front propagation into unstable states: Marginal stability as a dynamical mechanism for velocity selection" *Phys. Rev. A* **37**, 211 (1988); "Front propagation into unstable states. II. Linear versus nonlinear marginal stability and rate of convergence", *Phys. Rev. A* **39**, 6367 (1989).

[122] E. Ben-Jacob & P. Garik, "The formation of patterns in non-equilibrium growth", *Nature* **343**, 523 (1990).

[123] D.G. Aronson & H.F. Weinberger, "Multidimensional nonlinear diffusion arising in population genetics", *Adv. Math.* **30**, 33 (1978).

[124] P. Collet & J.P. Eckmann, *Instabilities and Fronts in Extended Systems* (Princeton University Press, Princeton, NJ, 1990).

[125] G.C. Paquette, L.Y. Chen, N. Goldenfeld & Y. Oono, "Structural stability and renormalization group for propagating fronts" *Phys. Rev. Lett.* **72**, 76 (1994).

[126] I. Goldhirsh, P.L. Sulem & S.A. Orszag, "Stability and Lyapunov stability of dynamical systems: a differential approach and numerical method", *Physica* **D27**, 311 (1987).

[127] F. Bagnoli, R. Rechtman & S. Ruffo, "Damage spreading and Lyapunov exponent in cellular automata", *Phys. Lett.* **A172**, 34 (1992).

[128] H.K. Moffat, "Transport effects associated with turbulence with particular attention to the influence of helicity", *Rep. Prog. Phys.* **46**, 621 (1983).

[129] A. Monin & A. Yaglom, *Statistical Fluid Dynamics*, (MIT Press, Cambridge, 1983).

[130] W.J. Cocke, "Turbulent hydrodynamic line stretching: consequences of isotropy", *Phys. Fluids* **12**, 2488 (1969);S.A. Orszag, "Comment on: Turbulent hydrodynamic line stretching: consequences of isotropy", *Phys. Fluids* **13**, 2203 (1970).

[131] P. Castiglione, A. Crisanti, A. Mazzino, M. Vergassola & A. Vulpiani, "Resonant enhanced diffusion in time-dependent flow", *J. Phys.*, **A31** 7197 (1998).

[132] G.I. Taylor, "Diffusion by continuous movements", *Proc. London Math. Soc.* **20**, 196 (1921).

[133] J.P. Bouchaud & A. Georges, "Anomalous diffusion in disordered media", *Phys. Rep.* **195**, 127 (1990).

[134] M. Avellaneda & A. Majda, "Stieltjes integral representation and effective diffusivity bounds for turbulent transport", *Phys. Rev. Lett.* **62**, 753 (1989); M. Avellaneda & M. Vergassola, "Stieltjes integral representation of effective diffusivities in time-dependent flows", *Phys. Rev. E* **52**, 3249 (1995).

[135] A.S. Pikovsky, "Statistical properties of dynamically generated anomalous diffusion", *Phys. Rev. A* **43**, 3146 (1991); P. Castiglione, A. Mazzino, P. Muratore-Ginanneschi & A. Vulpiani, "On *strong* anomalous diffusion", *Physica* **D134**, 75 (1999).

[136] T. Bohr & A.S. Pikovsky, "Anomalous diffusion in the Kuramoto-Sivanshinsky equation", *Phys. Rev. Lett.* **70**, 2892 (1993).

[137] T.H. Solomon, E.R. Weeks & H.L. Swinney, "Chaotic advection in two-dimensional flow: Lèvy flights and anomalous diffusion", *Physica* **D76**, 70 (1994).

[138] D.Mc Laughlin, G.C. Papanicolau & O. Pironneau, "Convection of microstructure and related problems", *SIAM J. Appl. Math.*, **45**, 780 (1985); A. Bensoussan, J.L. Lions & G. Papanicolau, *Asymptotic Analysis for Periodic Structures*, (Noth-Holland, Amsterdam, 1978).

[139] L. Biferale, A. Crisanti, M. Vergassola & A. Vulpiani, "Eddy diffusivities in scalar transport", *Phys. Fluids* **7**, 2725 (1995).

[140] G. Buffoni, P. Falco, A. Griffa & E. Zambianchi, "Dispersion processes and residence times in a semi-enclosed basin with recirculating gyres: an application to the Tyrrhenian sea", *J. Geophys. Res.* **102**, 18699 (1997).

[141] R. Sabot & M.A. Dubois, "Diffusion coefficient in a finite domain from exit times and application to the tokamak magnetic structure", *Phys. Lett.* **A212**, 201 (1996).

[142] G. Boffetta, A. Celani, A. Crisanti & A. Vulpiani, "Relative dispersion in fully developed turbulence: Lagrangian statistics in synthetic flows", *Europhys. Lett.* **42**, 177 (1999); "Pair dispersion in synthetic fully developed turbulence", *Phys. Rev. E*, in press (1999).

[143] L.F. Richardson, "Atmospheric diffusion shown on a distance-neighbor graph", *Proc. Roy. Soc. A* **110**, 709 (1926).

[144] S. Benkadda, Y. Elskens, B. Ragot & J.T. Mendoça, "Exit times and Chaotic Transport in Hamiltonian Systems", *Phys. Rev. Lett.* **72**, 2859 (1994); A.N. Yannacopoulos & G. Rowlands, "Calculation of diffusion coefficients for chaotic maps", *Physica* **D65**, 71 (1993).

[145] M. Falcioni & A. Vulpiani, "Diffusion properties of test particles in a two dimensional flows", *J. Phys.* **A22**, 1201 (1989).

[146] L.D. Landau & E.M. Lifshiz, *Fluid Mechanics*, 2nd ed., (Pergamon Press, Oxford, 1987).

[147] T.H. Solomon & J.P. Gollub, "Chaotic particle transport in time-dependent Rayleigh-Bénard convection", *Phys. Rev. A* **38**, 6280 (1988); "Passive transport in steady Raleigh-Bénard convection", *Phys. Fluids* **31**, 1372 (1988).

[148] G. Boffetta, A. Celani & P. Franzese, "Trapping of Passive Tracers in a Point Vortex System", *J. Phys.* **A29**, 3749 (1996).

[149] M. Miozzi, G. Querzoli & G.P. Romano, "The investigation of an unstable convective flow using optical methods", *Phys. Fluids* **10**, 2995 (1998).

[150] J.H. Misguich, J.D. Reuss, Y. Elskens & R. Balescu, "Motion in a stochastic layer described by symbolic dynamics", *Chaos* **8**, 248 (1998).

[151] M. Cencini, G. Lacorata, A. Vulpiani & E. Zambianchi, "Mixing in a meandering jet: a Markovian approximation", *J. Phys. Oceanogr.* in press (1999).

[152] R.W. Easton, J.D. Meiss & S. Carver, "Exit times and transport for Symplectic Twist Maps", *Chaos* **3**, 153 (1993).

[153] P. Castiglione, M. Cencini, A. Vulpiani & E. Zambianchi, "Transport in finite size systems: an exit time approach", *Chaos* To appear (1999).